Equations of motion for viscoelastic moving crack problems

Goleniewski, G.

Award date:
1988

Awarding institution:
University of Bath

Equations of motion for viscoelastic moving crack problems.

submitted by G.Goleniewski

for the degree of PhD

of the University of Bath

1988

Copyright

G.Goleniewski

ProQuest LLC
789 East Eisenhower Parkway
P.O. Box 1346
Ann Arbor, MI 48106-1346

CONTENTS Page

Abstract.

The problem of steady-state crack propagation under antiplane strain in a Maxwell liquid is considered, using the critical crack opening displacement fracture criterion and incorporating a finite craze zone over which cohesive forces act. Stress and displacement fields are obtained by use of the Wiener-Hopf technique, and from these plots of nominal stress intensity factor and work-rate of applied tractions are generated, demonstrating variation with respect to the craze zone length (the energy absorbed by the zone being held constant) and relaxation time (relative to a characteristic timescale). The curves for a finite craze zone size deviate considerably from those near the sharp crack limit.

Quasi-static crack propagation in a standard linear solid is investigated for two different crack geometries, one semi-infinite, the other finite. Viscoelastic displacements are obtained from their elastic counterparts by use of a correspondence principle. The fracture initiation time is evaluated in each case, and from this it is possible to deduce quasi-static crack motion is possible in a certain range of loading for a viscoelastic material. Time histories of the crack tip position are evaluated from the fracture criterion equation using numerical methods.

The method of matched asymptotic expansions is used to investigate accelerating crack growth in a standard linear solid (in the subsonic velocity range). The outer problem is found to reduce to the elastic accelerating crack problem in Mode III, while the inner problem is one of steady-state motion. Stress intensity factor matching is performed for various choices of crack face loading.

This thesis is concluded with an extension of the steady-state work on the Maxwell liquid to the standard linear solid, and treatments of the inner matched expansions problem for the supersonic range of the latter material and for the subsonic range of the power law material.

Acknowledgements

The author would like to thank Professor J.R. Willis for many helpful suggestions during the course of the work, and also for his continual encouragement in this endeavour. This work was funded by the Science and Engineering Research Council. Thanks are due to the numerous individuals who freely offered assistance in the fields of computing and numerical analysis, and those who evaluated various drafts of the material in Chapter 2, especially Professor J.R. Walton who made certain invaluable points. Finally, the author appreciates Dr.J. Sivaloganathan's helpfulness in looking over the completed work.

Chapter 1 - Introduction.

This thesis concerns itself with time-dependent crack propagation problems in linear viscoelastic materials. There are two sources of time-dependence: one is inertia (mathematically the second time derivative of displacement as appears in the equations of motion) and the other is the viscoelasticity itself, i.e the relaxation function(s) or creep function(s) vary with time, unlike in the elastic case.

There are a number of crack propagation models that can be set up depending on the presence or otherwise of certain ingredients. The central three of these are the nature of the loading on the crack (or on the adjacent intact material), the specimen geometry and whether or not a craze zone is present ahead of the actual crack. In addition, a choice of relaxation function has to be made, and also a fracture criterion: the constant crack opening displacement criterion is a natural choice when a craze zone is included in the model.

For simplicity, the work contained in this thesis is based solely on Mode III (antiplane strain) loading, or in other words, shearing or tearing. The problems tackled, which do not include the presence of inertia, could relatively easily be generalised to Mode I, the opening mode of loading. This, however, is not the case when inertia is taken into account. Either crack face traction loading or remote loading (at infinity) are utilised in various problems. In the former case, a step function is chosen as a means of reducing the multiplicity of the integrals present by one.

All the work is done using either semi-infinite (primarily) or double-ended cracks in an infinite medium. This removes the complications that would otherwise result from wave reflection effects at the boundaries of a finite specimen, but limits the approximate validity of the results to pieces of material of large

dimension relative to a characteristic length based on, for Mode III, the shear wave speed for the material and its relaxation time.

A significantly novel aspect of the work presented is the incorporation of a finite, as opposed to infinitesimal, craze zone, also variously referred to, among other terminology, as a Dugdale or failure zone. This is an intermediate zone between the actual physical crack tip and the, as yet, intact material on the line of the crack. Although this is observed in certain polymers e.g. in PMMA (perspex) to be three-dimensional in nature, for the purposes of mathematical modelling it is customarily taken to be represented by a one-dimensional strip of cohesive forces. Taking a constant cohesive stress over this zone makes the resulting mathematics less complicated, but this is not a prerequisite of the model. Physically, a craze zone can be thought of as a set of fibrils keeping together the two faces of what will be the next section of crack if there is any further propagation, i.e. it is an intermediate failure zone. Mathematically, the craze zone is treated as if it were an integral part of the crack.

The primary choices of relaxation function made for this thesis are those of the Maxwell liquid and standard linear solid, although a feasibility study of what is possible with the power law material appears in chapter 6. The Maxwell liquid is the most rudimentary example of a viscoelastic material. Although it does not have a finite long-time modulus, and so cannot be considered to be a solid, nevertheless it possesses the essential attributes of a viscoelastic material, and its very mathematical simplicity makes much analytic progress possible which would be a non-starter for more realistic materials. The results obtained from this material, although coming from a highly artificial model, do in fact give some idea as to what behaviour may be expected from more realistic materials.

The standard linear solid has the simplest, usable relaxation function that models a solid: it has finite short and long-time moduli. However, containing only three parameters, it does not possess sufficient complexity to realistically model an actual polymer (this is thought to need at least a four or five parameter model (Bland, 1960)). Abstract generalisations of the standard linear solid's constitutive equation are a possibility, but are algebraically unwieldy. Therefore, there is a conflict between realistic modelling and mathematical tractability, with the result that much of the work presented here is semi-analytic in nature.

Contained in chapter 2 is the Maxwell liquid analogue of Willis' 1967 paper on steady state crack motion in a standard linear solid. Steady-state crack propagation problems are the least troublesome of all types involving inertia because the time-dependence can be masked by a change of variable, making solution of the equations of motion possible by use of the Wiener-Hopf technique, a process based fundamentally on analytic continuation. Apart from its simplicity, the choice of the Maxwell liquid is motivated by Freund and Hutchinson's 1985 paper on high strain-rate crack growth in an elastic-plastic material. In chapter 2, formulae are derived for stress and displacement in an infinite body containing a semi-infinite crack with its faces loaded by step function surface tractions. These are used to generate curves of nominal stress intensity factor and work-rate of loading stresses per unit of crack extension vs velocity. Although not absolutely guaranteeing correctness, elastic and quasi-static limits are taken of the computed quantities and these are found to agree with well established or easily derivable results. Also, the sharp crack, or as it is referred to subsequently, the Griffith limit is investigated: this limit is taken while keep-

ing the total energy absorbed by the craze zone constant.

Chapter 3 contains an investigation of the quasi-static growth of a semi-infinite crack in a standard linear solid. The model includes a craze zone and transient motion arising solely from viscoelastic effects. However, for the chosen loading, the motion is found to tend to a steady state eventually. Application of the fracture criterion to the displacement, which is calculated using Graham's (1968) extended correspondence principle, is used to derive a formula for fracture initiation time. This quantity is the interval which elapses from the onset of loading to the commencement of crack motion. From its formula, it is possible to ascertain the range of loading stresses for which it is possible to have motion in the absence of inertia, and above which the motion must become dynamic (then the present analysis becomes inadequate). An expression for the terminal velocity can also be derived. Further progress can be made with degenerate cases of the standard linear solid, such as the Maxwell liquid and Voigt solid, and it is shown how some of the results can be interpreted as specific instances of an equation derived for the case of a general viscoelastic material with finite short and long-time moduli under time-independent loading. Chapter 3 can be considered as complementary to the quasi-static work of Knauss (1970) and Schapery (1975) which contained infinitesimal craze zones and numerous approximations - the present work concentrates instead on attempting to solve the non-standard integro-differential controlling equation, which has the added complication of history, by a mixture of numerical techniques.

The finite or double-ended crack analogue of the model in chapter 3 is examined in chapter 4, with the important exception that the loading has changed in view of the new geometry. There are several papers by Graham (1969,1975)

that address the problem of whether or not a finite crack will extend in the absence of inertia under a certain loading. The current model is more complicated as it involves craze zones at either end of the crack, and that an attempt is made to predict the extent of the symmetrically growing crack as a function of time. An analytic argument to approach Graham's conclusions from the starting point of the viscoelastic equations in this chapter is given: these were that quasi-static crack growth in a viscoelastic material is not possible in the case of a Griffith crack and in the absence of inertia.

The problem of an accelerating semi-infinite crack in an infinite medium is tackled by the method of matched asymptotic expansions in chapter 5. The underlying motivation for this approach is that the only reasonably simple solution (for stresses and displacements) in the literature for an accelerating crack is Kostrov's 1966 paper for a crack in an elastic medium under antiplane strain. There are more complicated solutions for the corresponding Mode I problem by Freund (1972a,b, 1973) for various special loadings and by Kostrov (1974) for general loading. Atkinson and Coleman (1977) treat a series of mechanical problems by matched asymptotic expansions, the second of which is a steady-state semi-infinite crack propagating in a standard linear solid. The author knows of no viscoelastic solutions for accelerating cracks.

On applying the matched asymptotic expansions technique to the problem, it transpires that the outer problem is identically Kostrov's. The inner problem is of standard steady-state type and can be dealt with by the techniques of chapter 2. Since the outer limit of the inner problem and vice-versa are equal, it is reasonable to match stress intensity factors from the outer and inner problems. This is done for various elementary choices of crack face loading on the

macroscopic scale, generating curves of crack tip position vs time.

Chapter 6 first deals with a hybridised extension of some of the problems of chapters 2 and 5 for the case of the standard linear solid. It goes on to investigate how much of the technique used for that choice of relaxation function can be carried through for the power law material, in view of Walton's 1987 work on the energy-release rate of general viscoelastic materials. The differences in behaviour observed between the two materials are primarily accounted for by the fact that the power law material does not have a finite short-time modulus. This thesis is concluded with a summary of what has been achieved and some suggestions as to what could still be done in this area.

Chapter 2 - Dynamic crack growth in a Maxwell liquid.

1. Background to and description of problem.

Freund and Hutchinson (1985), using approximate analysis, investigated high strain-rate crack growth in an elastic-plastic material - the terminology arising because the strain-rates in the vicinity of the crack tip are so large as to offset any propagation slowdown effects attributable to rate-dependent plasticity. Contained within their model are three zones of material, described by different constitutive relations, radiating outwards from the crack tip and defined in terms of strain-rate intervals: two of these describe the material behaviour in the plastic zone. In the highest strain-rate range, a plastic strain-rate increase is linearly proportional to a stress increase. Employing certain approximations to calculate the plastic strain-rates and utilising K-field type remote loading, a relation between the near tip and remote fields (or, equivalently, between the corresponding energy release rates) is derived. The authors employ a critical near-tip energy release rate criterion to obtain a crack propagation equation. From this it turns out that the whole process, as approximated, is essentially controlled by a single non-dimensional combination of material constants, which is much simpler than what one might expect from such a problem.

Freund, Hutchinson and Lam (1986) give a concise summary of the analysis contained in the previously mentioned paper, and conduct a numerical investigation into its validity, essentially based on the finite element method. Plastic zone shapes for the two strain-rate ranges are computed. A check on the computations was carried out by evaluating the path-independent J-integral for a number of contours surrounding the crack tip (this integral measures the energy flux into the immediate crack tip region under suitably defined conditions).

They conclude by acknowledging deficiencies in the approximate analysis for temperatures above those for which cleavage crack growth is known to occur, but otherwise they demonstrate the effectiveness of the modelling contained in the 1985 paper.

A similar set-up to that of the aforementioned authors is investigated in this chapter. The material description chosen is that of a Maxwell liquid, this resulting from taking the dominant term of the constitutive equation from their paper in the region of the plastic zone nearest the crack tip (i.e. the region corresponding to the highest strain-rate range of the three). The analysis contained in this chapter is different in that the same rate-dependent constitutive equation is taken in all of the material as opposed to only in the zone within which strain-rates are high. This reduces the problem to a linear one which can be solved explicitly. Apart from the wish to facilitate comparison with the work of Freund and Hutchinson, the choice of the material representation is governed in part by the need to minimise the scale of the computations. A set of more realistic calculations for the standard linear solid for the same problem appears in section 1 of chapter 6.

A new feature of the present analysis is the consideration of the effects of a finite cohesive zone, in which a constant cohesive stress σ_0 acts, whose extent may be comparable with the length scale of the applied loads. A critical crack opening displacement fracture criterion is used. When σ_0 is sufficiently large, this is demonstrated to reduce to the energy release-rate criterion (Willis, 1967a, contains a comparison of the Griffith and Barenblatt fracture criteria, which essentially is what is present here). Finite σ_0 provides a rudimentary model of a craze zone such as exists adjacent to a crack tip in a viscoelastic

polymer. The solution to be presented thus serves the dual purpose of providing an explicit realisation of the near-tip situation discussed in Freund and Hutchinson (1985), and of assessing the influence of a craze zone during dynamic fracture of a polymer.

There is a small but significant literature on dynamic steady-state crack propagation in viscoelastic materials, and more often than not the material chosen is the standard linear solid. However, there are relatively few papers that include transient effects. The first paper in the category is thought to be Atkinson and List's 1972 treatment of a semi-infinite crack which starts growing with uniform velocity at time t=0: the authors, by use of the Fourier transform for the spatial variable and the Laplace transform for time, reduce the problem to that of solving a Wiener-Hopf equation. The (time-dependent) stress intensity factor is evaluated for the Maxwell liquid (as it is referred to throughout this thesis) and the standard linear solid.

Willis (1967b) used the Wiener-Hopf technique to solve for stress and displacement fields for steady-state motion in antiplane strain. This paper apparently gives the first solution to any moving boundary value problem in the dynamic theory of crack propagation in viscoelastic materials. There are also a series of contributions as regards steady-state propagation in a two-dimensional strip of standard linear solid. Atkinson and Popelar (1979) dealt with the Mode III problem as treated by Atkinson and Coleman (1977) in a limiting case for Mode I as part of a series of problems on the application of matched asymptotic expansions to linear viscoelasticity theory. Numerical, as opposed to analytic, factorisation of the Wiener-Hopf equation proves to be necessary. Popelar and Atkinson (1980) deal with the more general Mode I problem, their

results agreeing closely with the asymptotic formulae of Atkinson and Coleman. The standard technique of introducing potential functions to separate out the equations resulting from a Mode I problem is employed by the latter authors.

Having reformulated the Wiener-Hopf problem as a Riemann-Hilbert problem, and considering a general viscoelastic material subject to certain analytic conditions on the relaxation function, Walton (1982) obtained expressions for stress fields in the plane of the crack as well as the stress intensity factor. The technique rests on the mapping properties of a certain coefficient function which appears in the Riemann-Hilbert equation of the reformulated problem. His work includes an infinitesimal cohesive zone, and so there is scope for comparison with some of the material presented in this work, which incorporates a finite zone. Throughout this thesis, the Wiener-Hopf technique is used. There is little, if anything, to distinguish the two methods. The current work is computationally displacement intensive, in view of the fracture criterion chosen, and Walton acknowledges that very little can in general be done to rework a raw displacement formula (for a point on the crack line) into a useful form. When using the Wiener-Hopf technique for materials other than those with simple relaxation function forms, numerical factorisation is found to be necessary.

Similar techniques were used by Walton to solve the corresponding problem for a layer of general viscoelastic material (1985) and to derive an expression for the energy release rate (1988). Herrmann and Walton (1988) add an infinitesimal craze zone to Atkinson and List's 1972 transient model, and treat the problem using Walton's Riemann-Hilbert techniques. They found that the presence or absence of a failure zone affects the ERR (energy-release rate) con-

siderably, and they state that this has important implications as far as making stability inferences from a critical ERR criterion is concerned.

In this chapter, steady-state motion with uniform velocity V is studied, the crack faces being loaded with stresses travelling in tandem. Only antiplane strain (Mode III) is considered, and body forces are ignored. The Wiener-Hopf technique is used to solve for stress and displacement in the manner of Willis (1967b) which dealt with a parallel calculation for the standard linear solid. The loading is then specialised to a step function to enable a simpler formula (in terms of single integrals) for the displacement to be obtained. Plots of the work performed by the loading forces, per unit of crack extension (which is analogous to G as used by Freund and Hutchinson), vs V, crack velocity, are drawn, showing a similar U-shape to the $\frac{G}{G_{tip}^c}$ vs V curves of those authors. The behaviour at $V=0$ is consistent with the relation $K^2=2\mu G$, since, for the Maxwell liquid, $\mu\to 0$ as $t\to\infty$ (treating μ as a function of time) and K, the stress intensity factor, is finite.

2. Solution of the moving boundary problem by the Wiener-Hopf technique.

The constitutive equations for the Maxwell liquid (in shear) are

$$\mu\frac{\partial \dot{w}}{\partial x_i}=\dot{\sigma}_{i3}+\frac{\sigma_{i3}}{t_*},\quad i=1,2, \tag{2.1}$$

where $w=w(x_1,x_2,t)=u_3$ is the 3-component of displacement, σ_{i3}, $i=1,2$ are the two non-zero components of the stress tensor, μ is a shear modulus and t_* is the relaxation time.

Equation (2.1) can be written as

$$\sigma_{i3}=G_1 * de_{i3}=\int_{-\infty}^{t} G_1(t-t')de_{i3}(t'),\quad i=1,2, \tag{2.2}$$

where * denotes Riemann-Stieltjes convolution,

$$G_1(s)=2\mu e^{-\frac{s}{t_*}} \tag{2.3}$$

is the relaxation function, and

$$e_{i3}=\frac{1}{2}\frac{\partial w}{\partial x_i},\quad i=1,2, \tag{2.4}$$

are the only two non-zero (infinitesimal) strains.

Substituting (2.4) into (2.2) leads to

$$\sigma_{i3}=\frac{1}{2}\frac{\partial}{\partial x_i}(G_1 * dw),\quad i=1,2. \tag{2.5}$$

The only non-trivial equation of motion is

$$\sigma_{13,1}+\sigma_{23,2}=\rho\frac{\partial^2 w}{\partial t^2}, \tag{2.6}$$

where e.g. ,1 denotes differentiation with respect to x_1.

Substituting for stresses from (5), the following equation in w is obtained:

$$\frac{1}{2}\left(\frac{\partial^2}{\partial x_1^2}+\frac{\partial^2}{\partial x_2^2}\right)(G_1 * dw)=\rho\frac{\partial^2 w}{\partial t^2}. \tag{2.7}$$

Now consider the following moving boundary problem:

Solve equation (2.7) subject to

$$\sigma_{23}(x_1,0,t)=f(x_1-Vt),\quad x_1-Vt<0, \tag{2.8a}$$

$$w(x_1,0,t)=0,\quad x_1-Vt>0, \tag{2.8b}$$

$$\sigma_{ij}(x_1,x_2,t)\to 0 \text{ as } \sqrt{x_1^2+x_2^2}\to\infty. \tag{2.8c}$$

Equation (2.8a) describes the crack being driven by a following applied traction f. A solution with the following properties is desired:

$$w(x_1,x_2,t)=w(x,y)=w(x,-y), \tag{2.9}$$

where $x=x_1-Vt$, $y=x_2$. In view of the anti-symmetry with respect to y, we need consider only $y>0$.

Rewriting the boundary value problem in the new variables, the number of independent variables is reduced to two since $\frac{\partial}{\partial t}=-V\frac{\partial}{\partial x}$.

We thus require to solve

$$\frac{1}{2}\left(\frac{\partial^2}{\partial x^2}+\frac{\partial^2}{\partial y^2}\right)(G_1*dw)=\rho V^2\frac{\partial^2 w}{\partial x^2} \tag{2.10}$$

subject to

$$\sigma_{23}(x,0)=\frac{1}{2}\frac{\partial}{\partial y}(G_1*dw)=f(x),\quad x<0, \tag{2.11a}$$

$$w(x,0)=0,\quad x>0, \tag{2.11b}$$

$$\sigma_{ij}(x,y)\to 0 \text{ as } \sqrt{x^2+y^2}\to\infty, \tag{2.11c}$$

where now

$$G_1*dw=-\int_x^\infty G_1\left(\frac{x'-x}{V}\right)dw(x'). \tag{2.12}$$

As in Willis (1967b), assume that solutions satisfy

$$|w(x,y)|<M_1\ \forall x,y, \tag{2.13a}$$

$$\int_0^\infty|\sigma_{23}(x,0)|dx<M_2 \tag{2.13b}$$

for some $M_1, M_2\in\mathbf{R}$ and

$$\left.\begin{matrix}\sigma_{23}(x,0)\\ w(x,y)\end{matrix}\right\}=O(e^{-\kappa x}),\quad x\to+\infty \text{ for some } \kappa>0. \tag{2.13c}$$

Define

$$W_+(p,y)=\int_0^\infty e^{ipx}w(x,y)dx, \tag{2.14a}$$

$$W_-(p,y)=\int_{-\infty}^0 e^{ipx}w(x,y)dx, \tag{2.14b}$$

which are analytic for $\mathrm{Im}(p)>-\kappa$, $\mathrm{Im}(p)<0$ respectively, in view of (2.13c).

Fourier-transforming (2.10) and rearranging gives

$$\frac{d^2}{dy^2}\hat{w}(p,y)-\gamma_*^2\hat{w}(p,y)=0, \tag{2.15}$$

where

$$\hat{w}(p,y)=\int_{-\infty}^{\infty} e^{ipx}w(x,y)dx \tag{2.16}$$

is analytic for $-\kappa<\mathrm{Im}(p)<0$ and

$$\gamma_*^2=ap(p+i\frac{b}{a}), \tag{2.17}$$

where

$$a=1-\frac{V^2}{c^2}, \tag{2.18a}$$

$$b=\frac{V}{c^2 t_*} \tag{2.18b}$$

and

$$c=\sqrt{\frac{\mu}{\rho}}, \tag{2.18c}$$

where c is the shear wave speed.

(2.15) is a second order linear ordinary differential equation. Solving subject to the requirement that $\hat{w}(p,y)$ is bounded as $y\rightarrow\infty$ yields

$$\hat{w}(p,y)=A(p)e^{-\gamma_* y}. \tag{2.19}$$

Define

$$\Phi_+(p)=\int_0^{\infty} e^{ipx}\Phi(x)dx, \tag{2.20a}$$

where

$$\sigma_{23}(x,0)=\Phi(x),\ \ x>0, \tag{2.20b}$$

is unknown and

$$F_-(p)=\int_{-\infty}^{0} e^{ipx}f(x)dx. \tag{2.20c}$$

Then transforming the boundary conditions (2.11a,b) gives

$$-\frac{\mu ip}{\frac{1}{Vt_*}+ip}\gamma_*(p)A(p)=\Phi_+(p)+F_-(p), \tag{2.21a}$$

$$W_+(p,0)=0, \tag{2.21b}$$

$$W_-(p,0)=A(p). \tag{2.21c}$$

Equation (2.20a) is now solved by the Wiener-Hopf technique for $W_-(p,0)$ and $\Phi_+(p)$. First we solve for a load of the form

$$f(x)=g(\lambda)e^{-i\lambda x},\quad x<0, \tag{2.22}$$

and then generate the result for general f by superposition as the problem is linear. For this simple f,

$$F_-(p)=\frac{g(\lambda)}{i(p-\lambda)}. \tag{2.23}$$

The branch cuts chosen are $-\infty<\mathrm{Re}(p)<-\frac{b}{a}$ and $0<\mathrm{Re}(p)<\infty$. If the Wiener-Hopf equation is rewritten as

$$\frac{\mu ip}{\frac{1}{Vt_*}+ip}a^{1/2}p^{1/2}W_-(p,0)-\frac{g(\lambda)}{i(p-\lambda)(\lambda+i\frac{b}{a})^{1/2}}$$
$$=\frac{\Phi_+(p)}{(p+i\frac{b}{a})^{1/2}}+\frac{g(\lambda)}{i(p-\lambda)}\left\{\frac{1}{(p+i\frac{b}{a})^{1/2}}-\frac{1}{(\lambda+i\frac{b}{a})^{1/2}}\right\}, \tag{2.24}$$

the left (right) hand side is analytic for $\mathrm{Im}(p)<0$ ($>-\kappa$). By analytic continuation and Liouville's Theorem (using conditions (2.13a,b) to prove boundedness), both sides identically vanish.

This gives

$$W_-(p,0)=\frac{g(\lambda)(\frac{1}{Vt_*}+ip)}{\mu a^{1/2}p^{3/2}(p-\lambda)(\lambda+i\frac{b}{a})^{1/2}}, \tag{2.25}$$

$$\Phi_+(p)=\frac{ig(\lambda)}{p-\lambda}\left\{1-\left[\frac{p+i\frac{b}{a}}{\lambda+i\frac{b}{a}}\right]^{1/2}\right\}. \tag{2.26}$$

A general stress can be expressed in the form

$$f(x)=\frac{1}{2\pi}\int_{-\infty+i0}^{\infty+i0} e^{-i\lambda x}d\lambda \int_{-\infty}^{\infty} e^{i\lambda u}f(u)du. \qquad (2.27)$$

The inner integral plays the part of $g(\lambda)$ in the previous formulae, and inverting the transforms (using Erdelyi *et al*, 1954) yields $\sigma_{23}(x,0)$, $x>0$ and $w(-s,0)$, $s>0$.

After inverting the transforms and evaluating some integrals, the following formulae for stress and displacement are derived:

$$\frac{d}{ds}w(-s,0)=-\frac{1}{\pi\mu a^{1/2}}\left(\frac{1}{Vt_*}+\frac{d}{ds}\right)\int_{-\infty}^{0}f(u)du\int_{u}^{\xi}\frac{e^{\frac{b}{a}u'}du'}{(-u')^{1/2}(s+u-u')^{1/2}}, \quad s>0, \qquad (2.28a)$$

$$\xi=\min\{(s+u),0\} \qquad (2.28b)$$

and

$$\sigma_{23}(x,0)=\frac{e^{-\frac{b}{a}x}}{\pi x^{1/2}}\int_{-\infty}^{0}\frac{e^{\frac{b}{a}u}f(u)(-u)^{1/2}du}{u-x}, \quad x>0. \qquad (2.29)$$

Appendix 1 gives a sample of the techniques used to deal with the integrals in this chapter.

Inversion of equation (2.19) gives a formula involving the displacement at a general point:

$$\frac{d}{ds}w(-s,y)=-\frac{yb}{2\pi^2\mu a}\left(\frac{1}{Vt_*}+\frac{d}{ds}\right)\int_{-\infty}^{0}f(u)du\int_{u}^{0}\frac{e^{\frac{b}{a}u'}h(u-u'+s)du'}{(-u')^{1/2}} \qquad (2.30)$$

where

$$h(t)=\left[\frac{H(t)}{t^{1/2}}\right]*\left[\frac{e^{\frac{bt}{2a}}K_1\left(\frac{b}{2a}\sqrt{t^2+ay^2}\right)}{\sqrt{t^2+ay^2}}\right] \qquad (2.31)$$

and K_1 is a modified Bessel function of the second kind.

3. Asymptotic results.

Using a result relating the value of a function at ∞ to the value of its transform at 0 (Lighthill, 1958), it is possible to deduce asymptotic results for $w(x,y)$ as $x\to\pm\infty$.

As $x\to-\infty$,

$$w(x,y)\sim\frac{ki^{1/2}}{2\pi}\int_{-\infty-0i}^{\infty-0i}\frac{e^{-ipx-(ib)^{1/2}p^{1/2}y}dp}{p^{3/2}}, \tag{3.1}$$

where

$$k=\frac{1}{\mu b^{1/2}Vt_*}\int_{-\infty}^{0}\operatorname{erf}\left(\sqrt{\frac{b}{a}}(-u)^{1/2}\right)f(u)du. \tag{3.2}$$

Although no large parameter is now involved, the integral in (3.1) can be evaluated by the method of steepest descent and the use of the standard Laplace transform

$$\int_0^\infty\frac{e^{-pt}dt}{t^{1/2}(t+a)}=\pi a^{-1/2}e^{ap}\operatorname{erfc}\sqrt{ap} \tag{3.3}$$

where

$$\operatorname{erfc}(x)=\frac{2}{\sqrt{\pi}}\int_x^\infty e^{-u^2}du, \tag{3.4a}$$

$$\operatorname{erf}(x)+\operatorname{erfc}(x)=1. \tag{3.4b}$$

This yields the formula

$$w(x,y)\sim 2k(-x)^{1/2}e^{-2a^2}\{\sqrt{2}ae^{2a^2}\operatorname{erfc}\sqrt{2a^2}-\frac{1}{\pi^{1/2}}\}H(-x), \tag{3.5}$$

where now

$$a^2=\frac{y^2b}{8|x|}. \tag{3.6}$$

From this it can be shown that $w(x,y)\to0$ as $y\to\infty$. This latter fact can be shown independently by proving

$$\forall K>0,\ \exists\delta>0 \text{ s.t.} |w(x,y)|<\delta\ \forall |y|>K \text{ (for } x \text{ fixed)}. \tag{3.7}$$

This requires the displacement formulae (2.30,31) together with the asymptotic behaviour of K_1 for large values.

When $y=0$, formula (3.5) reduces to

$$w(x,0)\sim\frac{-2k}{\pi^{1/2}}(-x)^{1/2}H(-x) \text{ as } x\to-\infty, \tag{3.8}$$

the result obtained by taking the leading term in $W_-(p,0)$, i.e. the term proportional to $\frac{1}{p^{3/2}}$.

Since $w(x,y)\to0$ as $y\to\pm\infty$ for x fixed and as $x\to+\infty$ for y fixed, the value of the path-independent J-integral defined (for Mode III) by

$$J=\oint\left(W dx_2-\sigma_{23}\frac{\partial w}{\partial x_1}ds\right), \tag{3.9a}$$

where

$$W=\int\sigma_{ij}de_{ij}, \tag{3.9b}$$

could in principle be calculated solely on the values of stresses and displacements as $x\to\infty$, but this is not attempted here due to the complexity of the integrals involved. Equation (3.9a) defines a special case of the J-integral given by Willis (1975), whose more general formula includes heat flux.

4. Specialisation to step function loads.

The step function

$$f(x)=\begin{cases}-\sigma_0, & -d<x<0\\ F, & -(d+L)<x<-d\\ 0, & x<-(d+L)\end{cases} \tag{4.1}$$

provides for both a shearing stress along a length L of the crack from the crack tip $x=-d$ and a cohesive stress $-\sigma_0$ from the crack tip to the end of the cohesive zone at $x=0$. A relation between F and σ_0 is established by specifying

that the stress intensity factor for the crack tip at $x=0$ identically vanish:

$$\int_{-\infty}^{0} \frac{\exp(\frac{b}{a}u)f(u)du}{(-u)^{1/2}}=0. \tag{4.2}$$

This gives

$$\frac{F}{\sigma_0}=\frac{\text{erf}\sqrt{(\frac{b}{a}d)}}{\text{erf}\sqrt{(\frac{b}{a}(d+L))}-\text{erf}\sqrt{(\frac{b}{a}d)}}. \tag{4.3}$$

Evaluating (2.28a) in integrated form for the step function given by equation (4.1) leads to

$$w(-s,0)=\frac{\sigma_0}{\pi\mu a^{1/2}}\{A_1(s)+B_1(s)\} \tag{4.4}$$

where

$$\begin{aligned} A_1(s)=&-2\exp(-\frac{b}{a}d)H(s,d,1)(1+\frac{F}{\sigma_0}(d)) \\ &+2\exp(-\frac{b}{a}(d+L))H(s,d+L,1)\frac{F}{\sigma_0}(d), \end{aligned} \tag{4.5}$$

$$\begin{aligned} B_1(s)=&\frac{1}{Vt_*}\int_0^s A_1(s')ds' \\ =&\frac{1}{Vt_*}\{-\frac{4}{3}\exp(-\frac{b}{a}d)H(s,d,3)(1+\frac{F}{\sigma_0}(d)) \\ &+\frac{4}{3}\exp(-\frac{b}{a}(d+L))H(s,d+L,3)\frac{F}{\sigma_0}(d)\} \end{aligned} \tag{4.6}$$

and $H(s,x,\alpha)$ is defined as

$$\int_0^{\min\{x,s\}} \exp(\frac{b}{a}v)\frac{(s-v)^{\frac{\alpha}{2}}}{(x-v)^{1/2}}dv. \tag{4.7}$$

Formula (4.4) was checked by taking elastic ($t_* \to \infty$) and static ($\rho \to 0$) limits and these were in agreement with known results.

5. Computations

Figure 2.1 shows $w(-d,0)=\frac{1}{2}COD$, considered as a function of Dugdale zone length d and velocity V (the term COD is an abbreviation for crack opening displacement, widely used in fracture mechanics; it is used here by analogy even although the crack shears rather than opens). A family of $w(-d,0;V)$ vs V curves was plotted for various values of d, the other values being $L=8, c=t_*=\mu=\sigma_0=1$. At fixed V, COD is a monotone increasing function of d. For fixed d, the increasing behaviour of the curves as $V\to c$ is similar to that of the corresponding linear elastic curves, the difference being in what happens as $V\to 0$. In the elastic case, the curve tends to a finite static value as $V\to 0$, and is monotone increasing on the interval $(0,c)$. In contrast, a Maxwell liquid can creep indefinitely, leading to a large COD when V is small.

Using the fracture criterion COD=δ (δ constant), the equation $w(-d,0)=\frac{\delta}{2}$ was solved numerically (using bisection) for each V, yielding a value of d. The corresponding values of $K=K(d,V)$, nominal stress intensity factor, are plotted in Figure 2.2 for various σ_0,δ pairs such that $\sigma_0\delta=2\gamma$, where γ is the surface energy per unit width. It may be noted that

$$2\int_{-d}^{0} -\sigma_0 \dot{w}\,dx = 2\sigma_0 V\int_{-d}^{0}\frac{\partial w}{\partial x}\,dx = 2\sigma_0 V[w(0)-w(-d)] = -\sigma_0\delta V \qquad (5.1)$$

so $\sigma_0\delta$ represents the energy dissipated in the Dugdale zone per unit of crack extension. K is defined by $K=2\sqrt{\frac{2}{\pi}}F\sqrt{L}$. Figure 2.2 was generated for the values $\alpha=0.125$ and $\mu=1$, where α is a dimensionless parameter defined by $\alpha=\frac{ct_*}{L}$. All the curves tend to the origin, except in the limit $\sigma_0\to\infty$ with $\sigma_0\delta=2\gamma$. The monotone increasing nature of the K vs V graphs implies that

crack motion is stable at all speeds $V\in(0,c)$ for the particular value of α chosen. Increasing α makes the material more elastic, and a decreasing section appears in each of the K vs V curves in an ever larger interval strictly contained in $(0,c)$: this behaviour is exhibited in Figure 2.5.

The total work done by the applied loading is

$$2\int_{-(d+L)}^{-d} F\dot{w}dx=2FV[w(-(d+L))-w(-d)]. \qquad (5.2)$$

The corresponding total work done by the applied loading, per unit of crack extension, $2F[w(-(d+L))-w(-d)]$ is plotted against V in Figure 2.3, again for various σ_0,δ such that $\sigma_0\delta=2\gamma$ and $\alpha=0.125,\mu=1$. This total work per unit of extension corresponds to the total rate of energy absorption, both by viscoelastic dissipation in the bulk of the material and by absorption of energy in the craze zone, and is analogous to the overall energy release-rate in the sense used by Freund and Hutchinson (1985). The latter quantity, $\sigma_0\delta=2\gamma$, is also plotted in Figure 2.3, and is seen to represent only a small fraction of the total energy absorbed. Stored energy does not enter into the energy balance as it is constant, this being a steady-state problem. Walton (1987) defined the energy release rate G as the work done by cohesive forces: thus in Walton's terminology, $G=\sigma_0\delta$ for the present model.

As σ_0 increases, the curves converge to what we choose to call the Griffith limit, in which the cohesive zone shrinks to a point but nevertheless a finite amount of energy, 2γ per unit of crack extension is absorbed there. This can be viewed either as plastic dissipation or, alternatively, the cohesive stress σ_0 can be regarded as resisting the breaking of bonds and hence giving rise to a specific surface energy γ. The curves demonstrate that a finite yielding zone

(with σ_0 small) induces more dissipation throughout the material than does the Griffith limit, except for small V. As σ_0 increases, the domain of the stable branch of the curves ($V>V_{min}$, the velocity where the minimum is attained) is reduced. However, Figure 2.2 suggested that crack motion is stable for all velocities (with small α) with the dead loading that we have been using. A precise stability comparison with Freund and Hutchinson's work is made difficult by the differences in loading, and the nonlinearity which is present in that model.

In Figure 2.4, having fixed $\sigma_0=100$ and $\delta=0.01$, t_* is varied to demonstrate the decrease in viscous dissipation (en route from the loading zone to the plastic zone) with increasing t_* (as $t_* \to \infty$, the constitutive equation tends to

$$\sigma_{i3}=2\mu e_{i3}, \tag{5.3}$$

which is the case of linear elasticity, where there is no viscous dissipation).

Walton's work also includes a finite cohesive zone, but considers exponential forms for both the applied loading and the cohesive stresses. Unlike the current model, the zones of application for the two types of loading are not disjoint, and the assumption is made that $\varepsilon=\frac{a_f}{a_e} \ll 1$ where a_f, a_e are length scales associated with the cohesive stresses and applied loads respectively. An expression is derived for the energy release rate, and this is mainly studied as a function of crack speed for the cases of a standard linear solid and power law material, when $\varepsilon \ll 1$. Walton chooses to base stability inferences on the energy release rate. This leads, in general, to different conclusions than those based on the shape of K vs V curves. However it can be demonstrated relatively easily that these two different bases for deciding stability are equivalent in certain circumstances. The parameter analogous to α in the present work would be

$\varepsilon=\frac{d}{L}$. Of course a strict stability analysis must depend explicitly on the precise loading conditions and should also allow for non-steady motion. A limited case is taken up in chapter 5. The work of the present chapter is less general than that of Walton in that it concentrates on a Maxwell liquid but the case of finite σ_0 and δ (and hence d) is considered so that deviations from the limit $\varepsilon \ll 1$ are shown explicitly.

Figure 2.5 shows a series of nominal stress intensity factor vs V plots for varying values of α ($\sigma_0=10, \delta=1, \mu=1$): these are computed for choices of α slightly above the transition value where these particular curves lose their monotone increasing nature (as exhibited in Figure 2.2 for $\alpha=0.125$). As α is progressively increased, the curves take on a predominantly monotone decreasing appearance (except at either end of the interval). In the elastic limit, the graph would be decreasing on the entire interval, so transitional behaviour of the sort observed in Figure 2.5 is consistent with the limiting case and the behaviour in Figure 2.2.

Figure 2.1:
COD variation

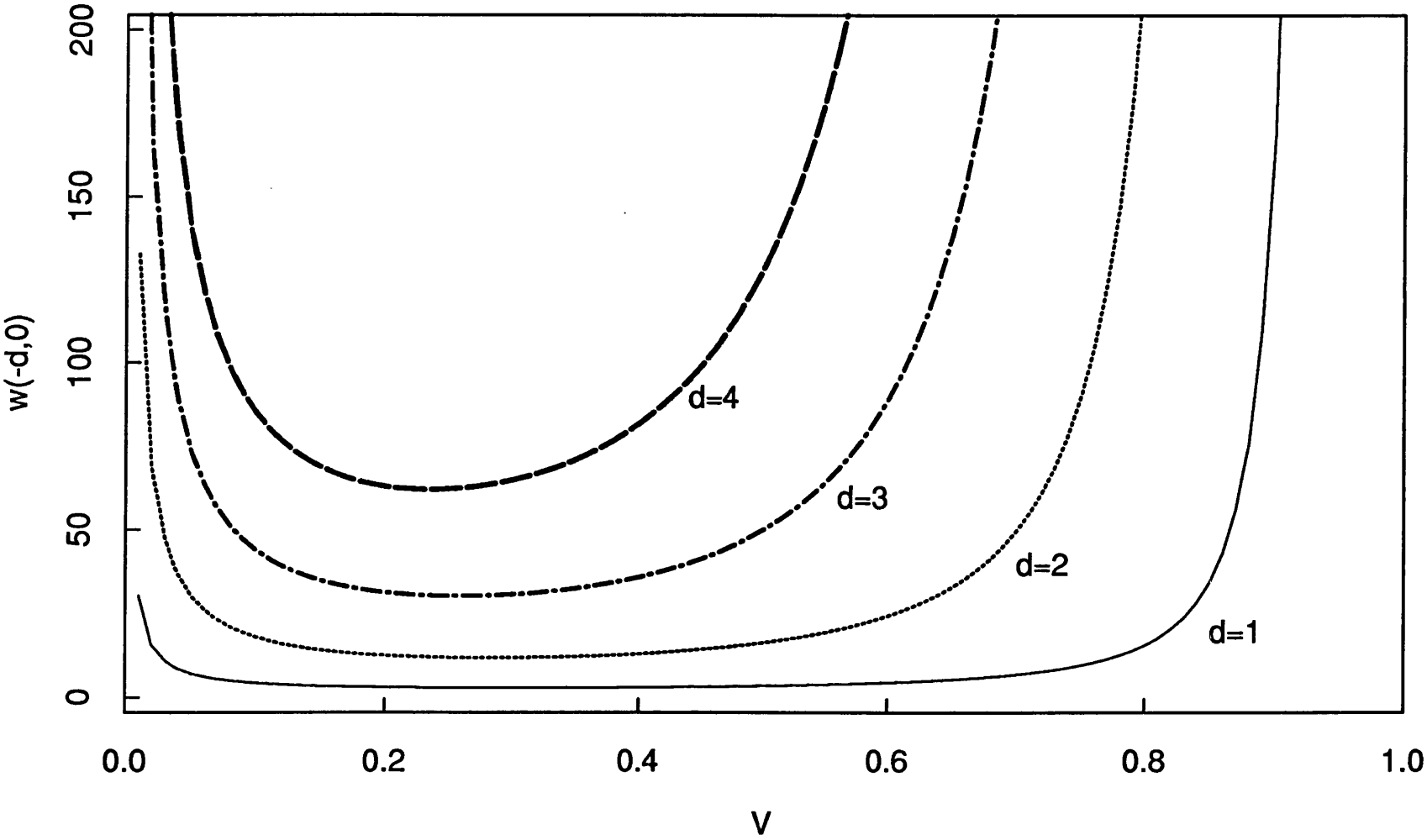

Figure 2.2: craze zone varies

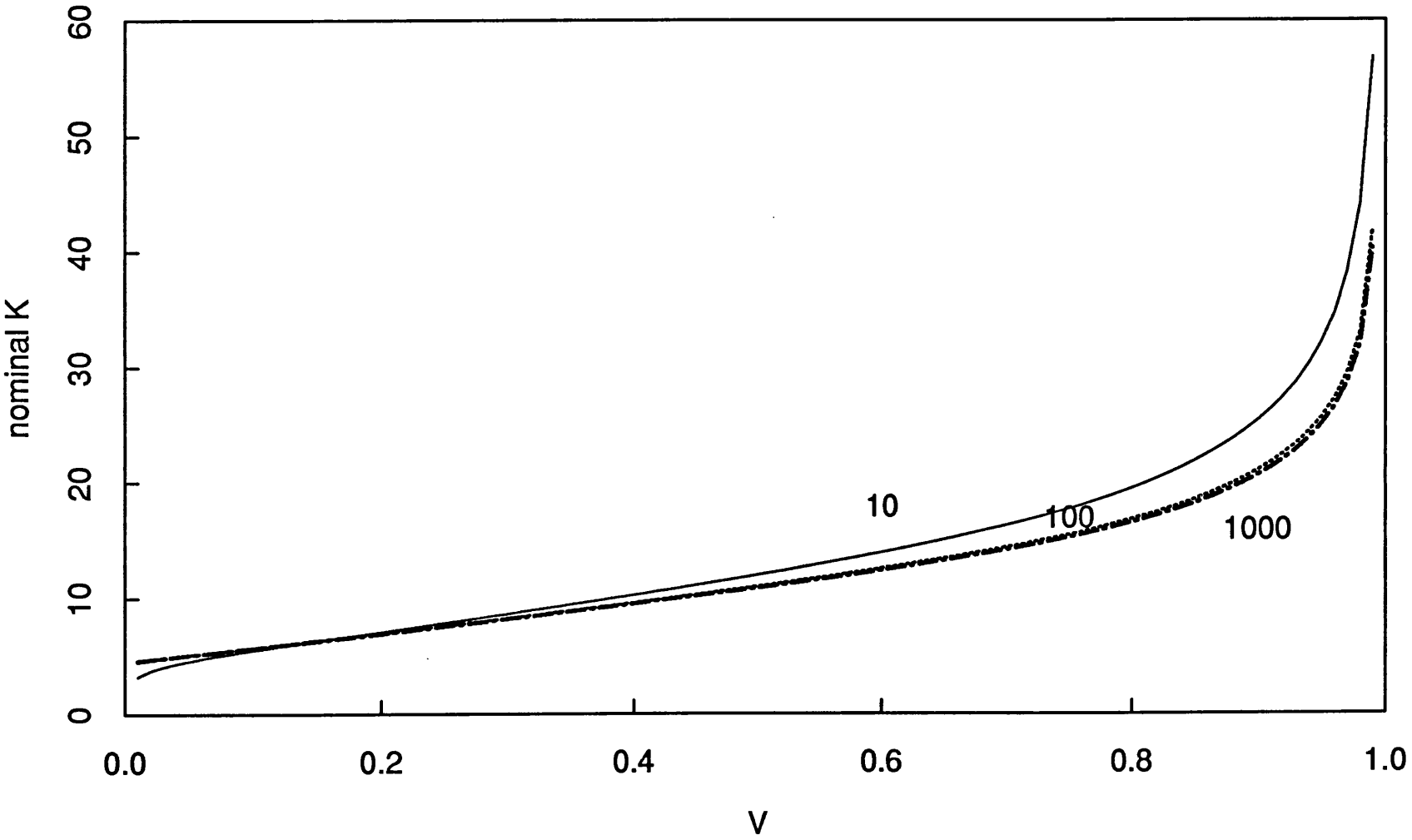

Figure 2.3:
craze zone varies

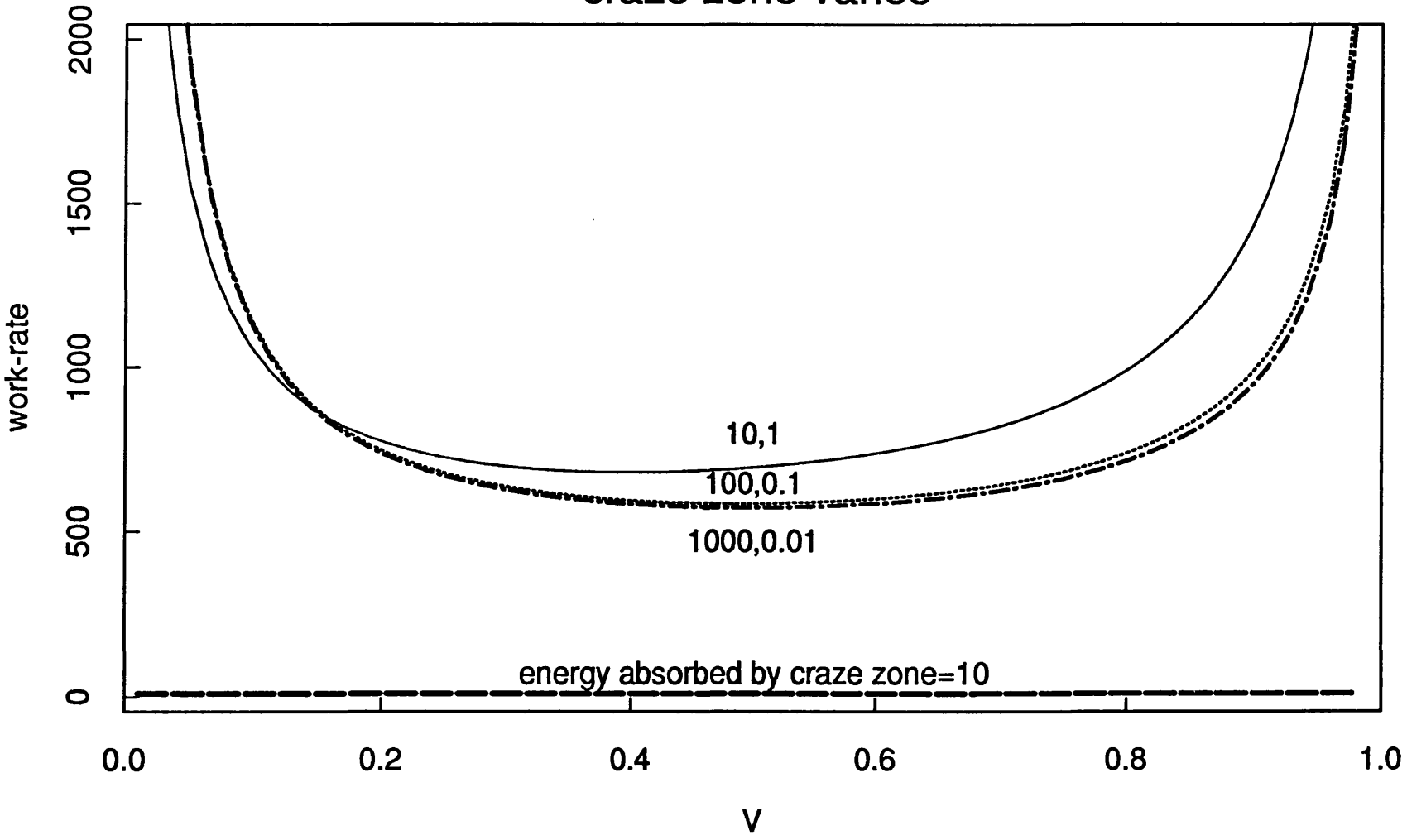

Figure 2.4:
relaxation time varies

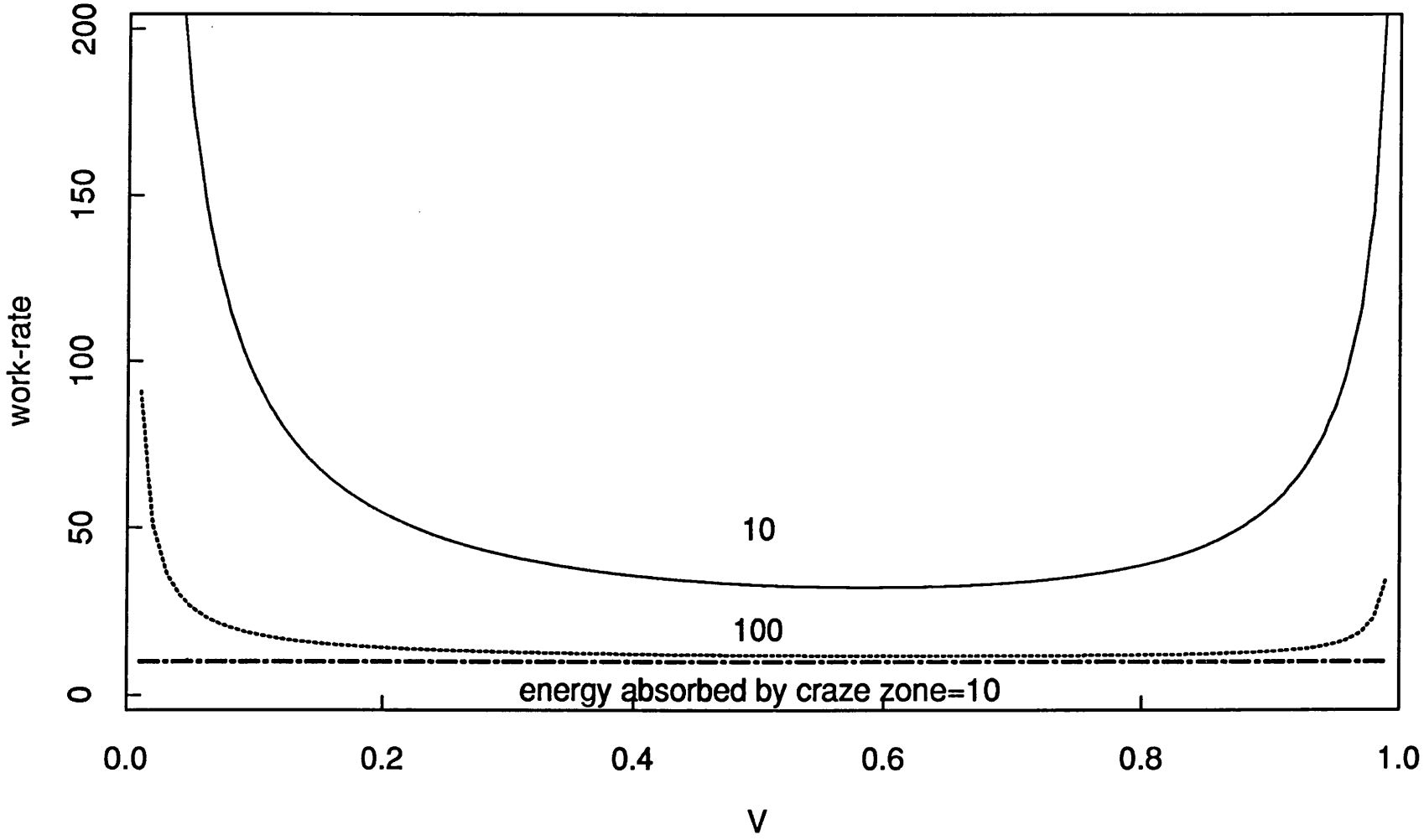

Figure 2.5:
alpha varies

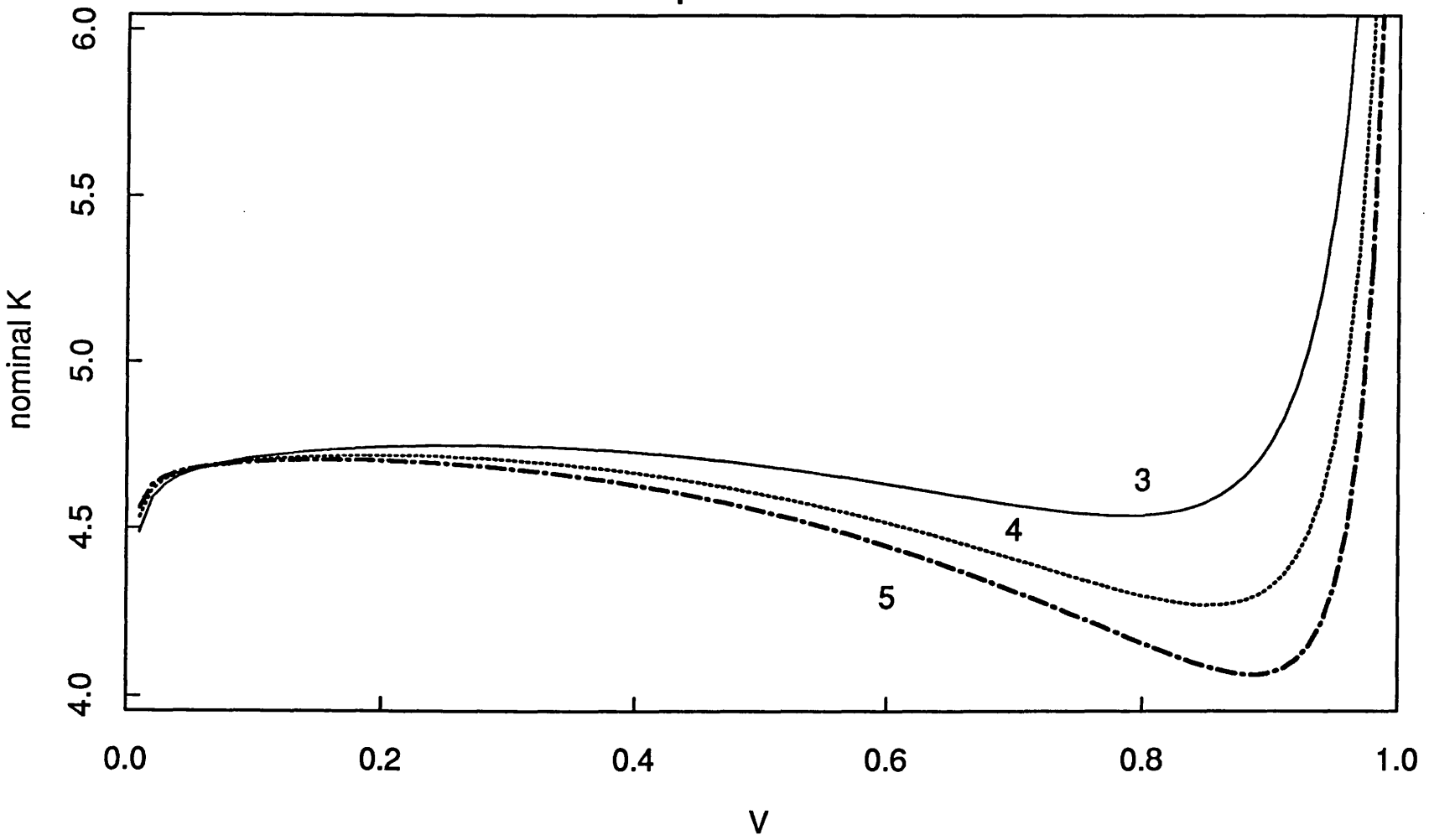

Chapter 3: Quasi-static crack growth in viscoelastic materials.

1. Introduction

This chapter considers the conditions under which non-uniform crack growth in a viscoelastic medium, in the absence of inertia, is possible. The primary material model considered is the standard linear solid, but certain aspects of behaviour can be analysed more explicitly for the cases of the Maxwell liquid and, to a lesser extent, the Voigt solid. Attention is focused on the semi-infinite geometry and the analysis is restricted to the case of antiplane strain (Mode III).

The displacement fields on which the subsequent numerical solution of the crack motion problems is based are derived from the corresponding elastic fields by means of an extended correspondence principle (Graham, 1968). A strip of cohesive forces, of the type introduced into elastoplastic fracture by Dugdale (1960) and Bilby, Cottrell and Swinden (1963) to simulate a craze zone, is incorporated into the model. It is therefore appropriate to employ a constant crack opening displacement (COD) fracture criterion to fix the path of the crack tip in (x,t) space. On differentiation, the character of the controlling equation for crack tip position as a function of time is found to be integro-differential with history, and this necessitates use of a combination of numerical techniques in order to obtain a solution.

The literature contains a large number of papers on quasi-static fracture of viscoelastic materials, certainly in comparison to the number of dynamic counterparts. In 1973, Knauss published a comprehensive review article entitled "The Mechanics of Polymer Fracture" which summarises the known work at that time in this particular subject area, and includes many papers which treat

aspects of the subject from a materials science perspective. At that time, most analytic work on cracks in viscoelastic materials excluded inertial considerations. In keeping with the nature of this thesis, attention will be restricted to a sample of those papers which include an analytic stress derivation.

Williams (1965), using an energy balance (Griffith) approach, investigated the initiation and subsequent growth of a spherical cavity in a viscoelastic material: although this is not failure of crack type as considered throughout this thesis, it does bring out the influence of viscoelasticity in the process (the inclusion of inertia considerations proves difficult). The paper by Kostrov and Nikitin (1970) is considerable in scope, dealing with many aspects of quasi-static fracture, including in particular extensive sections on the Griffith criterion. The important point is made that not all possible fracture criteria lead to the same result, and the effects of what is usually called the Dugdale (or Barenblatt) model are investigated. For this latter case, a relationship between fracture initiation time and the level of loading is derived. This is explicitly carried out for the standard linear solid later in this chapter. A large, book-style article by Knauss (1972) is similar in style of presentation to the last paper: it is extensively discursive in nature, and, in view of its author, gives a mixed perspective on the subject, taking into account experimental work. Wnuk and Knauss (1970) employ a penny-shaped crack geometry, modelling the adjacent crazing by Crochet's viscoplasticity theory: expressions are derived for the fracture initiation time for time-dependent and time-independent plasticity. Knauss and Dietmann use an energy balance (thermodynamic power) equation to obtain a nonlinear differential equation relating the speed of the crack tip to a near tip stress intensity factor history: it is proves possible to simplify this equation to a

more amenable form in certain circumstances. Mueller and Knauss (1971) consider crack propagation in an infinite linearly viscoelastic strip: as tends to be the case with papers of this vintage, an energy balance equation is set up, and comparisons are made with experimental data using Solithane 113.

A decade later, Nikitin (1984) used a thermo-mechanical quasi-static approach and a Griffith type criterion to investigate fracture in linear viscoelastic materials. The crack is deemed to be stable for one of the loading types considered and unstable for the other. Nikitin finds that, in the terminology used in this thesis, that, in the case of the unstable crack, the fracture initiation time for a certain range of loading is finite and strictly positive, whereas, for the stable case, the crack progresses in a jumplike manner. This latter phenomenon does not correspond to anything observed in the course of the current work: this is possibly due to a combination of the chosen loadings and the presence of finite craze zones.

Recently, the study of craze mechanics to a certain extent divorced from cracks has gained in prominence. Walton and Weitsman (1984) presented techiques, both analytical and numerical, to determine stress and displacement fields in an infinite elastic body due to a craze zone modelled as a distributed spring. This more detailed representation than the Dugdale zone is a feasible proposition because complicating features such as cracks are absent. Passaglia (1982) addresses the problem of how the viscoelastic nature of the craze material influences the rate of craze extension, in the presence of a crack and in a viscoelastic material. The Dugdale model used throughout this thesis is so basic as to be inadequate for these purposes: it is one-dimensional so the concept of a constitutive description does not apply. The size of the craze zone

based on small-scale yielding is recoverable from Passaglia's work. In this and the subsequent chapter, the length of any craze zone present is assumed to be constant. Passaglia does not base his inferences on the crack opening displacement fracture criterion, but on stress intensity factor considerations.

There are two main general theories on quasi-static crack growth in a linearly viscoelastic material which include an infinitesimal craze zone, namely those of Knauss (1970) and Schapery (1975). Knauss' paper deals with what is basically a Griffith problem (understood to be one involving a crack with a Griffith fracture criterion - energy flux into the crack tip region is constant) with the addition of a length α over which cohesive forces act, and is backed up by experimental data for the polymer Solithane. The material presented in this chapter is for finite as well as small α, and is consistent with Knauss in predicting that crack motion is slow in the latter case. Knauss gives limit theorems on crack behaviour in various loading ranges for a general viscoelastic material: this chapter includes not only explicit realisations of these for the standard linear solid but also, in the final section, a sketch proof of a result of this type.

In a series of papers beginning in 1975, Schapery develops a general theory of crack initiation and growth in viscoelastic materials, using a failure zone adjacent to the crack tip and a local energy fracture criterion. Like Knauss, Schapery considers large cohesive stresses over a small length, but in this case the analysis is asymptotically rigorous. Graham's extended correspondence principle (1968) is used to arrive at the displacement, and finite stresses at the crack tip are specified. Since the log-log plot of creep-compliance can be linearised for most materials without the loss of too much accuracy, Schapery's theory covers a large number of materials. In Part II (1975), approximate

expressions are derived for crack tip velocity and fracture initiation time. Part III (1975) compares experimental results with theoretical ones, as well as considering the effects of nonlinear behaviour at the crack tip. Schapery (1978) makes predictions relating to crack growth in nonhomogeneous viscoelastic materials, again with a failure zone present. More recently, Schapery (1984), using certain correspondence principles and "a generalised J-integral", investigates similar problems, now taking into account the complications of nonlinearity and improved material modelling near the crack tip region, where heavy degradation has taken place.

2.Analysis of semi-infinite crack geometry

In shear the standard linear solid has constitutive equation

$$\dot{\sigma}+\frac{(1+f)}{\tau}\sigma=2\mu_c(\dot{e}+\frac{e}{\tau}), \tag{2.1}$$

where σ, e, μ_c, τ and f represent, respectively, stress, strain, a shear modulus, a relaxation time and a real positive parameter.

The relaxation function corresponding to antiplane strain is

$$G_1(t)=\frac{2\mu_c}{1+f}(1+f\exp(-\frac{1+f}{\tau}t)). \tag{2.2}$$

It can be deduced from (2.1) that

$$\frac{\partial w}{\partial x}=\mu^{-1}*\sigma_{13} \tag{2.3}$$

where the symbol * denotes the operation of convolution and

$$\mu^{-1}=\frac{1}{\mu_c}(\delta(t)+\frac{f}{\tau}\exp(-\frac{t}{\tau})H(t)). \tag{2.4}$$

Here and throughout the chapter generalised functions are employed. The problem to be solved is one of non-steady motion of a semi-infinite crack without inertia in an infinite standard linear solid, driven by tractions on the

crack faces. In particular, the case of a constant load over a fixed length of crack, next to a zone of cohesive forces representing crazing, both travelling behind the crack tip, is considered.

First the corresponding solution for the elastic problem is used, in which the operator μ^{-1} is replaced by $\frac{1}{\mu_c}$, where μ_c designates an ordinary elastic shear modulus. The same elastic stresses solve the viscoelastic problem defined above - these are derived in Appendix 2. Equation (2.3) is used to get the following formula for the displacement derivative with respect to x on the crack line, the technique being justified by Graham's extended correspondence principle (1968):

$$\frac{\partial w}{\partial x}(x+0i,t)=\frac{1}{2i}\int_{t_1(x)}^{t}\frac{1}{\mu}(\delta(t-t')+\frac{f}{\tau}\exp(-\frac{t-t'}{\tau})H(t-t'))dt'$$
$$\cdot\frac{2}{\pi i}(x_1(t')-x)^{-\frac{1}{2}}\int_{-\infty}^{x_1(t')}\frac{(x_1(t')-x')^{\frac{1}{2}}g_1(x',t')dx'}{x'-x} \qquad (2.5)$$

where, in the notation of Figure 3.1,

$x_1(t_1(x))=x$,

$x_1(t')$ denotes the crack tip position at time=t'

$\sigma_{23}=g_1(x',t')$ is the loading at position x' and time t' in the general case

and the inner integral is to be interpreted as a Cauchy principal value.

In (2.5) and from now on in this chapter, the subscript is dropped from μ_c.

The three preconditions given by Graham for application of the extended correspondence principle are satisfied here. As they relate to this problem, they are: 1. Displacement, w, is zero for $x>x_1(t)$. 2. x_1 is a monotone increasing function of t. 3. In the corresponding elastic problem, the boundary condition

corresponding to $x<x_1(t)$ has the elastic constants separated in a multiplicative factor.

Integration with respect to x and some simplification yields:

$$w(x_0(t)+0i,t)=\frac{1}{\pi\mu}\Big[\int_{x_0(t)}^{x_1(t)}(x_1(t)-x)^{-\frac{1}{2}}dx\int_{-\infty}^{x_1(t)}\frac{(x_1(t)-x')^{\frac{1}{2}}g_1(x',t)dx'}{x'-x}$$

$$+\frac{f}{\tau}\exp(-\frac{t}{\tau})$$

$$\int_{x_0(t)}^{x_1(t)}dx\int_0^t\exp(\frac{t'}{\tau})(x_1(t')-x)^{-\frac{1}{2}}H(x_1(t')-x)dt'\int_{-\infty}^{x_1(t')}\frac{(x_1(t')-x)^{\frac{1}{2}}g_1(x',t')dx'}{x'-x}\Big]. \tag{2.6}$$

We specialise to travelling step function loading:

$$g_1(x,t)=\begin{cases}F.H(t), & x_0(t)-L<x<x_0(t),\\ -\sigma_0.H(t), & x_0(t)<x<x_1(t)=x_0(t)+d,\end{cases} \tag{2.7}$$

where d and L are the craze and loading zone lengths respectively. F and σ_0 are related by the condition of zero stress concentration at $x_1(t)$.

Define

$$g(s)=2\sigma_0\Big[\frac{\sqrt{d}}{\sqrt{d+L}-\sqrt{d}}(s+L)\ln\Big|\frac{\sqrt{s+L}}{\sqrt{d+L}+\sqrt{d-s}}\Big|$$
$$-\Big(\frac{\sqrt{d+L}}{\sqrt{d+L}-\sqrt{d}}\Big)s\ln\Big|\frac{\sqrt{s}}{\sqrt{d}+\sqrt{d-s}}\Big|\Big]H(d-s). \tag{2.8}$$

Then

$$w(x_0(t)+0i,t)=\frac{1}{\pi\mu}[g(0)+\frac{f}{\tau}\exp(-\frac{t}{\tau})\int_0^t\exp(\frac{t'}{\tau})g(x_0(t)-x_0(t'))dt']. \tag{2.9}$$

Since it can be shown that g is a negative function, we require to solve the equation

$$-\frac{\delta}{2}=w(x_0(t)+0i,t), \tag{2.10}$$

where $\delta>0$. This equation represents $COD=COD_{crit}$, where $COD_{crit}=\delta$.

If the applied loading F is too small, it is demonstrated below that (2.10) may never be satisfied, even as $t\to\infty$, and the crack will remain stationary. On the other hand if F is sufficiently large, $|w(x_0(t)+0i,t)|$ may exceed $\frac{\delta}{2}$ for all $t>0$, implying the need to allow for inertia from the beginning. This current analysis only applies in an intermediate F range, in which (2.10) first becomes satisfied at some finite time. Accordingly define crack initiation time, t_0, by

$$x_0(t)=0, t\le t_0. \tag{2.11}$$

For $t\ge t_0$, (2.10) simplifies to

$$\tau(\exp(\frac{t_0}{\tau})-1)g(x_0(t))+\int_{t_0}^{t}\exp(\frac{t'}{\tau})g(x_0(t)-x_0(t'))dt'$$
$$=\frac{\tau}{f}(-\frac{\delta\pi\mu}{2}-g(0))\exp(\frac{t}{\tau}). \tag{2.12}$$

Putting $t=t_0$ in (2.12) and solving for t_0 yields

$$t_0=\tau\ln|\frac{g(0)}{g(0)+\frac{1}{f}(\frac{\delta\pi\mu}{2}+g(0))}|. \tag{2.13}$$

The requirement of a finite positive initiation time dictates that the following inequality must be satisfied:

$$-\frac{\delta\pi\mu}{2}<g(0)<-\frac{\delta\pi\mu}{2(1+f)}. \tag{2.14}$$

This can be rewritten in terms of loading constants as

$$\frac{\delta\pi\mu}{2(1+f)}<FL\ln(1+2\frac{F}{\sigma_0})<\frac{\delta\pi\mu}{2}. \tag{2.15}$$

Therefore $\exists F_1, F_2\in\mathbf{R}$ such that (2.14) becomes

$$F_1<F<F_2 \tag{2.16}$$

i.e. the postulated crack motion is only possible in a certain range of crack

loading forces.

By putting $x_0(t) \sim A+Vt$, where A is a constant, into (2.10), the following implicit formula for terminal velocity V can be obtained:

$$\frac{1}{\pi\mu}[g(0)+\frac{f}{\tau V}\int_0^d \exp(-\frac{s}{\tau V})g(s)ds]=-\frac{\delta}{2}. \qquad (2.17)$$

This can be solved numerically, e.g. by bisection, to provide an independent check on the terminal velocity as computed by the algorithm described in section 3.

3.Details of numerical algorithm

This section describes a predictor-corrector method for solving equation (2.10) at the times $t_0+ih, i=1,2,\ldots$ where h is a time step. It is based on the Newton-Raphson method for solving nonlinear equations iteratively, together with the trapezoidal rule for approximating integrals. Initially, the crack tip is at $x=0$.

Considering equation (2.12) when $t=t_1=t+h$, replacing the integral by a single trapezium gives

$$\begin{aligned}&\tau(1-\exp(-\frac{t_0}{\tau}))g(x_1)+\frac{h}{2}(g(x_1)+\exp(\frac{h}{\tau})g(0))\\&=\frac{\tau}{f}(-\frac{\delta\pi\mu}{2}-g(0))\exp(\frac{h}{\tau})\end{aligned} \qquad (3.1)$$

where $x_1=x_0(t_0+h)$.

Rearranging for $g(x_1)$:

$$g(x_1)=c_1(h)g(0) \qquad (3.2)$$

where

$$c_1(h)=\frac{\tau(1-\exp(-\frac{t_0}{\tau}))-\frac{h}{2}}{\tau(1-\exp(-\frac{t_0}{\tau}))+\frac{h}{2}}\exp(\frac{h}{\tau}). \qquad (3.3)$$

It can be verified that $\exists l_1 \in \mathbf{R}^+$ such that for all $h \in [0, l_1]$,

$$0 \leq c_1(h) \leq 1. \tag{3.4}$$

It is therefore possible to solve (3.2) for x_1, provided h is small enough, using the additional information that g is monotone increasing and negative on the interval $[0,d]$. Having discovered the solution at the initial step, it is now possible to proceed using the main algorithm.

Using Newton-Raphson, equation (2.12) is rewritten as

$$\begin{aligned}
&\tau(\exp(\frac{t_0}{\tau})-1)[g(x_0^*(t))+(x_0(t)-x_0^*(t))g'(x_0^*(t))] \\
&+\int_{t_0}^{t}\exp(\frac{t'}{\tau})g(x_0^*(t)-x_0(t'))dt' \\
&+(x_0(t)-x_0^*(t))\int_{t_0}^{t}\exp(\frac{t'}{\tau})g'(x_0^*(t)-x_0(t'))dt' \\
&=\frac{\tau}{f}(-\frac{\delta\pi\mu}{2}-g(0))\exp(\frac{t}{\tau})
\end{aligned} \tag{3.5}$$

where $x_0^*(t)$ is a predictor of the true value $x_0(t)$ (in this case it will be taken to be the linear extrapolant of the last two actual values).

Rearranging (3.5) gives

$$x_0(t)=x_0^*(t)-\frac{c_u(t)}{c_l(t)}, \tag{3.6}$$

where $c_u(t)$, $c_l(t)$ are respectively defined by

$$\begin{aligned}
c_u(t)&=\frac{\tau}{f}(\frac{\delta\pi\mu}{2}+g(0))\exp(\frac{t}{\tau})+\tau(\exp(\frac{t_0}{\tau})-1)g(x_0^*(t)) \\
&+\int_{t_0}^{t}\exp(\frac{t'}{\tau})g(x_0^*(t)-x_0(t'))dt',
\end{aligned} \tag{3.7}$$

$$c_l(t)=\tau(\exp(\frac{t_0}{\tau})-1)g'(x_0^*(t))+\int_{t_0}^{t}\exp(\frac{t'}{\tau})g'(x_0^*(t)-x_0(t'))dt'. \tag{3.8}$$

Equation (3.6), with the integrals replaced by their trapezoidal approximations based on the mesh points t_0+ih, $i=0,1,2,\ldots$ is used to compute Figure 3.2,

which shows acceleration for a finite time after initiation, after which the motion assumes a steady state. The $x_0(t)$ which appears on the right hand side of (3.6) is replaced by $x_0^*(t)$. One portion of the integral in (3.8) is treated separately to avoid a singularity in g': the argument is assumed linear on $[t-h,t]$ and a change of variable is made which enables that part to be evaluated explicitly. The plot of Figure 3.2 is nominally for the values

$$F=0.4316624;\tau=f=1;\mu=2;L=10;\delta=0.5;\sigma_0=2;h=5e-6.$$

These can be interpreted physically if time is measured in units of τ, the relaxation time, and lengths are measured in units of a macroscopic length L_1, except that displacement w is measured in units of critical crack opening displacement, δ, so that strains are effectively scaled to $\frac{\delta}{L_1}$. Then, if the stresses (including σ_0) are measured in units of σ_1 and μ is taken as as an arbitrary multiple of σ_1 or, equivalently, of σ_0, the above values yield

$$\frac{F}{\sigma_0}=0.2158312$$

$$\frac{\mu}{\sigma_0}=K$$

$$\frac{\delta}{L_1}=\frac{1}{2K}$$

$$\frac{L}{L_1}=10$$

so that $L=20K\delta$.

4.Other materials

Similar analysis has been carried out for the Maxwell liquid and Voigt solid. The mathematics involved is comparable and the resulting graphs similar in character, but the simplicity of the Maxwell liquid allows an explicit formula for terminal velocity to be obtained.

In antiplane strain the Maxwell liquid has relaxation function

$$G_1(t)=2\mu\exp(-\frac{t}{t_*}), \tag{4.1}$$

where μ is a shear modulus and t_* a relaxation time.

The corresponding formula for terminal velocity is

$$V=\frac{L[g(0)+2\sigma_0 d\frac{\sqrt{d+L}}{\sqrt{d+L}-\sqrt{d}}]}{2t_*[\frac{\pi\mu\delta}{2}+g(0)]}, \tag{4.2}$$

where $F,L,g(0)$ are related by

$$\frac{F}{\sigma_0}=\frac{\sqrt{d}}{\sqrt{d+L}-\sqrt{d}} \tag{4.3}$$

and

$$g(0)=-FL\ln|1+2\frac{F}{\sigma_0}|. \tag{4.4}$$

Taking a Griffith limit of (4.2) i.e. letting $\sigma_0\to\infty$ subject to $\sigma_0\delta=2\gamma$, constant surface energy, yields a zero limit for the terminal velocity V, leading to the conclusion that quasi-static crack motion is not possible without a finite craze zone. This is illustrated in Figure 3.3, where terminal velocity is plotted against F for various σ_0,δ pairs such that $\sigma_0\delta=1$, and for $\mu=10,t_*=1,L=10$. A similar result can be proved for the standard linear solid case, starting from equation (2.17). While the Maxwell liquid has a finite positive initiation time for $F<F^{ml}_{crit}$, this is true for the Voigt solid in the case $F>F^{v}_{crit}$, where $F^{ml}_{crit},F^{v}_{crit}\in\mathbf{R}$ and are dependent on geometrical, loading and constitutive parameters. In the case of the Maxwell liquid, quasi-static crack motion is not possible when F is too large and inertia terms must come into the analysis. In contrast, for the Voigt solid, the crack will remain stationary if F is too small.

5. The fracture initiation time for a general constitutive relation.

For completely general time-dependent loading $g_1(x,t)$ and relaxation operator μ, application of the fracture criterion

$$w(x_0(t)+0i,t)=\frac{\delta}{2} \tag{5.1}$$

at $t=t_0$ gives

$$\frac{\delta}{2}=\frac{1}{\pi}\int_0^d (d-x)^{-\frac{1}{2}}dx\int_0^{t_0}\mu^{-1}(t_0-t')dt'\int_{-\infty}^{0}\frac{(-x')^{\frac{1}{2}}g_1(x',\,t')dx'}{x'-x}. \tag{5.2}$$

Assume, without loss of generality, that g_1 has been amended if necessary so that $\delta>0$. Unfortunately not much progress can be made in deriving information about t_0 unless the loading is time-independent i.e. $g_1=g_1(x)$. In particular, the loading represented by equation (2.7) falls into two parts, the first an integral of creep compliance and the second a function of the loading stresses. Only the first of these involves t_0:

$$\frac{\delta}{2}=\frac{1}{\pi}\int_0^{t_0}\mu^{-1}(t')dt'.\int_0^d (d-x)^{-\frac{1}{2}}dx\int_{-\infty}^{0}\frac{(-x')^{\frac{1}{2}}g_1(x')dx'}{x'-x}. \tag{5.3}$$

This can be rewritten as

$$\frac{\delta}{2}=\chi(t_0)\Phi(g_1(x)), \tag{5.4}$$

where

$$\chi(t_0)=\int_0^{t_0}\mu^{-1}(t')dt'. \tag{5.5}$$

Assuming t_0 is finite and positive, the following inequality follows from μ^{-1} being a positive operator:

$$\chi(0)<\chi(t_0)<\chi(\infty), \tag{5.6}$$

and this combined with equation (5.4) gives

$$\frac{\delta}{2\chi(\infty)}<\Phi(g_1(x))<\frac{\delta}{2\chi(0)}. \tag{5.7}$$

Now providing Φ is a monotone increasing function of the non-cohesive loading stresses, as it proved to be in section 2, this gives a restriction on the range of admissable stresses - in particular for step loading, writing

$$\Phi(g_1(x))=\varphi(F), \tag{5.8}$$

F is found to be restricted by the inequalities

$$\varphi^{-1}(\frac{\delta}{2\chi(\infty)})<F<\varphi^{-1}(\frac{\delta}{2\chi(0)}). \tag{5.9}$$

Using the Abelian theorems for the Laplace Transform, $\chi(0)$ can be related to the short-time modulus and $\chi(\infty)$ to the long-time modulus. Knauss (1970) states a general result of this nature, without analytic proof.

Figure 3.1: the semi-infinite crack geometry

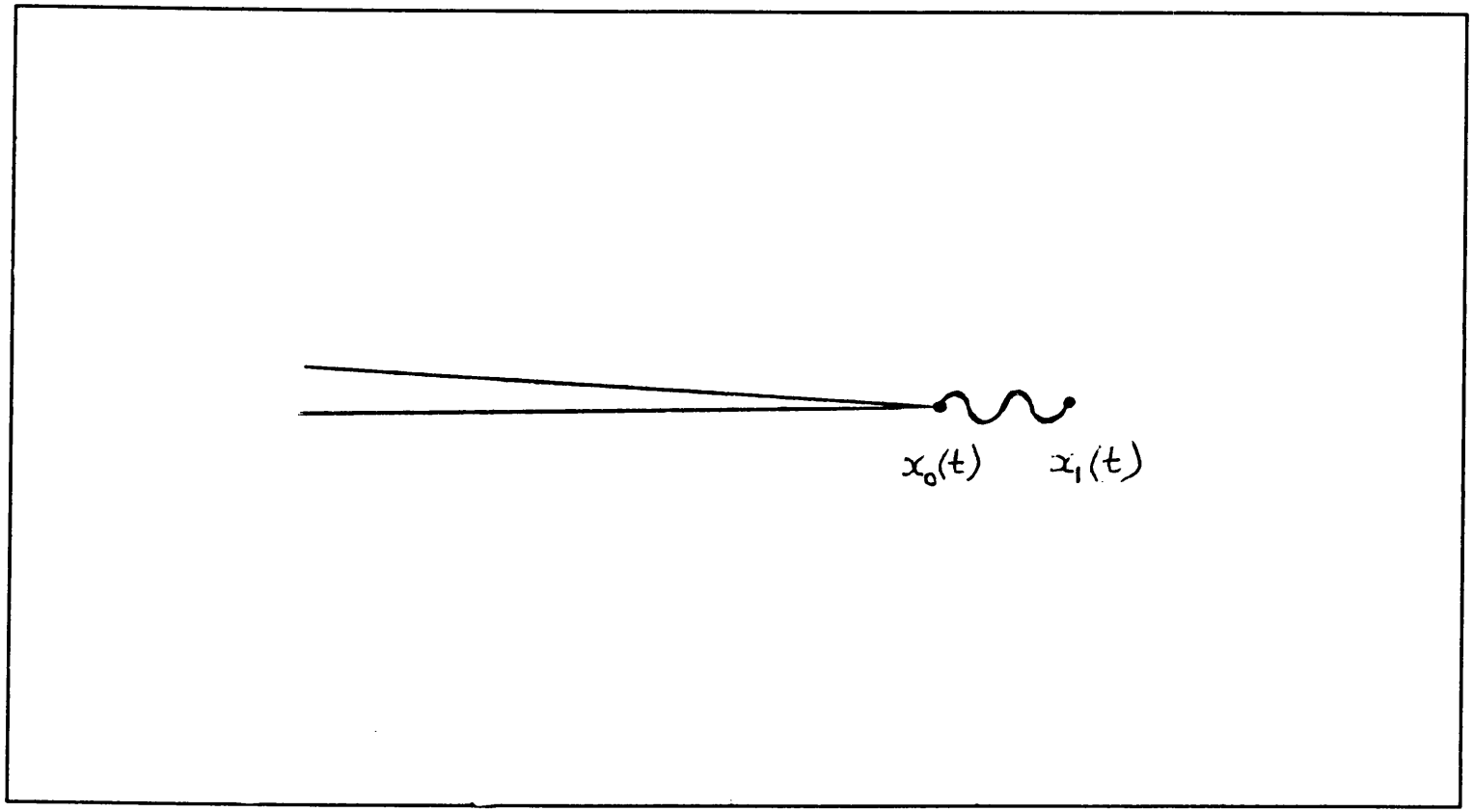

Figure 3.2:
semi-infinite geometry

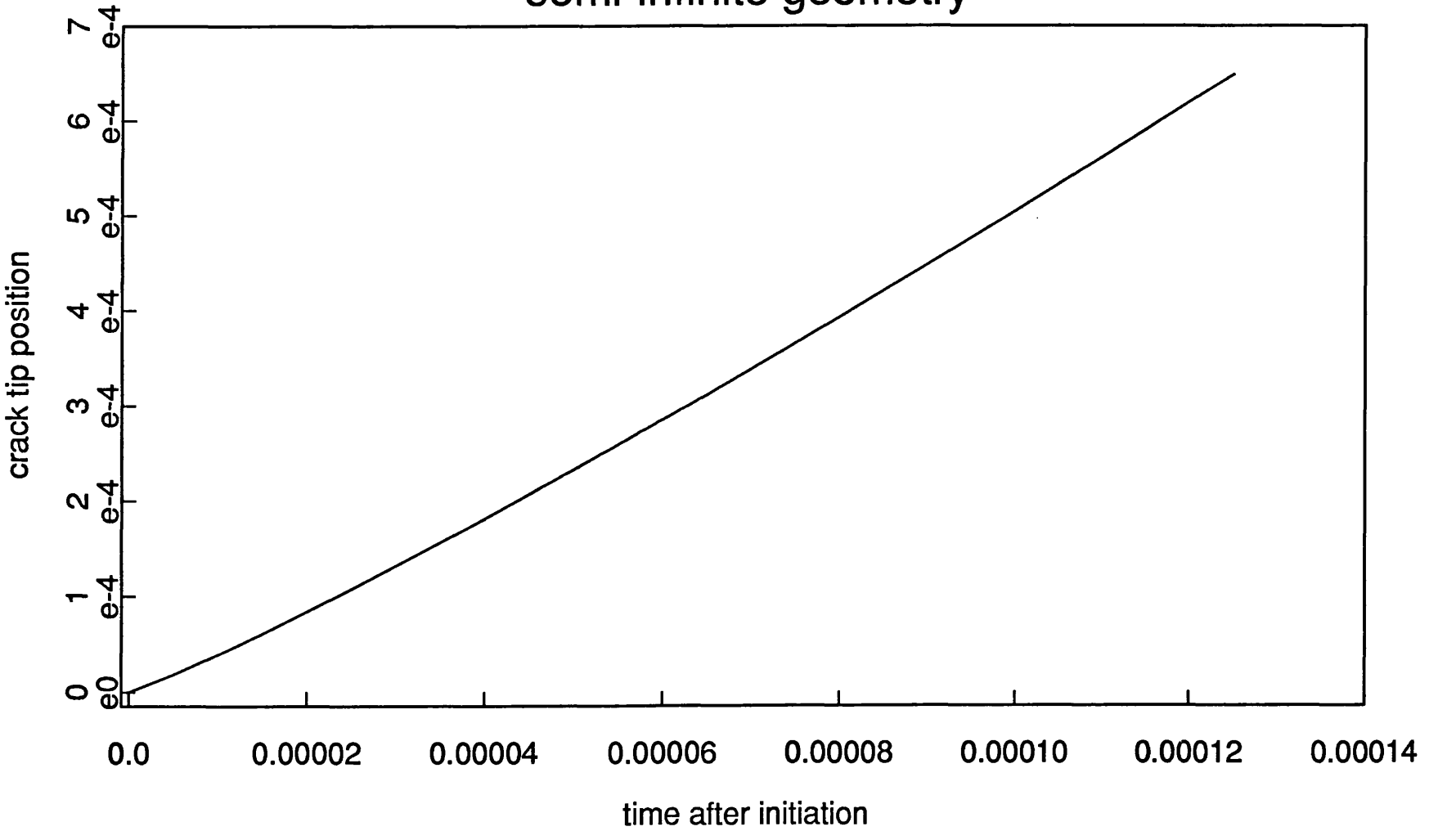

Figure 3.3:
approach to Griffith limit

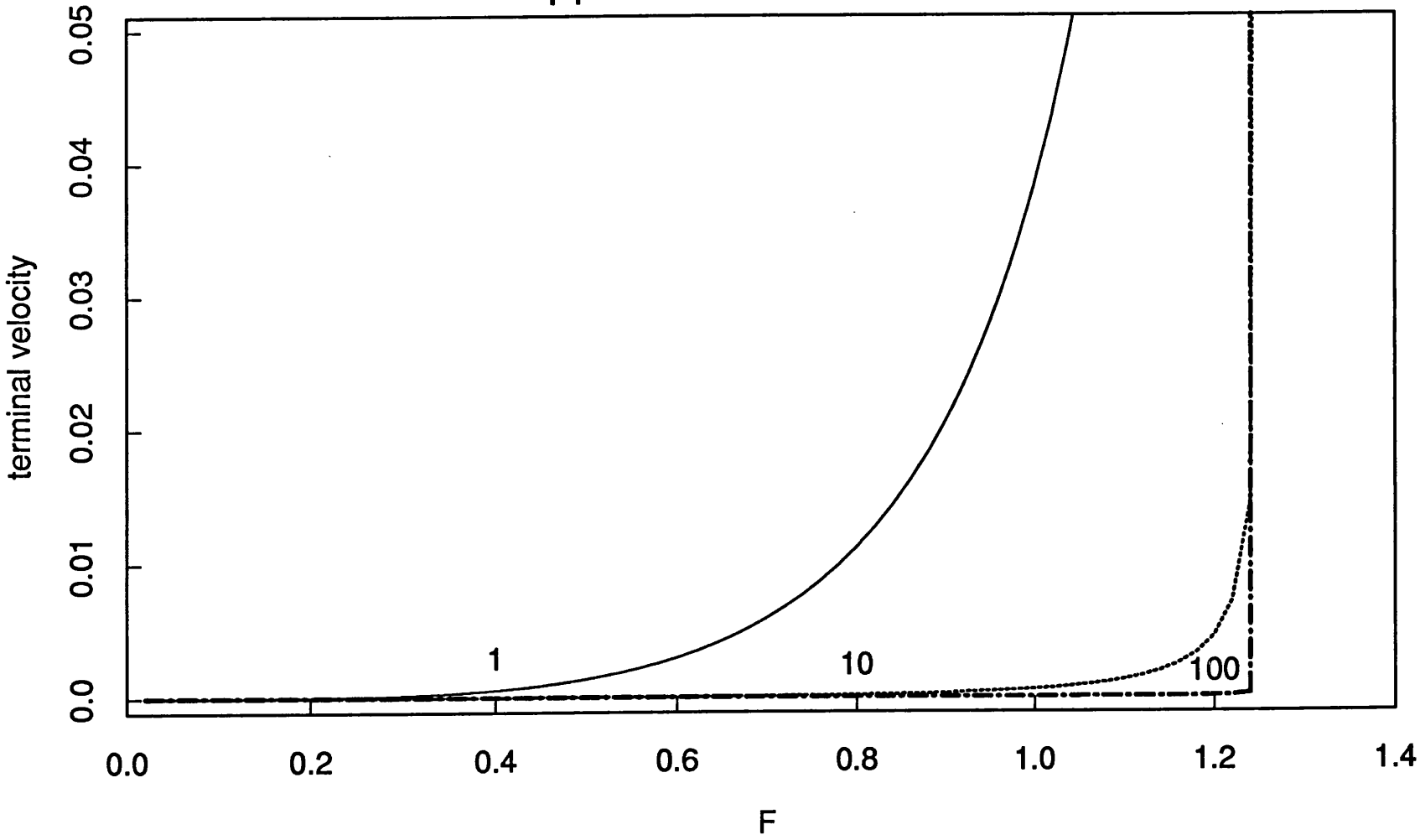

Chapter 4: Quasi-static double-ended crack growth.

1. Introduction.

This chapter deals with the more realistic double-ended crack problem in the standard linear solid, which is nonetheless similar in many respects to that considered in chapter 3. One important difference is that the total loading increases as the crack extends, whereas it remains the same in the semi-infinite case considered earlier. The main consequence of this is that non-steady crack growth without inertia is possible only for a limited time, after which the motion becomes dynamic and the current analysis inapplicable. Although finite cracks occur in reality and semi-infinite ones are a mathematical convenience, no claim is made here pertaining to the credibility of the loading that has been chosen for this chapter's model. As is the case throughout this thesis, the loading is one aspect of the crack models considered which is kept as simple as possible to facilitate progress in obtaining information such as the time history of the crack tip position. Since the computed displacement (as a function of length along the crack line) turns out to be non-monotonic, care has to be taken in the application of the constant COD criterion.

Graham (1968) introduced an extended version of the classical correspondence principle for linear viscoelasticity (which is a means of salvaging the extensive number of solutions known for elastic crack problems) for the solution of mixed boundary value problems which include time-dependent boundary regions. Often non-static crack problems have a displacement boundary condition as well as a stress one (on the crack faces), separated by the moving boundary of the crack tip. Traction loading problems certainly fall into this category. Graham (1969) proceeds to apply his technique to two moving crack problems

in linear viscoelasticity theory, using a Griffith energy balance approach. After obtaining stresses and displacements, he obtains what are known, from the elastic theory, as Griffith instability criteria, which are inequalities specifying the level of loading necessary for initiation of crack motion. In the presence of finite craze zones, as in the quasi-static chapters of this thesis, the nature of this instability criterion changes. An interval of loading stresses appears in which quasi-static crack motion is possible (this cannot happen in the elastic case). This interval disappears in the Griffith limit, so conclusions resembling those of Graham are recovered by this means.

The analysis of Graham and Sabin (1973) involves the application of an extended correspondence principle to the consideration of thermal effects for an extending penny-shaped crack as well as a cylinder problem. Graham (1975), followed by Graham and Sabin (1976, 1978 and 1981), investigate the effect of alternating tensile and compressive loads on quasi-static crack extension in a linearly viscoelastic material. A Griffith type approach is used to obtain conditions for crack growth. The 1976 paper includes analysis for the Maxwell liquid, while the 1981 one addresses the standard linear solid.

2. Displacement and crack initiation time.

The analogous equation to (3.2.6) is

$$w(x_0(t)+0i,t)=\frac{1}{\mu\pi}\Big[\int_{-x_1(t)}^{x_0(t)}(x_1(t)^2-x'^2)^{-\frac{1}{2}}dx'\int_{-x_1(t)}^{x_1(t)}g(x'',t)\frac{\sqrt{x_1(t)^2-x''^2}}{x''-x'}dx''$$

$$+\frac{f}{\tau}\exp(-\frac{t}{\tau})$$

$$\cdot\int_{-x_1(t)}^{x_0(t)}dx'\int_{t_1(x)}^{t}\exp(\frac{t'}{\tau})(x_1(t')^2-x'^2)^{-\frac{1}{2}}dt'\int_{-x_1(t')}^{x_1(t')}g(x'',t')\frac{\sqrt{x_1(t')^2-x''^2}}{x''-x'}dx''\Big] \tag{2.1}$$

where, using the notation of Figure 4.1,

$x_1(t_1(x))=|x|$,

$x_0(t)$ is the end of the crack proper,

$x_1(t)=x_0(t)+d$ is the end of the craze zone

and $g=\sigma_{23}$ is the loading function (of time and space variables).

The innermost integrals are to be interpreted as Cauchy principal values.

We specialise $g(x,t)$ to

$$\begin{cases} F.H(t), & -x_0(t)<x<x_0(t) \\ -\sigma_0.H(t), & x_0(t)<x<x_1(t), -x_1(t)<x<-x_0(t). \end{cases} \tag{2.2}$$

Changing the order of integration in the second term, and utilising the known COD derivation in the elastic case (Bilby, Cottrell & Swinden, 1963), the following formula is arrived at:

$$w(x_0(t)+0i,t)=\frac{F+\sigma_0}{\mu\pi}\{2c\ln\frac{1}{r}$$
$$+\frac{f}{\tau}\exp(-\frac{t}{\tau})\int_0^t\exp(\frac{t'}{\tau})[(c+c')\cosh^{-1}|\frac{a'^2-c'^2}{a'(c+c')}+\frac{c'}{a'}|$$
$$-(c-c')\cosh^{-1}|\frac{a'^2-c'^2}{a'(c'-c)}+\frac{c'}{a'}|]H(a'-c)dt'\}, \tag{2.3}$$

where

$$a=x_1(t)$$
$$a'=x_1(t')$$
$$c=x_0(t)$$
$$c'=x_0(t')$$
$$\text{and } r=\cos(\frac{\pi}{2}\frac{F}{F+\sigma_0})=\frac{c}{a}. \tag{2.4}$$

This last relation represents zero stress concentration at $x_1(t)$.

Eliminating a,a' gives

$$w(x_0(t)+0i,t)=\frac{F+\sigma_0}{\mu\pi}\{2c\ln\frac{1}{r}$$
$$+\frac{f}{\tau}\exp(-\frac{t}{\tau})\int_0^t\exp(\frac{t'}{\tau})[(c+c')\cosh^{-1}|\frac{c'+r^2c}{r(c'+c)}|$$
$$-(c-c')\cosh^{-1}|\frac{c'-r^2c}{r(c'-c)}|]H(c'-rc)dt'\}. \tag{2.5}$$

Let t_0 be the time at which the crack first extends. Then,

$$x_0(t)=c_0, \quad t\leq t_0. \tag{2.6}$$

Consider the equation

$$w(x_0(t)+0i,t)=\frac{\delta}{2} \tag{2.7}$$

for $t=t_0(\delta>0)$.

This gives

$$\frac{\delta}{2}=\frac{F+\sigma_0}{\mu\pi}2c_0\ln\frac{1}{r}[1+f(1-\exp(-\frac{t_0}{\tau}))]. \tag{2.8}$$

Solving for t_0 yields

$$t_0=\tau\ln|\frac{f\ln\frac{1}{r}}{(1+f)\ln\frac{1}{r}-\frac{\delta\mu\pi}{4c_0(F+\sigma_0)}}|. \tag{2.9}$$

Define

$$h(x)=(1+x)\ln\sec(\frac{\pi}{2}\frac{x}{1+x}) \tag{2.10}$$

Requiring t_0 to be non-negative and finite produces the inequalities

$$\frac{\delta\mu\pi}{4c_0\sigma_0(1+f)}\leq h(\frac{F}{\sigma_0})\leq\frac{\delta\mu\pi}{4c_0\sigma_0}. \tag{2.11}$$

It can be deduced from the monotone increasing nature of h that $\exists F_3,F_4\in\mathbf{R}$ such that

$$t_0>0 \text{ iff } F_3<F<F_4, \tag{2.12}$$

which is a similar conclusion to that reached in the semi-infinite crack case. If the loading F exceeds F_4, then inertia must be allowed for from the outset; if, on the other hand, F lies below F_3 then motion does not occur. However, if F lies in the range specified in (2.12), there is a time t_1 where quasi-static crack extension occurs for $t_0<t<t_1$, after which dynamic terms must be taken into account.

3 .Numerical solution

Here equation (2.7) is solved at the times $t=t_0+ih$, $i=1,2,\ldots$ for $x_0(t)$, crack position. Define the following function which is based on a trapezoidal approximation to the displacement at the nth stage:

$$W_n(c;h)=\frac{F+\sigma_0}{\mu\pi}\{(1+\frac{hf}{2\tau})2c\ln\frac{1}{r}$$
$$+f\exp(-\frac{t}{\tau})[(1+\frac{h}{2\tau})\exp(\frac{t_0}{\tau})-1]f_0(c)$$
$$+\frac{hf}{\tau}\exp(-\frac{t}{\tau})\sum_{i=1}^{n-1}\exp(\frac{t_0+ih}{\tau})f_i(c)\}, \qquad (3.1)$$

where

$$f_i(c)=[(c+c_i)\cosh^{-1}|\frac{c_i+r^2c}{r(c_i+c)}|-(c-c_i)\cosh^{-1}|\frac{c_i-r^2c}{r(c_i-c)}|]H(c_i-rc), \qquad (3.2)$$

$t=t_0+nh=t_n$, $c_i=x_0(t_i)$ and $n\geq 1$.

Solving

$$W_n(c)=\frac{\delta}{2} \qquad (3.3)$$

for c yields $x_0(t_n)$.

For all the square bracketed terms to be nonzero,

$$c<\min\{\frac{c_i}{r}\} \qquad (3.4)$$

($=\frac{c_0}{r}$ if $\{c_i\}$ is an increasing sequence).

At stage n, an attempt is made to solve (3.3) on the interval $[c_{n-1}, \frac{c_0}{r})$. Simple calculus shows that $f_i(c)$ decreases on the interval $(c_i, \frac{c_i}{r})$. However the influence of the linear term in (3.1) is sufficient for $W_n(c)$ to turn upwards again. An inductive argument shows $W_n(c_{n-1}) > \frac{\delta}{2}$ provided it was possible to solve (3.3) in all previous steps. Identification of the minimum of $W_n(c;h)$ for $c > c_{n-1}$, $\min(n)$, provides an interval on which W_n is monotone in c, and (3.3) can be now solved provided

$$\frac{\delta}{2} \in (W_n(\min(n)), W_n(c_{n-1})) \tag{3.5}$$

and $h < h_{crit}$, where h_{crit} has to be bounded experimentally. There is a solution of (3.3) for $c > \min(n)$ but this is disregarded on the grounds that the condition $c_n \to c_{n-1}$ as $h \to 0$ must hold. Bisection is employed both to find the minimum and the solution at each stage.

Conditions (2.11 a,b) can be rewritten as

$$\frac{\delta\mu\pi}{4\sigma_0(1+f)h(\frac{F}{\sigma_0})} \leq c_0 \leq \frac{\delta\mu\pi}{4\sigma_0 h(\frac{F}{\sigma_0})} = c_d, \tag{3.6}$$

so it is only possible to initiate the solution procedure providing the initial crack length lies in this range. Results show that breakdown occurs in the solution before the crack grows to (half) length c_d. Analytically this is due to equation (3.5) no longer holding:

$$\frac{\delta}{2} \in (-\infty, W_n(\min(n))) \text{ for } n > n_{terminal} \tag{3.7}$$

i.e. the minimum of $W_n(c)$ lies above the line $y = \frac{\delta}{2}$.

Figure 4.2 shows crack tip position as a function of time until breakdown of the quasi-static analysis, and was obtained with the values

$$F=1;\sigma_0=5;f=\tau=\mu=\delta=1;h=0.02;c_0=3.$$

In relation to the scaling described in the previous chapter, these are equivalent to

$$\frac{F}{\sigma_0}=0.2,$$
$$\frac{\mu}{\sigma_0}=K,$$
$$\frac{\delta}{L_1}=\frac{1}{5K},$$
$$c_0=3L_1,$$

so that $c_0=15K\delta$.

This plot is repeated in Figure 4.3 for various σ_0,δ pairs such that $\sigma_0\delta=5$, the other parameter values being the ones used for Figure 4.2. It illustrates that stable crack growth is not possible in the case of a Griffith crack.

4. The limiting case of a Griffith crack.

This section details analytic arguments for the phenomenon demonstrated in Figure 4.3. Asymptotic analysis based on r taking the value

$$r=1-\varepsilon \tag{4.1}$$

where ε is small will be given: different reasoning is necessary depending on whether $c<\frac{c_0}{r}\sim(1+\varepsilon)c_0$ i.e. the crack has not extended far from its starting position or $c>\frac{c_0}{r}$ i.e. there has been considerable growth.

In the case of limited extension, where the crack tip position has not yet reached the end of the original craze zone,

$$c'\geq c_0>rc, \tag{4.2}$$

so formula (2.5) becomes

$$w(x_0(t)+0i,t)=\frac{F+\sigma_0}{\mu\pi}\{2c\ln\frac{1}{r}$$
$$+\frac{f}{\tau}\exp(-\frac{t}{\tau})\int_0^t\exp(\frac{t'}{\tau})[(c+c')\cosh^{-1}|\frac{c'+r^2c}{r(c'+c)}|$$
$$-(c-c')\cosh^{-1}|\frac{c'-r^2c}{r(c'-c)}|]dt'\}. \tag{4.3}$$

The following approximation (valid for α small) is used to facilitate evaluation of the integral:

$$\cosh^{-1}(1+\alpha)\sim\sqrt{(2\alpha)}. \tag{4.4}$$

The first argument of $\cosh^{-1}$ appearing in (4.3) can be algebraically re-arranged for the application of (4.4):

$$\frac{c'+r^2c}{r(c'+c)}=\frac{\frac{c'}{r}+rc}{c'+c}$$
$$\sim\frac{(1+\varepsilon+\varepsilon^2)c'+(1-\varepsilon)c}{c'+c}$$
$$=\frac{(c'+c)+\varepsilon(c'-c)+\varepsilon^2c'}{c'+c}$$
$$=1+\varepsilon\frac{c'-c}{c'+c}+\frac{\varepsilon^2c'}{c'+c}. \tag{4.5}$$

(4.4) is not suitable for use with the second such term, but the contribution arising from this term can be neglected. The post-initiation time part of the integral in the displacement formula is approximately

$$\int_{t_0}^t\exp(\frac{t'}{\tau})\sqrt{2\varepsilon(c'+c)(c'-c+\varepsilon c')}dt'. \tag{4.6}$$

Using $\ln\frac{1}{r}\sim\varepsilon$ and, for (4.6), $c'\sim c$, the integral in (4.3) can now be approximated by

$$2\varepsilon c_0\int_0^{t_0}\exp(\frac{t'}{\tau})dt'+2\varepsilon c\int_{t_0}^{t}\exp(\frac{t'}{\tau})dt'. \tag{4.7}$$

Applying the fracture criterion (2.7) gives

$$\frac{\delta}{2}\sim\frac{F+\sigma_0}{\mu\pi}\{2\varepsilon c+2\varepsilon f\exp(-\frac{t}{\tau}).$$
$$[c_0(\exp(\frac{t_0}{\tau})-1)+c(\exp(\frac{t}{\tau})-\exp(\frac{t_0}{\tau}))]\}. \tag{4.8}$$

Assuming now that $c-c_0=O(\varepsilon^{1+k})$, where $k>0$, equation (2.8) becomes (to leading order)

$$\frac{\delta}{2}\sim\frac{F+\sigma_0}{\mu\pi}2\varepsilon c\{1+f[1-\exp(-\frac{t}{\tau})]\}. \tag{4.9}$$

If (2.9) defines t_0 by the equation

$$t_0=T(c_0), \tag{4.10}$$

then (4.9) can be written in the form

$$t\sim T(c). \tag{4.11}$$

From these last two equations, the following local gradient approximation for the first portion of the curve after initiation can be derived:

$$\frac{c-c_0}{t-t_0}\sim\frac{c_0}{\tau}. \tag{4.12}$$

This stems from

$$\begin{aligned} t-t_0 &\sim T(c)-T(c_0)\\ &\sim\tau\ln|\frac{c}{c_0}|\\ &=\tau\ln|1+\frac{c-c_0}{c_0}|\\ &\sim\tau\frac{c-c_0}{c_0}. \end{aligned} \tag{4.13}$$

Proceeding to the second case where there has been considerable extension, theoretically the crack can extend quasi-statically to c_d, the upper bound in inequality (3.6). Define t_1 to be the time when

$$c(t_1)=rc(t). \tag{4.14}$$

Then

$$c(t')>rc \text{ for all } t_1<t'<t. \tag{4.15}$$

Since $|c-c'|<\varepsilon c$ in this time interval, c' is well approximated by c, and (2.5) can be written as

$$\begin{aligned} w(c(t)+0i,t) &\sim \frac{F+\sigma_0}{\mu\pi}\left[2c\ln\frac{1}{r}+\frac{f}{\tau}\exp(-\frac{t}{\tau})\int_{t_1}^{t}\exp(\frac{t'}{\tau}).2c\ln\frac{1}{r}dt'\right] \\ &= \frac{F+\sigma_0}{\mu\pi}.2\varepsilon c[1+f(1-\exp(-\frac{t-t_1}{\tau}))]. \end{aligned} \tag{4.16}$$

On application of the fracture criterion, it follows that

$$t-t_1 \sim T(c), \tag{4.17}$$

and this formula allows an approximation to be derived for the gradient $\dot{c}(t)$:

$$\begin{aligned} \dot{c}(t) &\simeq \frac{c(t)-c(t_1)}{t-t_1} \\ &\sim \frac{\varepsilon c(t)}{T(c(t))}. \end{aligned} \tag{4.18}$$

Measuring time in units of τ i.e. making the change of variable

$$t'=\frac{t}{\tau}, \tag{4.19}$$

allows (4.18) to be written in the form

$$\frac{dc}{dt'} \sim \frac{-\varepsilon c(t)}{\ln\left|\frac{1+f}{f}-\frac{\delta\mu\pi}{4(F+\sigma_0)f\varepsilon c(t)}\right|}. \tag{4.20}$$

This expression gives the expected behaviour for the gradient as $c\to c_d$, namely that $\frac{dc}{dt'}\to\infty$.

In conclusion, after remaining motionless at c_0 for a time t_0, the crack extends a length of order ε at finite velocity, after which the rate of extension becomes infinitesimal. Therefore the crack will take a very large time (of $O(\frac{1}{\varepsilon})$) to

reach c_d, where it will go dynamic. A numerical comparison with the method described in section 3, for the values used to generate the lowest of the curves in Figure 4.3, shows that the approximate formulae for extensive growth of this chapter over-estimate the "exact" ones.

Figure 4.1: the double-ended crack geometry

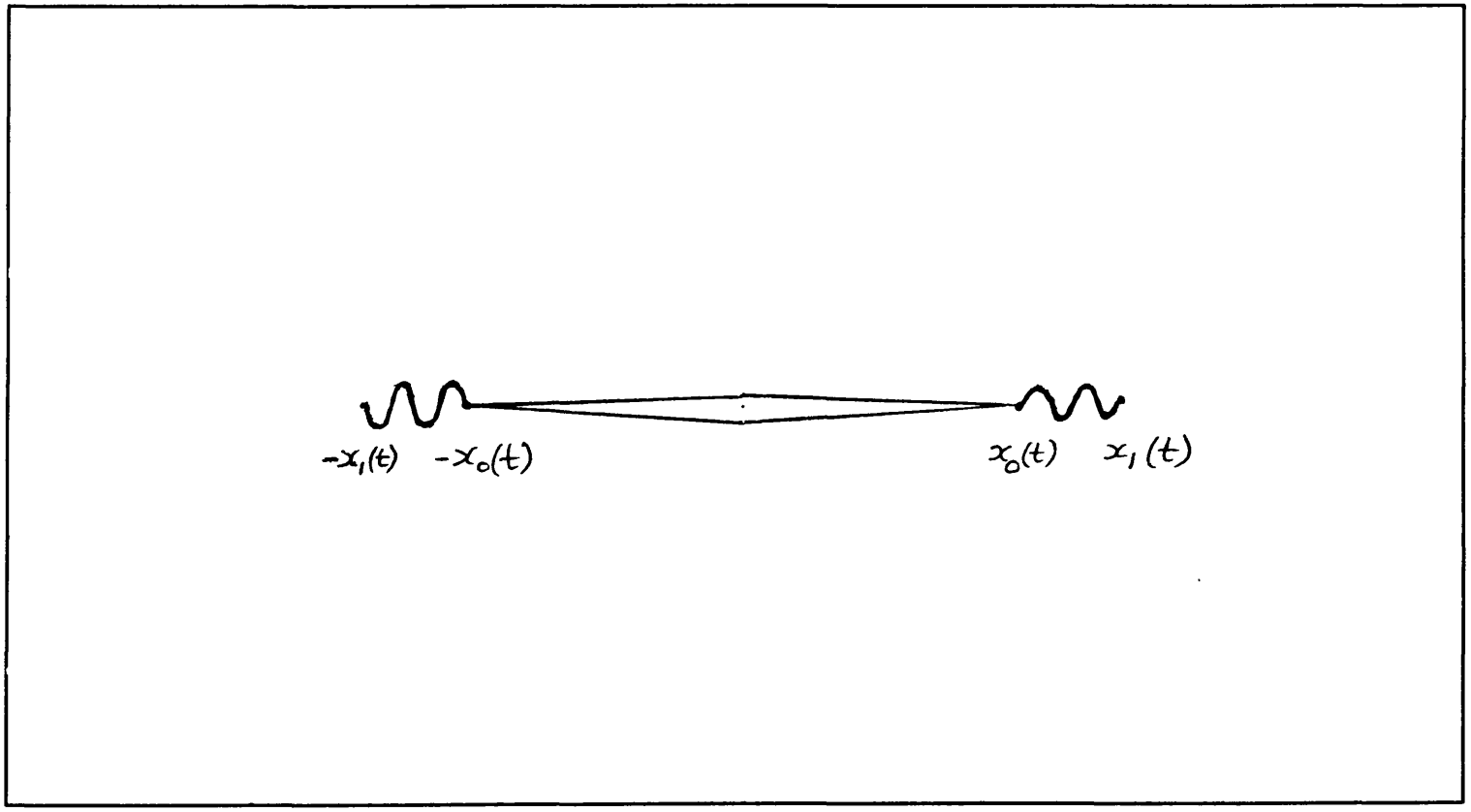

Figure 4.2:
double-ended geometry

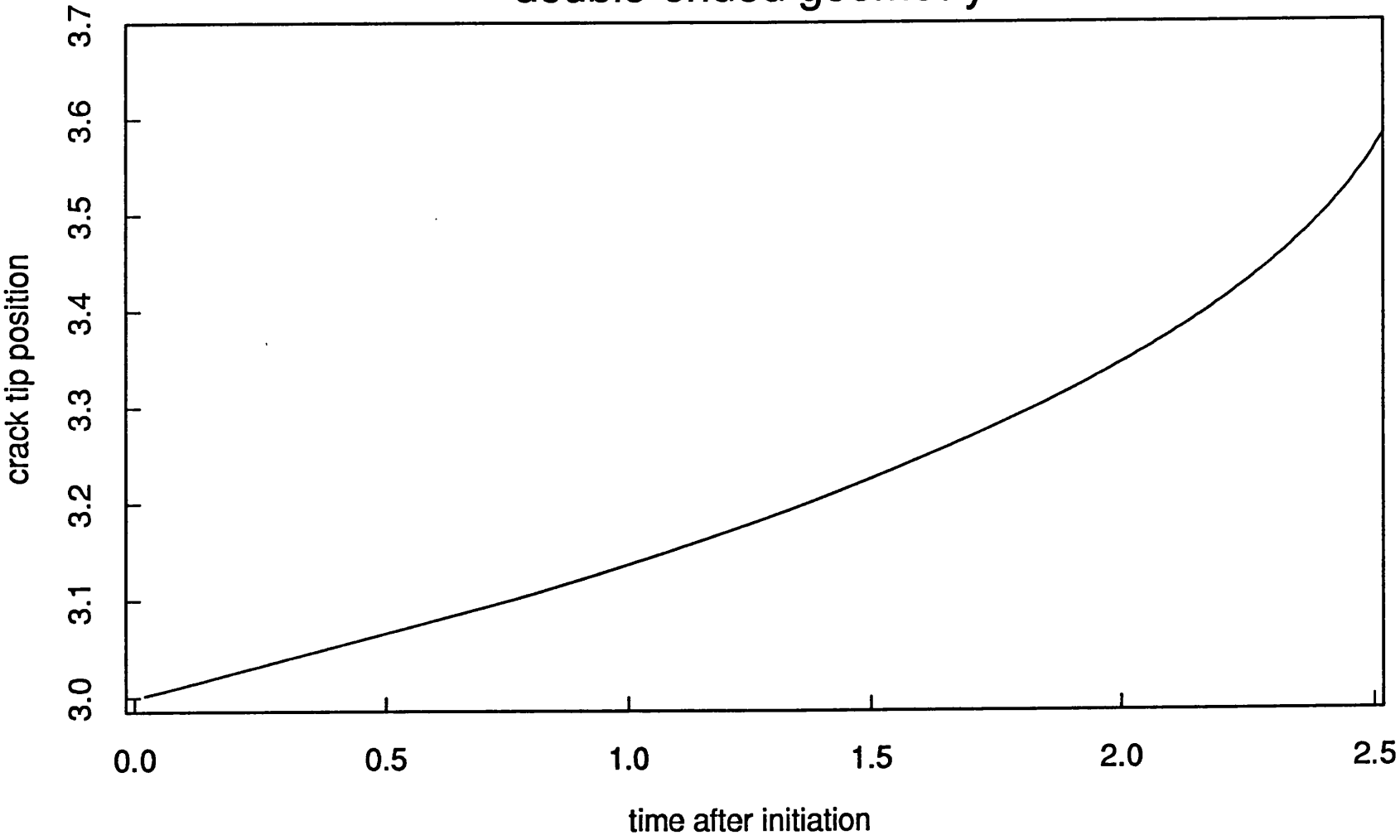

Figure 4.3:
approach to Griffith limit

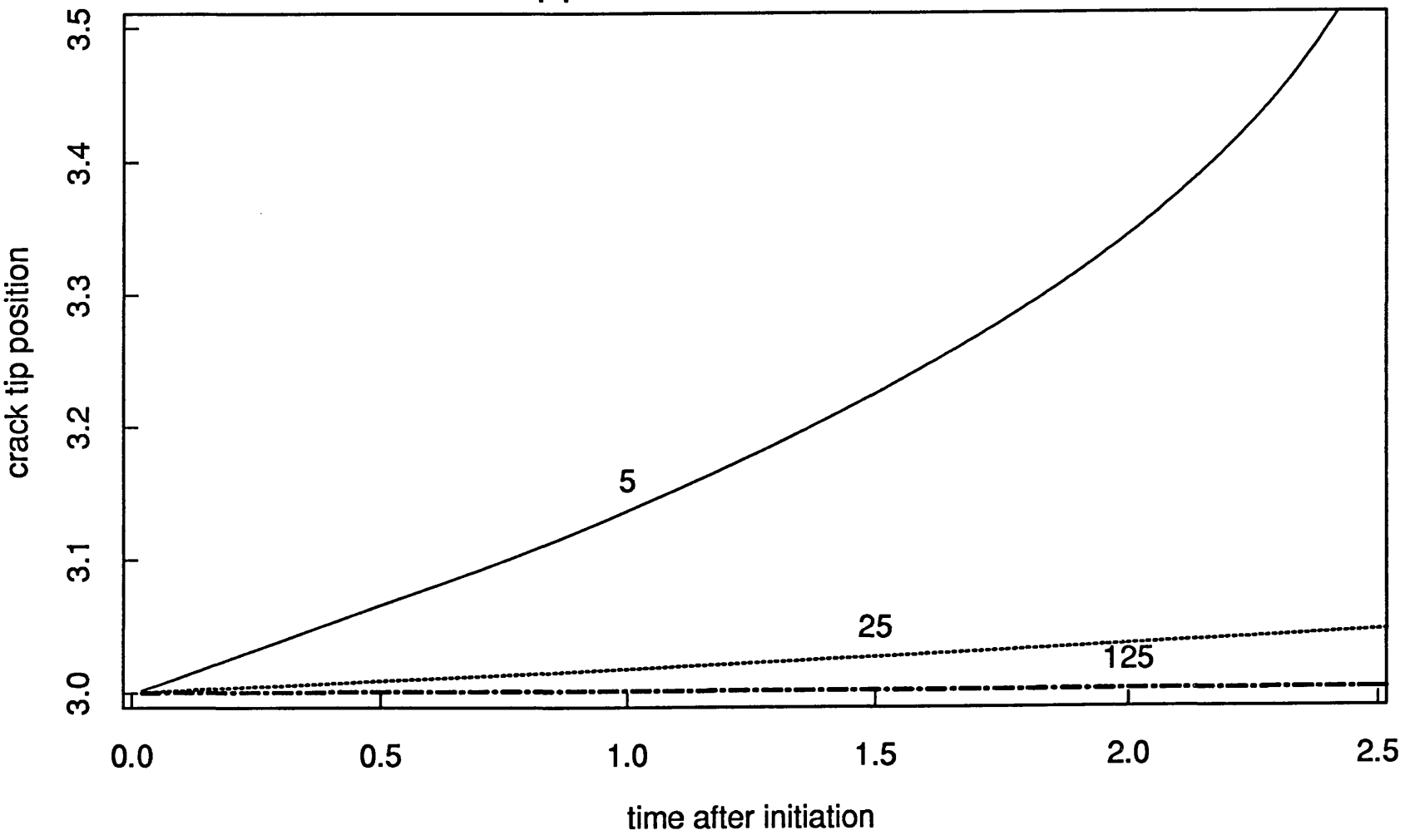

Chapter 5 - An accelerating crack in a viscoelastic material: solution by matched asymptotic expansions.

1. Formulation of problem.

Atkinson and Coleman (1977) used the method of matched asymptotic expansions to solve three problems in linear viscoelasticity, the first two concerned with crack propagation and the third with a steadily rolling cylinder in a half-space. All three contain a non-dimensional parameter $\varepsilon=\frac{V\tau}{L}$, where V is the crack tip speed (in the two cases involving cracks, the moving boundary speed in general), τ is the relaxation time of the material and L is a characteristic length scale. The second crack problem is based on the work of Yoffé (1951) and involves a finite crack moving in an infinite medium in such a way its length is preserved, i.e. one end zips up as the other advances. This problem does include inertia, but it is physically unreasonable.

The first, more realistic, problem involves steady-state Mode I (opening mode) propagation of a semi-infinite crack in a strip of standard linear solid with specified displacements on the strip faces. An inner problem is generated by introducing magnifying coordinates in the crack tip region, and this is related to the solution of the outer problem (based on the elastic version) by use of a matching principle. This relates certain derivatives of potentials expressed in terms of inner coordinates and functions to the corresponding 'outer' derivatives, solving for the arbitrary constants otherwise present in the outer problem. To avoid cumbersome analysis involving the use of potential functions to decouple the equations for a Mode I problem, the contents of this chapter are restricted to antiplane strain only. The complication of strip geometry present in

Atkinson and Coleman's work is not present here: this is offset by inertial complications of a transient nature (as opposed to steady-state).

The constitutive equation (in shear) of the viscoelastic material to be considered is

$$\sigma_{i3}=2\mu\{e_{i3}+\frac{d}{dt}(\beta_\varepsilon(t)*e_{i3}(t))\},\quad i=1,2, \tag{1.1}$$

where

$$\beta_\varepsilon(t)=\beta(\frac{t}{\varepsilon\tau}), \tag{1.2}$$

τ is a characteristic time, $\varepsilon\tau$ is a relaxation time with $\varepsilon\ll 1$ and μ is the long-time modulus of the material.

The equation of motion in terms of displacement becomes

$$\mu\nabla^2(w+\beta_\varepsilon*w_t)=\rho w_{tt} \tag{1.3}$$

which is to be solved with initial condition

$$w=0,\quad t\le 0 \tag{1.4}$$

and boundary conditions

$$\mu(w_y+\beta_\varepsilon*w_{yt})=-p(x,t),\quad y=0,\quad x\le x_2(t), \tag{1.5a}$$

$$w=0,\quad y=0,\quad x>x_2(t). \tag{1.5b}$$

The loading function p is taken to be

$$p(x,t)=\begin{cases} g(x,t), & x<x_2(t)-\varepsilon l, \\ -\dfrac{\sigma_0}{\varepsilon}, & x_2(t)-\varepsilon l<x<x_2(t). \end{cases} \tag{1.6}$$

When the solution to this moving boundary problem is smooth and providing that $\int_0^\infty \beta(u)du$ is finite, the terms involving convolutions are of $O(\varepsilon)$, and the problem reduces to the standard elastic accelerating crack problem as solved by Kostrov (1966):

$$\nabla^2 w=\frac{1}{c^2}w_{tt};\quad c^2=\frac{\mu}{\rho}, \tag{1.7}$$

$$\mu w_y=-p(x,t),\quad x\le x_2(t),\quad y=0, \tag{1.8a}$$

$$w=0,\quad x>x_2(t),\quad y=0. \tag{1.8b}$$

Near the crack tip, p becomes large over a very short interval and hence w will not be smooth in this vicinity.

Define inner co-ordinates by

$$X=\frac{(x-x_2(t))}{\varepsilon}, \tag{1.9}$$

$$Y=\frac{y}{\varepsilon}, \tag{1.10}$$

and a new displacement function W (assumed smooth in its variables) by

$$w(x,y,t)=W(X,Y,t). \tag{1.11}$$

Then

$$\begin{aligned}
(\beta_\varepsilon * w_t)(t)&=\int_0^t \beta(\frac{t'}{\varepsilon\tau})w_t(t-t')dt'\\
&=\int_0^t \beta(\frac{t'}{\varepsilon\tau})[-\frac{\dot{x}_2(t-t')}{\varepsilon}W_X(\frac{x-x_2(t-t')}{\varepsilon},Y,t-t')+W_t(\frac{x-x_2(t-t')}{\varepsilon},Y,t-t')]dt'\\
&=\varepsilon\int_0^{\frac{t}{\varepsilon}} \beta(\frac{t''}{\varepsilon})[-\frac{\dot{x}_2(t-\varepsilon t'')}{\varepsilon}W_X(\frac{x-x_2(t-\varepsilon t'')}{\varepsilon},Y,t-\varepsilon t'')\\
&\quad +W_t(\frac{x-x_2(t-\varepsilon t'')}{\varepsilon},Y,t-\varepsilon t'')]dt''\\
&\sim\int_0^\infty \beta(\frac{t''}{\tau})[-\dot{x}_2(t)W_X(X+t''\dot{x}_2(t),Y,t)]dt''\\
&=-\dot{x}_2(t)\int_0^\infty \beta(\frac{t''}{\tau})W_X(X+t''\dot{x}_2(t),Y,t)dt''.
\end{aligned} \tag{1.12}$$

In terms of the new notation, the equation of motion becomes

$$(1-\frac{\dot{x}_2^2}{c^2})W_{XX}+W_{YY}-\dot{x}_2\int_0^\infty \beta(\frac{t''}{\tau})(W_{XXX}+W_{XYY})dt''=0 \tag{1.13}$$

with stress boundary condition

$$\mu[W_Y-\dot{x}_2\int_0^\infty \beta(\frac{t''}{\tau})W_{XY}(X+\dot{x}_2t'',0,t)dt'']=\begin{cases}0, & X<-l\\ -\sigma_0, & -l<X<0,\end{cases} \qquad (1.14a)$$

and displacement boundary condition

$$W(X,0,t)=0, \quad X>0 \qquad (1.14b)$$

i.e. the inner problem is a steady-state one and can be solved by the Wiener-Hopf technique. In contrast to the situation considered in chapter 2, no loading (other than σ_0) is applied to the crack faces but stresses can no longer be assumed to decay so rapidly as $X^2+Y^2\to\infty$, since the present equations describe only the state near the crack tip. Correspondingly, the solution is allowed to contain the displacement due to a remote K-field such that the net local stress intensity factor is zero. In effect, the problem is decomposed into two parts, the first including the craze zone cohesive stresses with boundary conditions of the type assumed by Willis (1967b) and the second with no crack face tractions at all but relaxed boundary conditions at infinity.

2. Solution of the inner problem.

In this section, the upper case notation for the inner variables and W is replaced by lower case.

Define

$$\bar{w}(p,y)=\int_{-\infty}^{\infty} e^{ipx}w(x,y)dx \qquad (2.1)$$

and put

$$V=\dot{x}_2(t), \qquad (2.2)$$

where V is a parameter.

Then Fourier-transforming (1.13) yields

$$\frac{d^2\bar{w}}{dy^2}+\gamma^2\bar{w}=0, \tag{2.3}$$

where

$$\gamma^2=p^2[1-\frac{V^2}{c^2(1+ipV\tau\tilde{\beta}(-pV\tau))}], \tag{2.4}$$

$$\tilde{\beta}(p)=\int_0^\infty e^{ipt}\beta(t)dt \tag{2.5}$$

and

$$c^2=\frac{\mu}{\rho}. \tag{2.6}$$

Equation (2.3) has the solution

$$\bar{w}(p,y)=A(p)e^{-\gamma(p)y} \tag{2.7}$$

which vanishes as $y\rightarrow\infty$.

Transforming the stress boundary condition (1.14a) gives

$$-\mu(1+ipV\tau\tilde{\beta}(-pV\tau))\gamma(p)W_-(p,0)=-\frac{\sigma_0}{ip}[1-e^{-ipl}]+B_+(p), \tag{2.8}$$

where

$$W_-(p,0)=A(p) \tag{2.9}$$

and

$$B_+(p)=\int_0^\infty e^{ipt}\sigma_{23}(x,0)dx, \tag{2.10}$$

the half-transform of the unknown stresses ahead of the crack.

The function $\gamma(p)$ can be written in the form

$$\gamma(p)=p_+^{1/2}p_-^{1/2}[1-\frac{V^2}{c^2(1+ipV\tau\tilde{\beta}(-pV\tau))}]_-^{1/2}, \tag{2.11}$$

where $p_+^{1/2}=(p+i\varepsilon)_+^{1/2}$ with a branch cut from $-i\infty$ to $-i\varepsilon$, $p_-^{1/2}=(p-i\varepsilon)_-^{1/2}$ with a branch cut from $i\varepsilon$ to $i\infty$ and ε is a small real number which subsequently is

allowed to tend to zero. The function contained in the square brackets has neither any singularities nor any zeros (provided $0<V<c$) in the lower half plane $-\infty<\mathrm{Im}(p)<\varepsilon$ (as a result of β being a strictly positive, monotone decreasing function and a property of the Laplace transform) and is analytic in that region in view of the integral definition of $\tilde{\beta}$. From equation (2.11), it can be seen that $\mathrm{Re}\gamma(p)>0$ and so is consistent with the boundary condition at infinity for the non-homogeneous (traction loading) part of the problem.

Denoting

$$-\frac{\sigma_0}{ipp_+^{1/2}}[1-e^{-ipl}] \tag{2.12}$$

by $F(p)$, (2.8) can be factorised as

$$-\mu(1+ipV\tau\tilde{\beta}(-pV\tau))p_-^{1/2}[1-\frac{V^2}{c^2(1+ipV\tau\tilde{\beta}(-pV\tau))}]_-^{1/2}W_-(p,0)-F_-(p)$$
$$=F_+(p)+\frac{B_+(p)}{p_+^{1/2}} \tag{2.13}$$

in the strip $-\varepsilon<\mathrm{Im}(p)<\varepsilon$, where

$$F_-(p)=-\frac{1}{2\pi i}\int_{-\infty+iq}^{\infty+iq}\frac{-\sigma_0(1-e^{-ip_1l})dp_1}{ip_1p_1^{1/2}(p_1-p)} \quad (\max\{\mathrm{Im}(p),-\varepsilon\}<q<\varepsilon) \tag{2.14a}$$

and

$$F_+(p)=\frac{1}{2\pi i}\int_{-\infty-i0}^{\infty-i0}\frac{-\sigma_0(1-e^{-ip_1l})dp_1}{ip_1p_1^{1/2}(p_1-p)}. \tag{2.14b}$$

Since the function defined by analytic continuation of both sides is bounded and entire, both sides can be equated to a constant, which is zero due to the boundary conditions at infinity in (x,y)-space for the traction loading sub-problem. At this stage, the limit $\varepsilon\to0$ is taken.

This gives

$$W_-(p,0)=\frac{-F_-(p)}{\mu(1+ipV\tau\tilde{\beta}(-pV\tau))p_-^{1/2}[1-\frac{V^2}{c^2(1+ipV\tau\tilde{\beta}(-pV\tau))}]_-^{1/2}} \tag{2.15}$$

and

$$B_+(p)=-p_-^{\frac{1}{2}}F_+(p). \tag{2.16}$$

Inverting equation (2.16) for stress results in the equation

$$\sigma_{23}(x,0)=\frac{\sigma_0}{\pi x^{\frac{1}{2}}}\int_{-l}^{0}\frac{(-x_1'')^{\frac{1}{2}}dx_1''}{x-x_1''} \tag{2.17}$$

and the stress intensity factor due to the cohesive stresses, K, can be derived from this formula to be

$$K=\sigma_0\sqrt{\frac{8l}{\pi}}. \tag{2.18}$$

To this solution must be added that from the homogenous version of the problem i.e. with $F(p)=0$. The corresponding Wiener-Hopf equation is

$$-\mu(1+ipV\tau\tilde{\beta}(-pV\tau))p_-^{\frac{1}{2}}[1-\frac{V^2}{c^2(1+ipV\tau\tilde{\beta}(-pV\tau))}]_-^{\frac{1}{2}}W_-(p,0)=\frac{B_+(p)}{p_+^{\frac{1}{2}}} \tag{2.19}$$

and appropriate stresses can be obtained by equating both sides to $\frac{k}{p}$, where k is to be determined from the zero net stress intensity factor condition. The relaxed conditions at infinity in (x,y)-space for this second part of the problem allow a singularity at $p=0$.

Since $\sigma_{23}(x,0)$ is now

$$\frac{2^{\frac{1}{2}}ke^{-\frac{\pi}{4}}}{\sqrt{2\pi x}}, \tag{2.20}$$

k is taken to be $-2\sigma_0\sqrt{\frac{l}{\pi}}e^{i\frac{\pi}{4}}$.

The total displacement is the sum of two parts, one from each of the preceding problems, and is given by

$$w(-l,0)=-\frac{k}{2\pi\mu}\int_{-\infty-i0}^{\infty-i0}\frac{e^{ipl}dp}{pp_-^{\frac{1}{2}}[1-\frac{V^2}{c^2(1+ipV\tau\tilde{\beta}(-pV\tau))}]_-^{\frac{1}{2}}(1+ipV\tau\tilde{\beta}(-pV\tau))}$$

$$-\frac{1}{2\pi\mu}\int_{-\infty-i0}^{\infty-i0}\frac{e^{ipl}F_{-}(p)dp}{p_{-}^{1/2}[1-\dfrac{V^2}{c^2(1+ipV\tau\tilde{\beta}(-pV\tau))}]_{-}^{1/2}(1+ipV\tau\tilde{\beta}(-pV\tau))}. \tag{2.21}$$

For the purpose of numerical calculations, an equation for $\beta(t)$ corresponding to the standard linear solid is used:

$$\beta(t)=\alpha_* e^{-t}H(t), \tag{2.22}$$

where

$$\alpha_*=\frac{\mu_0}{\mu}-1, \tag{2.23}$$

μ_0 is the short-time modulus and μ is the long-time modulus ($\alpha_*>0$).

A constant *COD* fracture criterion is employed:

$$w(-l,0;V)=\frac{\delta}{2}; \tag{2.24}$$

this equation is solved for l as a function of V, and the resulting K vs V plots are shown in Figure 1 for various values of $\alpha=\dfrac{c\tau}{\delta}$. The other parameter values are $\alpha_*=0.5$, $c=\mu=\sigma_0=\delta=1$. As $\tau\to\infty$ or 0, the curves tend to those for a linear elastic material with the short-time modulus μ_0 or long-time modulus μ respectively. The limiting curves have equation

$$K=K(0)(1-(\frac{\dot{x}_2(t)}{c_*})^2)^{\frac{1}{4}} \tag{2.25}$$

where

$$K(0)=\begin{cases}\sqrt{2\mu_0\sigma_0\delta}, & \tau\to\infty,\\ \sqrt{2\mu\sigma_0\delta}, & \tau\to 0,\end{cases} \tag{2.26}$$

and

$$c_*=\begin{cases}c_0, & \tau\to\infty,\\ c, & \tau\to 0.\end{cases} \tag{2.27}$$

The curve for $\alpha=0.1$ shows slight fluctuations attributable to the use of unsophisticated uniform meshes to evaluate the contour integrals, resulting in the use of relatively large bisection tolerances to save function evaluations. All curves with finite τ tend to the value of $K(0)$ based on μ as $V\rightarrow 0$. Unlike their elastic K vs V counterparts, these viscoelastic curves rise initially before falling off again.

3. Solution of the outer problem.

We adhere to the following convention when defining K_0, the stress intensity factor for the outer problem:

$$\sigma_{23}(x,t)=\frac{K_0}{\sqrt{2\pi(x-x_2(t))}}. \tag{3.1}$$

Appendix 3 contains a summary of Kostrov's (1966) method. From the formula for stress, the following formula can be derived:

$$K_0=\sqrt{\frac{2}{\pi}}\sqrt{1-\frac{\dot{x}_2(t)}{c}}\int_{x_2(t)-ct}^{x_2(t)}\frac{p(x,\frac{ct-x_2(t)+x}{c})dx}{\sqrt{x_2(t)-x}}. \tag{3.2}$$

This is basically the same formula found in Kostrov's paper, apart from the fact that he considered only the case $c=1$ and had a different multiplicative factor.

4. Matching.

The method of matched expansions (van Dyke, 1964) postulates that both the outer limit of the inner problem and the inner limit of the outer problem are equal to the same steady-state elastic problem; hence it is reasonable to match inner and outer stress intensity factors. It is helpful to rewrite the matching equation $K=K_0$ in the form

$$g(\dot{x}_2(t))=\sqrt{\frac{2}{\pi}}\int_{x_2(t)-ct}^{x_2(t)}\frac{p(x,\frac{ct-x_2(t)+x}{c})dx}{\sqrt{x_2(t)-x}}, \tag{4.1}$$

where g is defined by

$$g(\dot{x}_2(t))=\frac{K(\dot{x}_2(t))}{\sqrt{1-\frac{\dot{x}_2(t)}{c}}} \tag{4.2}$$

(g is a monotone function and can therefore be inverted).

Equation (4.1) has been treated for three choices of the function $p=p(x,t)$. When

$$p(x,t)=F\delta(x+L)H(t), \tag{4.3}$$

this leads to the ordinary differential equation

$$\dot{x}_2(t)=g^{-1}(\sqrt{\frac{2}{\pi}}\frac{F}{\sqrt{x_2+L}}) \tag{4.4}$$

with initial condition

$$x_2(t)=0, \quad t\leq\frac{L}{c}, \tag{4.5}$$

as $\frac{L}{c}$ is the time it takes for the point stress to reach the crack tip. Equation (4.4) is separable and has solution

$$\int_0^{x_2(t)}\frac{dx_2}{g^{-1}(\sqrt{\frac{2}{\pi}}\frac{F}{\sqrt{x_2+L}})}=t-\frac{L}{c}, \quad t\geq\frac{L}{c}. \tag{4.6}$$

A graph of $x_2(t)$ vs t for $\alpha=0.01$ is shown in Figure 2. Figure 1 was used to generate values of g^{-1} (also for Figures 3 and 4), and the remaining parameters were $F=L=10$. The asymptotic crack length reached is given by the solution of the equation $\dot{x}_2(t)=0$ i.e.

$$\sqrt{\frac{2}{\pi}}\frac{F}{\sqrt{x_2+L}}=g(0)=\sqrt{2\mu\sigma_0\delta}.$$

Hence the terminal crack size (measured from the starting value $x_2=0$) is given by

$$x_2=\frac{F^2}{\pi\mu\sigma_0\delta}-L. \tag{4.7}$$

Hence, for any crack motion to occur, F must exceed $\sqrt{(\pi\mu\sigma_0\delta L)}$.

Consideration of a constant load

$$p(x,t)=F.H(t),\ \ x<x_2(t) \tag{4.8}$$

leads to the following equation for $x_2(t)$:

$$x_2(t)=\int_{t_{min}}^{t} g^{-1}(2\sqrt{\frac{2}{\pi}}F\sqrt{ct})dt,\ \ t\geq t_{min}, \tag{4.9}$$

where t_{min} is defined by the equation

$$t_{min}=\frac{\pi\mu\sigma_0\delta}{4F^2c}. \tag{4.10}$$

A graph of $x_2(t)$ vs t for this choice of $p(x,t)$ and for $\alpha=0.01$, $F=0.5$ is exhibited in Figure 3: its gradient is tending to c. The slightly serrated effect in this and the subsequent figure can be smoothed out by increasing the number of quadrature intervals used to evaluate the integrals in equations (4.9) and (4.13). The choice of constant loading differs from point loading in that the initiation time t_{min} can be made as small as desired by increasing the stress level F in the former case.

If $p(x,t)$ is modified so that the loading starts at $-L$ (instead of at minus infinity) i.e. if

$$p(x,t)=\begin{cases}F.H(t), & -L<x<x_2(t),\\ 0, & \text{otherwise},\end{cases} \tag{4.11}$$

then equation (4.9) holds up to time t_s defined by

$$x_2(t_s)=ct_s-L, \tag{4.12}$$

after when

$$\int_{x_2(t_s)}^{x_2(t)} \frac{dx_2}{g^{-1}(2F\sqrt{\frac{2}{\pi}}\sqrt{x_2+L})}=t-t_s,\ \ t\geq t_s. \tag{4.13}$$

The gradients of these curves also tend to c, as can be seen in Figure 4, which is a plot for the values $\alpha=0.01$, $F=0.5$, $L=10$. For there to be two distinct solution branches, t_{min} must not exceed $\frac{L}{c}$, or alternatively, F must not exceed $\sqrt{(\frac{\pi\mu\sigma_0\delta}{L})}$.

The leading order Kostrov approximation given by equations (1.7) and (1.8a,b) can be demonstrated to break down as V tends to the transition velocity by the use of Green's function methods. The inner problem for the supersonic case is treated in section 2 of the next chapter, but no attempt is made to perform matched asymptotic expansions. Finally, the choice of inner variables for this chapter is one of many that could be made, based on different powers of ε: perhaps the particular one in the first section could be considered to be the natural one.

Figure 5.1:
K variation with relaxation time

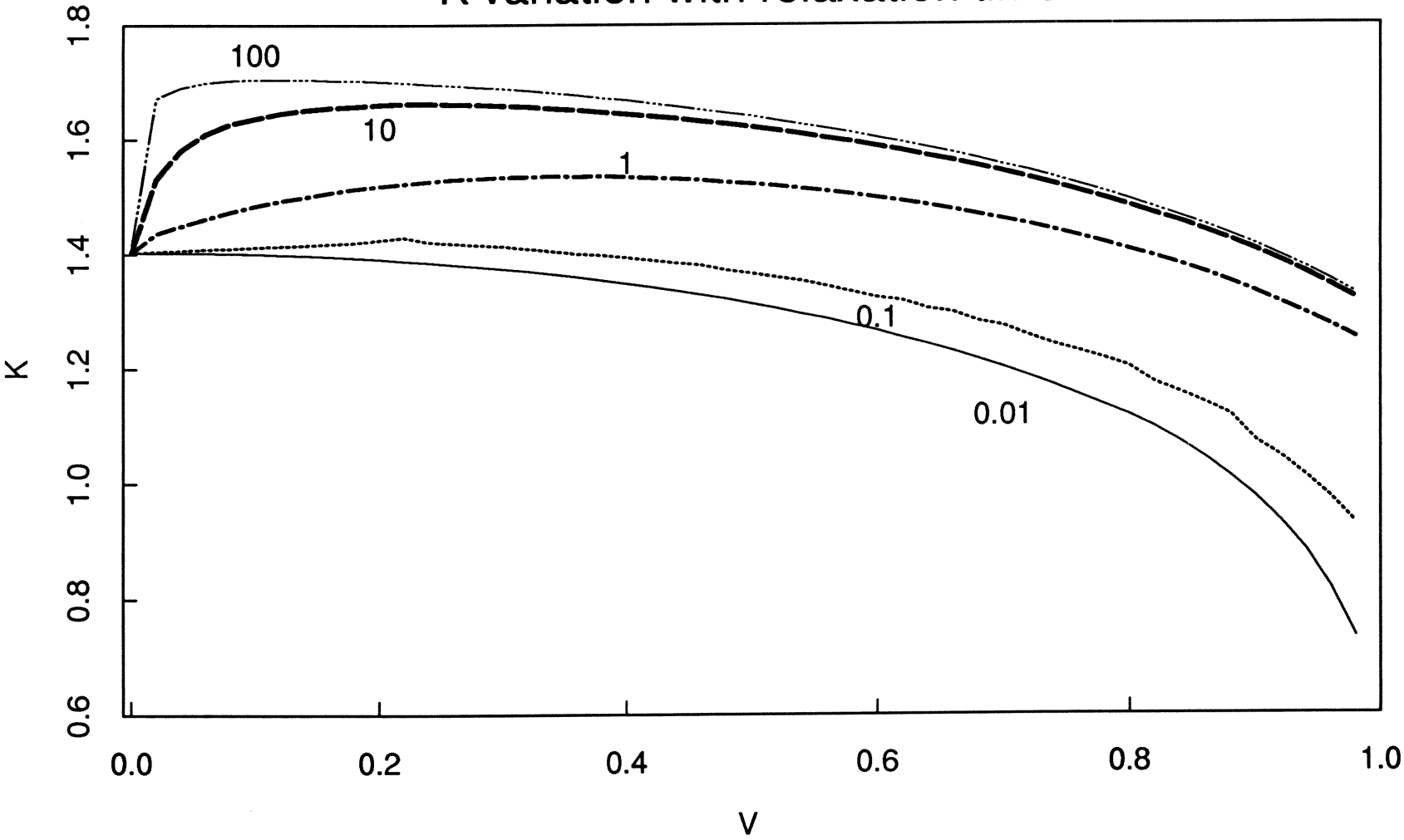

Figure 5.2: delta function loading

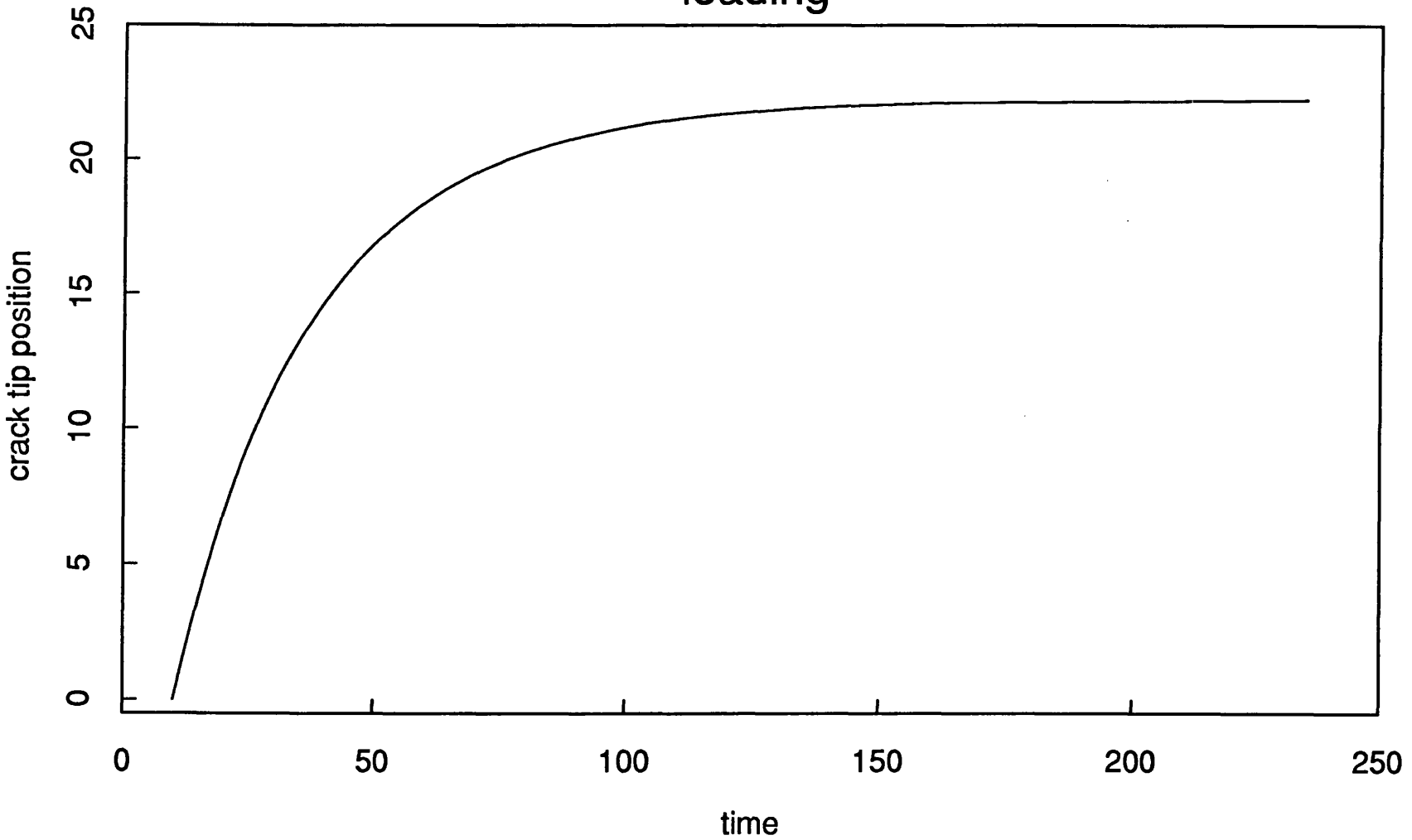

Figure 5.3: constant loading

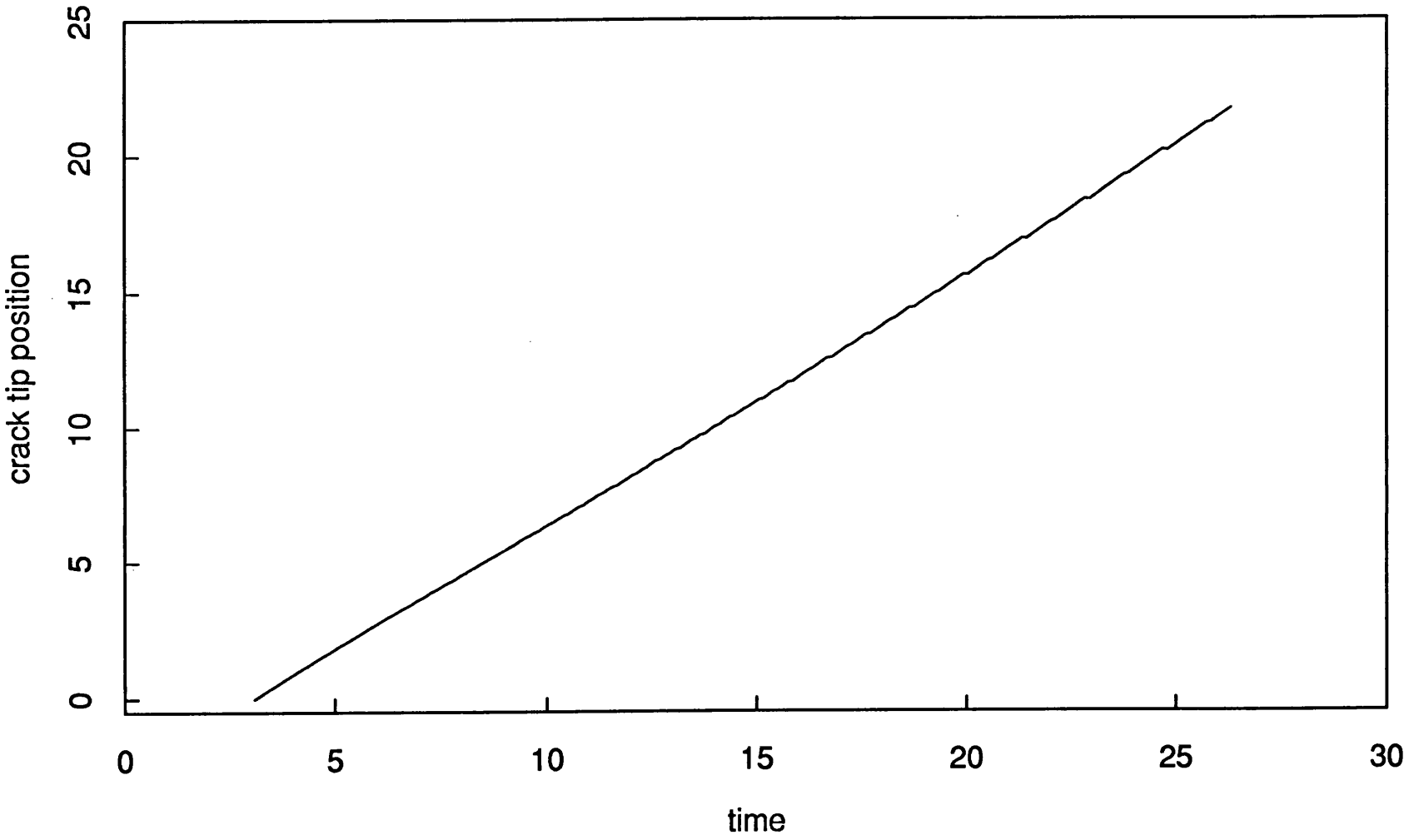

Figure 5.4: step function loading

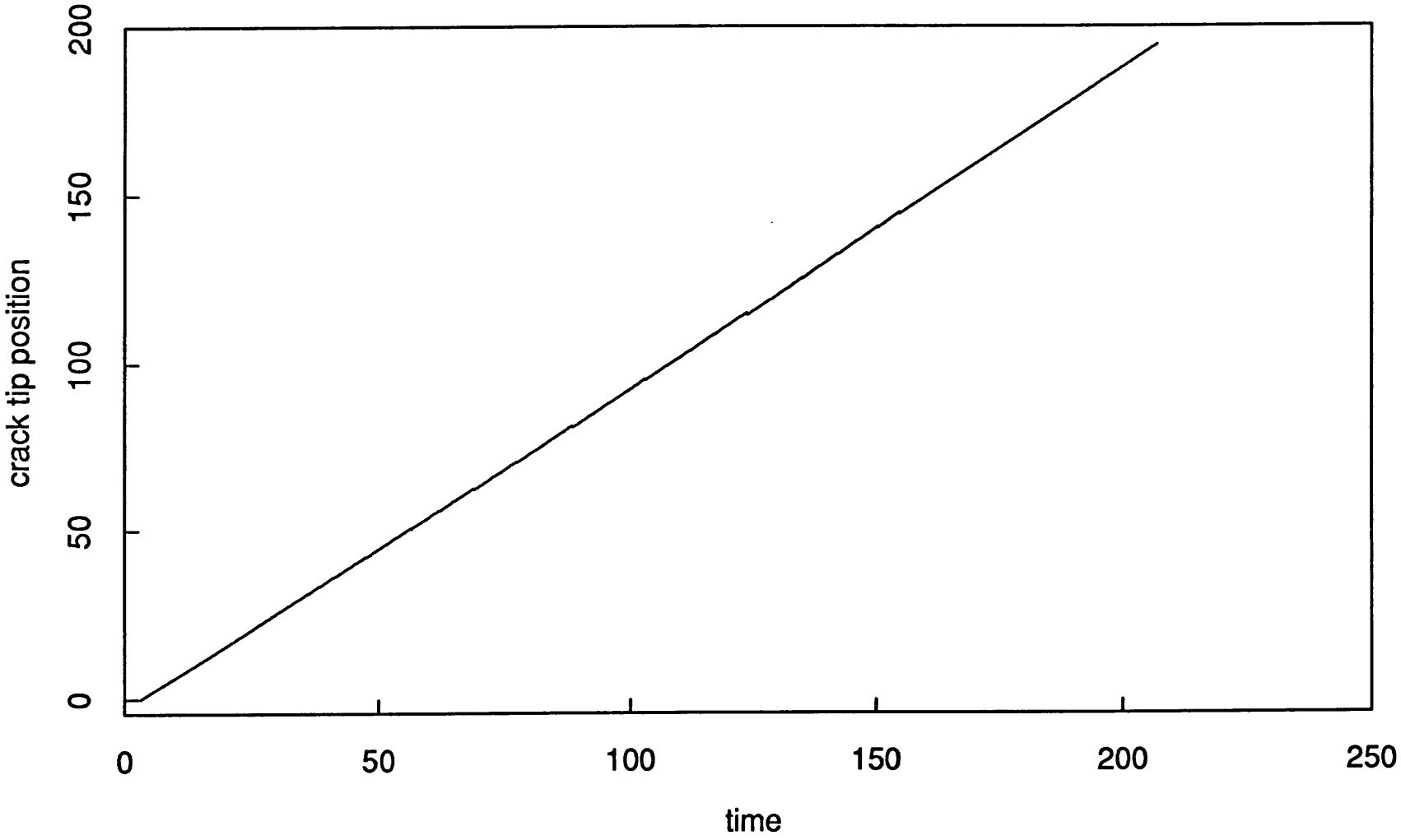

Chapter 6 - Aspects of dynamic crack growth in the standard linear solid and power law material.

1. The standard linear solid: stress and displacement formulae for the traction loading problem.

Willis (1967b) gives explicit formulae for stress and displacement for a crack moving under conditions of antiplane strain in a standard linear solid i.e. for the same problem considered in chapter 2 for the Maxwell liquid. The significant difference in the case of the standard linear solid is that the solution branches at the long-time wave speed. Also the scale of the computations is larger due to the presence of irreducible multiple integrals - this is particularly so in the range above the long-time wave speed where triple integrations are involved. Throughout this section we shall keep to Willis' original notation.

As they stand, Willis' formulae are unsuitable for immediate use as they contain integrable singularities. On use of appropriate changes of variable, the formula for displacement for $0<V<\frac{c}{\sqrt{1+f}}$ becomes

$$w(-s,0)=\frac{1}{\pi\mu\sqrt{(1-\frac{V^2}{c^2})}}(\text{auxel(s)}$$

$$+(\text{auxel(s)})*((a+(1+f)b)\exp(as)_1F_1\{\frac{1}{2},1,-(a+b)s\}$$

$$+\frac{a+b}{2}\exp(as)_1F_1\{\frac{3}{2},2,-(a+b)s\})) \tag{1.1}$$

where $g*h$ denotes the convolution

$$g*h=\int_0^s g(s')h(s-s')ds', \tag{1.2}$$

$$\text{auxel(s)}=\int_{-\infty}^{0}\log\left|\frac{\sqrt{s}-\sqrt{-u}}{\sqrt{s}+\sqrt{-u}}\right|f(u)du, \tag{1.3}$$

$$ {}_1F_1\{\frac{1}{2},1,-(a+b)s\}=\frac{2}{\pi}\int_0^{\frac{\pi}{2}}\exp(-s(a+b)\sin^2\theta)d\theta \qquad (1.4) $$

and

$$ {}_1F_1\{\frac{3}{2},2,-(a+b)s\}=\frac{-4}{\pi}\int_0^{\frac{\pi}{2}}\sin^2\theta\exp(-s(a+b)\sin^2\theta)d\theta. \qquad (1.5) $$

The quantities a and b which appear in this section are defined as functions of crack velocity V by the formulae

$$ a=\frac{\frac{V^2}{c^2}(1+f)-1}{(1-\frac{V^2}{c^2})V\tau} \qquad (1.6a) $$

and

$$ b=\frac{1}{V\tau}, \qquad (1.6b) $$

where $c=\sqrt{\frac{\mu}{\rho}}$ is the short-time wave speed.

For computational purposes, it is best to rewrite the second term in the convolution in (1.1) as a single function. In the short-time elastic limit i.e. $\tau\rightarrow\infty$, it proves expensive to calculate $w(-l,0)$ to high accuracy because this second term is tending to a delta function. The crack face tractions $f(u)$ only appear in the integral defined by equation (1.3) - for the purpose of calculations, the step function loading used in chapter 2 is used here. This has the advantage of making feasible the analytic evaluation of the integral previously referred to, and hence reducing computing time.

Adhering to the same traction function $f(u)$, the corresponding formula for $\frac{c}{\sqrt{1+f}}<V<c$ becomes

$$ w(-s,0)=\frac{-2\sigma_0}{\sqrt{\pi}\mu\sqrt{(1-\frac{V^2}{c^2})}}((1+f)b+\int_0^s ds)v(s), \qquad (1.7) $$

where

$$v(s)=\int_0^{\sqrt{as}} \exp(-\frac{b}{a}u^2)\{(1+\frac{F}{\sigma_0}\mathrm{erf}(u^2-as+ad)^{1/2}H(u^2-as+ad)$$

$$-\frac{F}{\sigma_0}\mathrm{erf}(u^2-as+ad+aL)^{1/2}H(u^2-as+ad+aL)\}du \qquad (1.8)$$

and

$$\frac{F}{\sigma_0}=\frac{\mathrm{erf}\sqrt{ad}}{\mathrm{erf}\sqrt{a(d+L)}-\mathrm{erf}\sqrt{ad}}. \qquad (1.9)$$

The last equation ensures zero stress intensity at the crack tip. For the low speed range, this formula is replaced by the static relation

$$\frac{F}{\sigma_0}=\frac{\sqrt{d}}{\sqrt{d+L}-\sqrt{d}}. \qquad (1.10)$$

As in chapter 2, a plot of nominal stress intensity factor vs velocity is made, where once again nominal $K=2\sqrt{\frac{2}{\pi}}F\sqrt{L}$ but this time F is defined differently in the two velocity ranges: (1.10) applies for $V\le\frac{c}{\sqrt{1+f}}$ and (1.9) for $V\ge\frac{c}{\sqrt{1+f}}$. This was done for the parameter values

$$f=\mu=c=1,\ L=8,\ \sigma_0=5,\ \delta=1$$

and for various values of the non-dimensional combination $\alpha=\frac{c\tau}{L}$. This plot is exhibited in Figure 6.1. The work-rate of the loading stresses appears in pictorial form in Figure 6.2 for the same parameter scheme: there appears to be a smooth transition between the two velocity regimes, unlike in the nominal K plot. Figures 6.3 and 6.4 illustrate Griffith convergence for nominal K vs V and work-rate vs V respectively. The parameters for these curves are as before except that now $\alpha=1$ and σ_0, δ vary such that $\sigma_0\delta=2\gamma=5$. Near convergence, the curves appear piecewise constant, due to the lower tolerance that has to be taken in the adaptive quadrature routine to achieve an acceptable computing

time. The routine itself is based on Simpson's rule, the number of points being doubled at each iteration, and convergence is taken to occur when the relative error based on the last two estimates is less than a pre-specified tolerance.

2. The remote loading problem: supersonic case.

The problem described in this section is the supersonic (i.e. $V>\frac{c}{\sqrt{1+f}}$) analogue of the inner problem from the matched expansion set-up of chapter 5. Unlike there, the notation of the previous section will be employed (Appendix 4 gives the correspondence between the two notations). Once again the displacement will be in two parts: the first arising from the cohesive forces in the craze zone, and the second from the remote loading whose influence appears through a singularity of strength k (though this is no longer a K-field as considered in the previous chapter, the viscoelasticity having a different effect in this higher velocity range). The strength of the singularity is still such that the local net stress intensity factor from the two sources is zero. The first of these contributions can be derived from equations (1.7) to (1.9), taking F, the non-cohesive crack face traction, to be zero. In this section, the derivation of the second contribution is concentrated upon.

As a starting point, Willis' (1967b) Wiener-Hopf equation in the absence of all crack face tractions is

$$-\frac{1}{2}iVp\hat{G}_1(-Vp)\gamma(p)A(p)=\Phi_+(p), \tag{2.1}$$

where

$$\hat{G}_1(-Vp)=\frac{2\mu(1+ipV\tau)}{iVp(1+f+iVp\tau)}, \tag{2.2}$$

G_1, A and Φ_+ are as defined in chapter 2 and

$$\gamma(p)=(1-\frac{V^2}{c^2})^{\frac{1}{2}}p(p+ia)^{\frac{1}{2}}(p-ib)^{-\frac{1}{2}}. \tag{2.3}$$

Equation (2.1) can easily be factored as

$$-\mu\frac{1+ipV\tau}{1+f+ipV\tau}\frac{p}{(p-ib)_-^{\frac{1}{2}}}(1-\frac{V^2}{c^2})^{\frac{1}{2}}A(p)=\frac{\Phi_+(p)}{(p+ia)_+^{\frac{1}{2}}} \tag{2.4}$$

in a strip. If both sides are equated to $\frac{k}{p}$, where $k\in\mathbf{C}$, a stress of appropriate singularity is generated: in this case,

$$\sigma_{23}(x,0)=\frac{k}{2\pi}\int_{-\infty}^{\infty}e^{-ipx}\frac{(p+ia)_+^{\frac{1}{2}}}{p}dp. \tag{2.5}$$

Differentiation of the integral with respect to x allows evaluation of $\sigma_{23}(x,0)$ to within a constant. Once k is known, this constant can be determined by an asymptotic result to be zero. To produce a net local stress intensity factor of zero, k has to be chosen such that

$$k=-\sigma_0\sqrt{\frac{i}{a}}\,\mathrm{erf}(\sqrt{al}). \tag{2.6}$$

The origins of the error function in (2.6) are in the stress intensity factor derived from the cohesive stresses alone, $K_{-\sigma_0}$. This has explicit velocity dependence as opposed to depending on V only through l, and is defined by

$$K_{-\sigma_0}=\sqrt{\frac{2}{a}}\sigma_0\mathrm{erf}(\sqrt{al}). \tag{2.7}$$

As $V\to\frac{c}{\sqrt{1+f}}$, $a\to 0$ and $K_{-\sigma_0}\to\sigma_0\sqrt{\frac{8l}{\pi}}$, which was to be expected in view of chapter 5.

$\sigma_{23}(x,0)$ eventually turns out to be defined by

$$\sigma_{23}(x,0)=\frac{k}{\sqrt{\pi i}}\{\frac{\exp(-ax)}{x^{\frac{1}{2}}}+\sqrt{a\pi}\,\mathrm{erf}(\sqrt{ax})\},\quad x>0. \tag{2.8}$$

and tends to $-\sigma_0\mathrm{erf}(\sqrt{al})$ as $x\to\infty$.

The contribution to w arising from the remote loading is

$$\frac{-k}{2\pi\mu(1-\frac{V^2}{c^2})^{\frac{1}{2}}}\int_{-\infty-i0}^{\infty-i0} e^{-ipx}\frac{p-i(1+f)b}{p^2(p-ib)^{\frac{1}{2}}}dp. \tag{2.9}$$

For evaluation purposes, an infinite rectangular contour symmetric about the y-axis (open-ended at the side where it would otherwise pass through the branch) is used. First, it is best to make a change of variable so that the branch point corresponding to the square root is independent of local parameters in force at any given time. Then the equation

$$w(-l,0;V)=\frac{\delta}{2} \tag{2.10}$$

is solved to obtain $l=l(V)$ for various values of $\alpha=\frac{c\tau}{\delta}$, generating plots of $K_{-\sigma_0}$ vs V which are exhibited in Figure 6.5. The other parameter values for this particular graph are $c=f=\mu=1$. This computation proves to be much more involved than the subsonic equivalent presented in the previous section. In view of this, the lowest value of α for which a curve is exhibited is 1. After deforming the contour of equation (2.9), special integration meshes are needed to cut down on the number of function evaluations necessary to work out the double integral. The thesis of Mendes (1988) contains a varied collection of such meshes for different kinds of integrand behaviour at zero and infinity as well as mixtures of these, in addition to certain asymptotic optimality results which are difficult to apply directly in this complex analytic context.

The obscuring effects of the complex-valued nature of the integrand contained in (2.9) will be removed temporarily in this discussion for the purpose of demonstrating the mesh usage choices. Then the pertinent integral is

$$\int_q^\infty \frac{e^{-bly}}{y^{3/2}}dy \tag{2.11}$$

where $0<q<1$ and $bl=\frac{l}{V\tau}$.

Depending on the range of the non-dimensional combination *bl*, either an exponential or power mesh is chosen. These are defined in the following way, assuming Simpson's rule is being used. The exponential mesh of n points on $[0,\infty]$, for use with the integral of a function which behaves like $\exp(-\alpha y)$ as $y\rightarrow\infty$, is defined by

$$a_i=\frac{4}{\alpha}\ln(\frac{n}{n-i}),\quad i=0,1,2,..,n-1. \tag{2.12}$$

The power mesh of n points on $[1,\infty]$, where now the integrand behaves like $\frac{1}{y^{3/2}}$ as $y\rightarrow\infty$, is defined by

$$a_i=(\frac{n}{n-i})^{\frac{8}{3}},\quad i=0,1,2,..,n-1. \tag{2.13}$$

This second mesh is a particular example of a more general formula for decaying powers. For *bl* less than some sufficiently small number, the overriding character of the integrand is that of a decaying power; therefore the mesh defined by (2.13) is an appropriate choice. Above this threshold, the influence of the exponential is greater than that of the power, necessitating the use of (2.12). Some computing time can be saved for certain parameter values by employing an upper threshold for *bl*, above which the integral is taken to be zero: this is acceptable because then the parts of the contour integral which are of essentially similar character to (2.11) are negligible compared with other terms present in the displacement formula.

For small values of $\alpha=\frac{c\tau}{\delta}$, the part of the displacement which arises from the non-homogeneous sub-problem is expensive to compute to high accuracy from equations (1.7) to (1.9) because many iterations within the adaptive quadrature

routine are necessary. Too high a tolerance can lead to the artefact of local non-monotonicity. Elimination of this phenomenon by decreasing the tolerance is prohibitive, so a cubic spline is assembled through a number of uniformly spaced points covering the bisection search interval for equation (2.10).

The particular motivation for carrying out this investigation is to see whether any of the K vs V curves increase in some or all of the supersonic regime. Such behaviour does occur in Willis (1967b) for a traction loading problem and Barenblatt fracture criterion, for certain ranges of the appropriate α-type parameter. In that case, exponential loading was considered. In the course of this work, the case of step function loading was considered for Willis' set-up and yielded similar insights. The same trend manifests itself in the nominal K vs V curves of Figure 6.5. However, the nature of the loading here is completely different in character.

3. The power law material.

Using a combination of notation from Willis (1967b) and Walton (1987), the constitutive relation of the power law material is taken to be

$$G_1(t)=2\mu_\infty(1+(\frac{\tau}{t})^n),\quad 0<n<1 \tag{3.1}$$

where μ_∞ is the material's long-time modulus and τ is a relaxation time. It is convenient to define m by the equation

$$m+n=1. \tag{3.2}$$

Now $\hat{G}_1(p)$, the Fourier transform of $G_1(t)$ on the positive real line as introduced in chapter 2, can be evaluated to be

$$\hat{G}_1(p)=2\mu_\infty\frac{i}{p}(1+(-ip\tau)^n)\Gamma(m) \tag{3.3}$$

by first evaluating in the first quadrant and extending the result to the upper half plane by use of the identity theorem / analytic continuation ($\hat{G}_1(p)$ is a "+" function in view of its definition in terms of an integral). The following equations utilise chapter 2 notation.

The function $\gamma(p)$ satisfies the equation

$$\gamma(p)=p\frac{[b+a(ip)^n]^{1/2}}{[1+a(ip)^n]^{1/2}}, \tag{3.4}$$

where a,b and c are defined by the equations

$$a=(V\tau)^n\Gamma(m), \tag{3.5a}$$

$$b=1-\frac{V^2}{c^2}, \tag{3.5b}$$

$$c^2=\frac{\mu_\infty}{\rho}. \tag{3.5c}$$

Assuming a crack face traction loading problem, the Wiener-Hopf equation for $f(x)=g(\lambda)e^{-i\lambda x}$ can be written in the form

$$-2\mu_\infty p[1+a(ip)^n]^{1/2}[b+a(ip)^n]^{1/2}A(p)=\Phi_+(p)+\frac{g(\lambda)}{i(p-\lambda)}. \tag{3.6}$$

The factorisation of equation (3.6) differs depending on whether $V<c$, the subsonic case, or $V>c$, the supersonic case. The complex plane must be cut for the function

$$\log(z)=\ln|z|+i\arg(z); \tag{3.7}$$

if this is done along the negative imaginary axis, then

$$-\frac{\pi}{2}<\arg(z)<\frac{3\pi}{2} \tag{3.8}$$

and this choice of branch cut is consistent with $\hat{G}_1(p)$ being a "+" function ($\hat{G}_1(-Vp)$ is consequently a "-" function). It can be shown that neither of the square root factors has zeros in the cut plane when $V<c$, and so both are analytic in a lower half plane. However, for $V>c$, $[b+a(ip)^n]^{1/2}$ must be split mul-

tiplicatively. The decomposition cannot easily be guessed, so the function must be split into integrals by a result found in the first chapter of Noble (1958) - the logs and exponentials arise because this is a corollary to an additive decomposition theorem, as used in chapter 5.

The function $[b+a(ip)^n]^{1/2}$, in the supersonic case, has branches on the imaginary axis described by $\mathrm{Im}(p)>0$, $\mathrm{Im}(p)<-(\frac{-b}{a})^{\frac{1}{n}}$. For any choice of $c,d\in\mathbf{R}$ such that $-(\frac{-b}{a})^{\frac{1}{n}}<c<d<0$,

$$f(p)=f_+(p)f_-(p), \tag{3.9}$$

where

$$f_+(p)=\exp\{\frac{1}{2\pi i}\int_{-\infty+ic}^{\infty+ic}\frac{\log[b+a(i\xi)^n]^{1/2}d\xi}{\xi-p}\}, \tag{3.10}$$

$$f_-(p)=\exp\{\frac{-1}{2\pi i}\int_{-\infty+id}^{\infty+id}\frac{\log[b+a(i\xi)^n]^{1/2}d\xi}{\xi-p}\} \tag{3.11}$$

and f_+, f_- are analytic for $\mathrm{Im}(p)>-(\frac{-b}{a})^{\frac{1}{n}}$, $\mathrm{Im}(p)<0$ respectively.

Although equation (3.6) can now be formally factored, it is likely that calculations for the supersonic case are likely to be computationally prohibitive on existing facilities. Therefore, to conclude this section, an investigation parallel to that of the inner problem of chapter 5 (for the standard linear solid) will be made i.e. a remote-loading, subsonic, steady-state combination.

The power law material does not have a finite short-time modulus, as can be seen from its constitutive equation (in shear). This effectively restricts checking based on elastic limits to the long-time case (the limiting case $n=0$ also yields a linear elastic constitutive relation).

The choice of $\beta(t)$ corresponding to equation (5.2.22) for the standard linear solid is

$$\beta(t)=t^{-n},\ 0<n<1. \tag{3.12}$$

The prescription of section 2 of chapter 5 is used to generate K vs V curves for various values of $\alpha=\frac{\sqrt{2}c\tau}{\delta}$ with $n=0.5$ and $\sigma_0=10$, $\delta=1$ fixed (also, throughout this section, $c=\frac{1}{\sqrt{2}}$, $\mu=0.5$). These are shown in Figure 6.6. As $\alpha\rightarrow 0$, it can be seen that the curves are approaching typically elastic behaviour as described by equation (5.2.25). The approach to the static value ($V\rightarrow 0$) is included for $\alpha=1$ only: in this case $K(0)\approx 3.16$. For larger values of α, the curves are increasing in nature unlike the corresponding ones for the standard linear solid: this is connected with the fact that there is no short-time elastic K vs V upper bound for the power law material. It does not appear that the curves tend to some other limiting case as $\alpha\rightarrow\infty$.

The curves in Figure 6.7 demonstrate n-variation for the values $n=0.1,\ 0.3,\ 0.5$ (throughout, $\sigma_0=10$, $\delta=\alpha=1$). For higher values, non-uniqueness is found to occur: not only are the solutions that fit into the displayed progression found, but also others. Curves for these values are not displayed: work on these solutions is currently in progress using the Pitcon (University of Pittsburgh continuation) program. Walton (1987) draws attention to the breakdown in monotonicity of a local energy release rate for certain ranges of n with this particular material: this, however, happens for low values of n in his case. There are many differences between Walton's model and the one presented here, the most prominent of which is the type of loading used.

Finally, to ascertain whether or not the K vs V curves tend to a Griffith limit

when σ_0, δ are varied subject to $\sigma_0\delta=10$ (this was done with the parameters $n=0.5$, $\tau=1$), Figure 6.8 was produced. Although there are other non-dimensional combinations apart from α that are affected by the σ_0, δ variation, there is a tie-up between the behaviour as $\sigma_0\to\infty$ with $\sigma_0\delta$, α fixed, and that for $\alpha\to\infty$ with σ_0, δ fixed (i.e. a short-time elastic limit). Therefore the apparent lack of a Griffith limit is also attributable to the infinite short-time elastic modulus.

Figure 6.1:
alpha varies

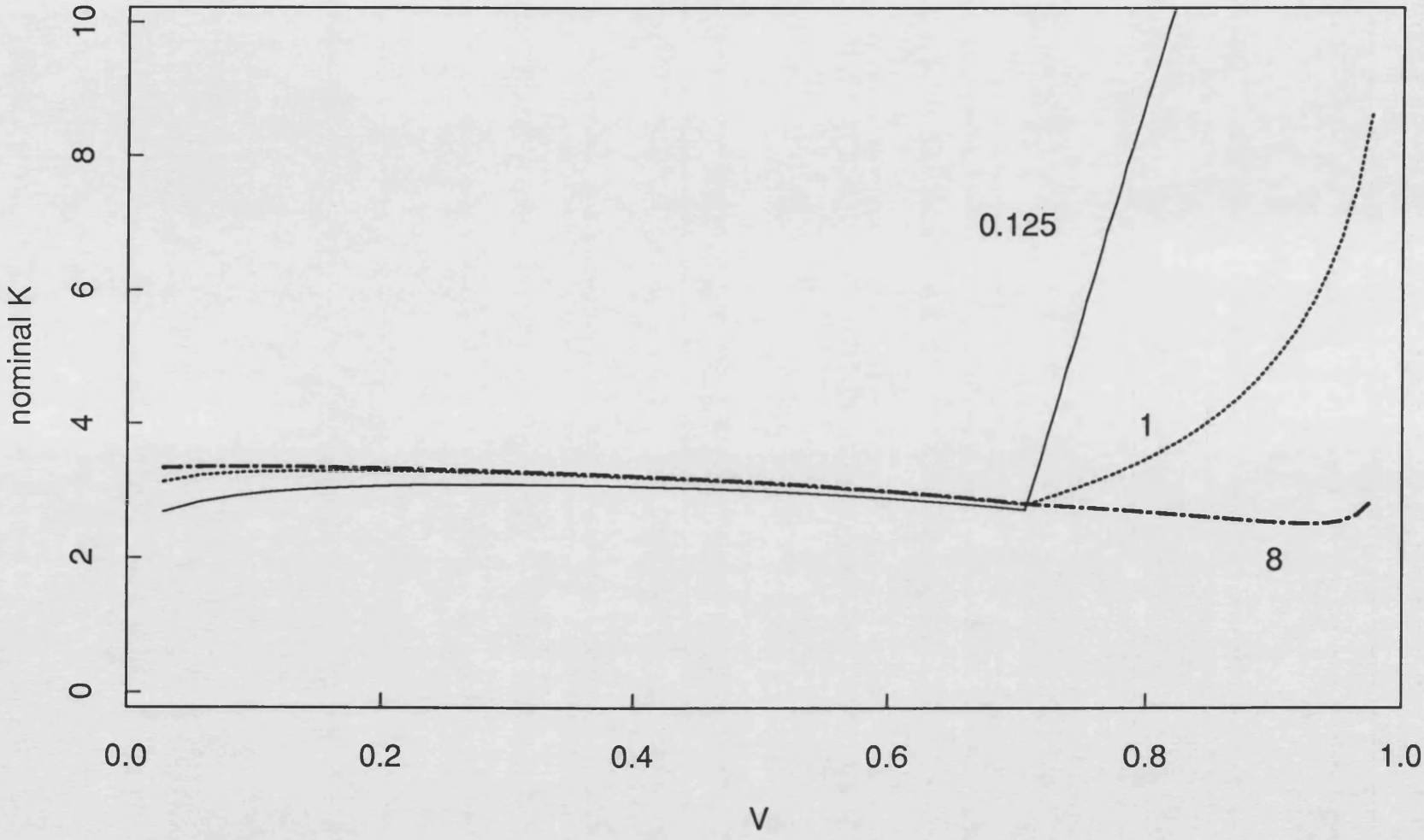

Figure 6.2:
alpha varies

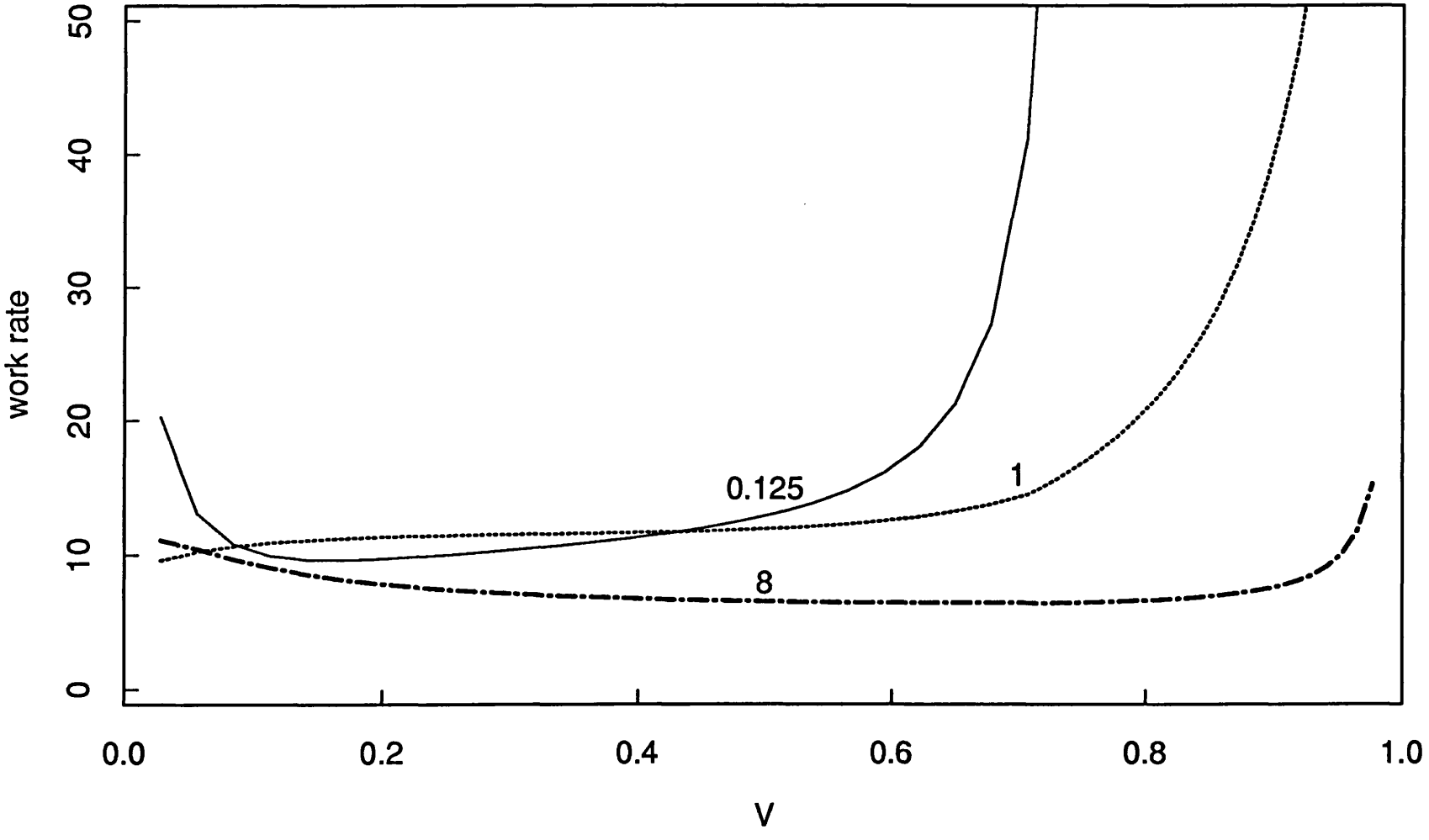

Figure 6.3:
Griffith limit

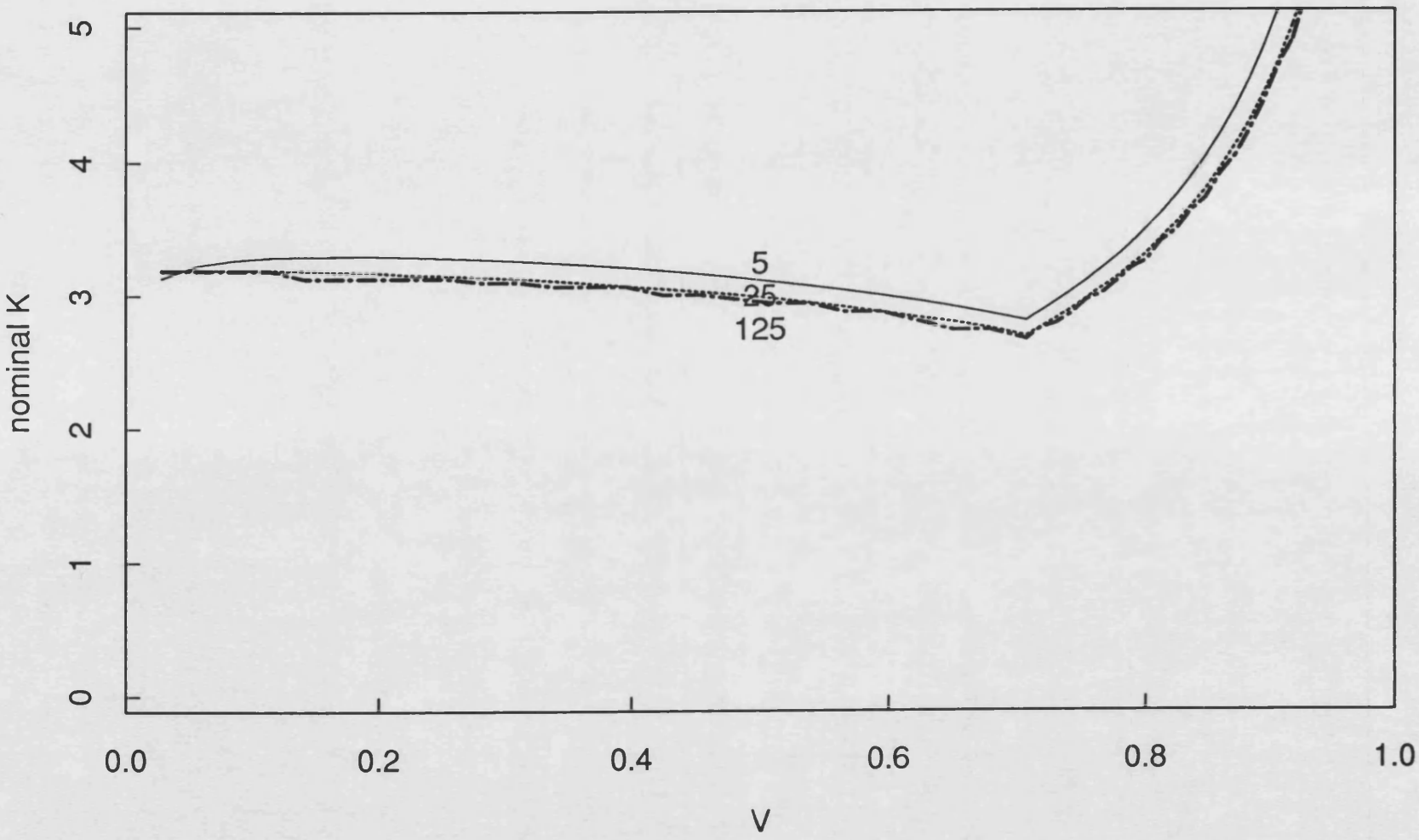

Figure 6.4:
Griffith limit

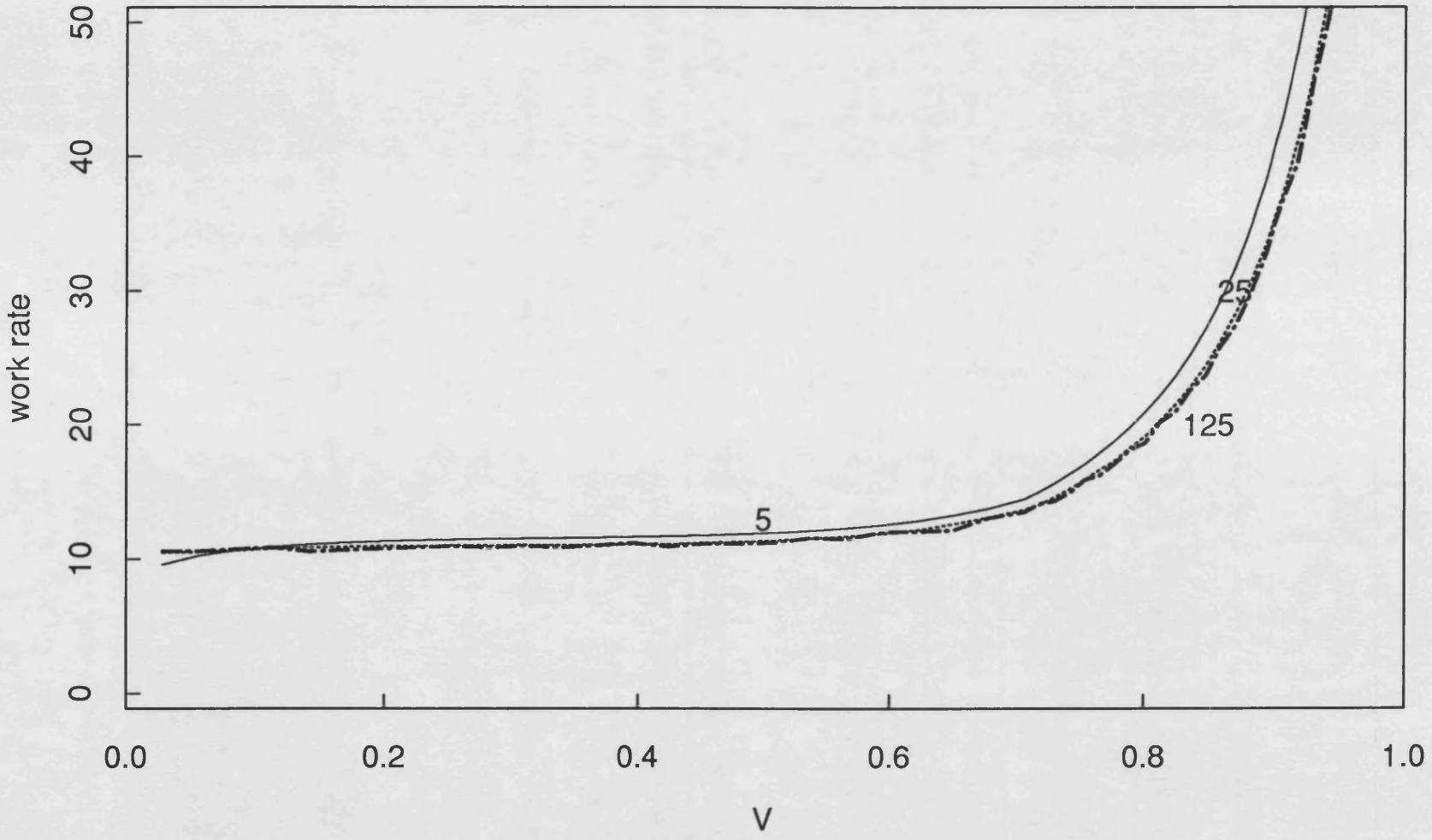

Figure 6.5:
alpha varies

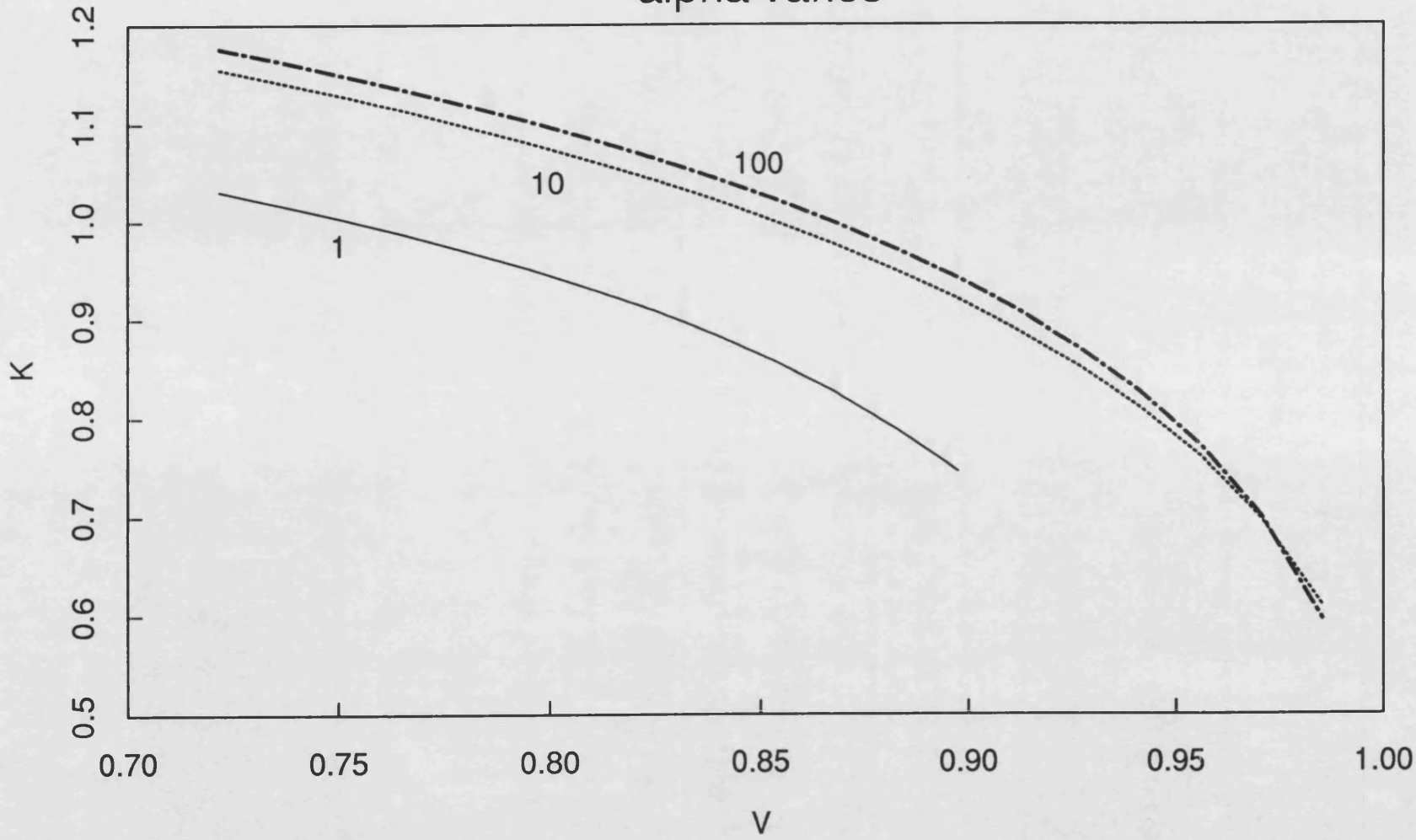

Figure 6.6:
alpha varies

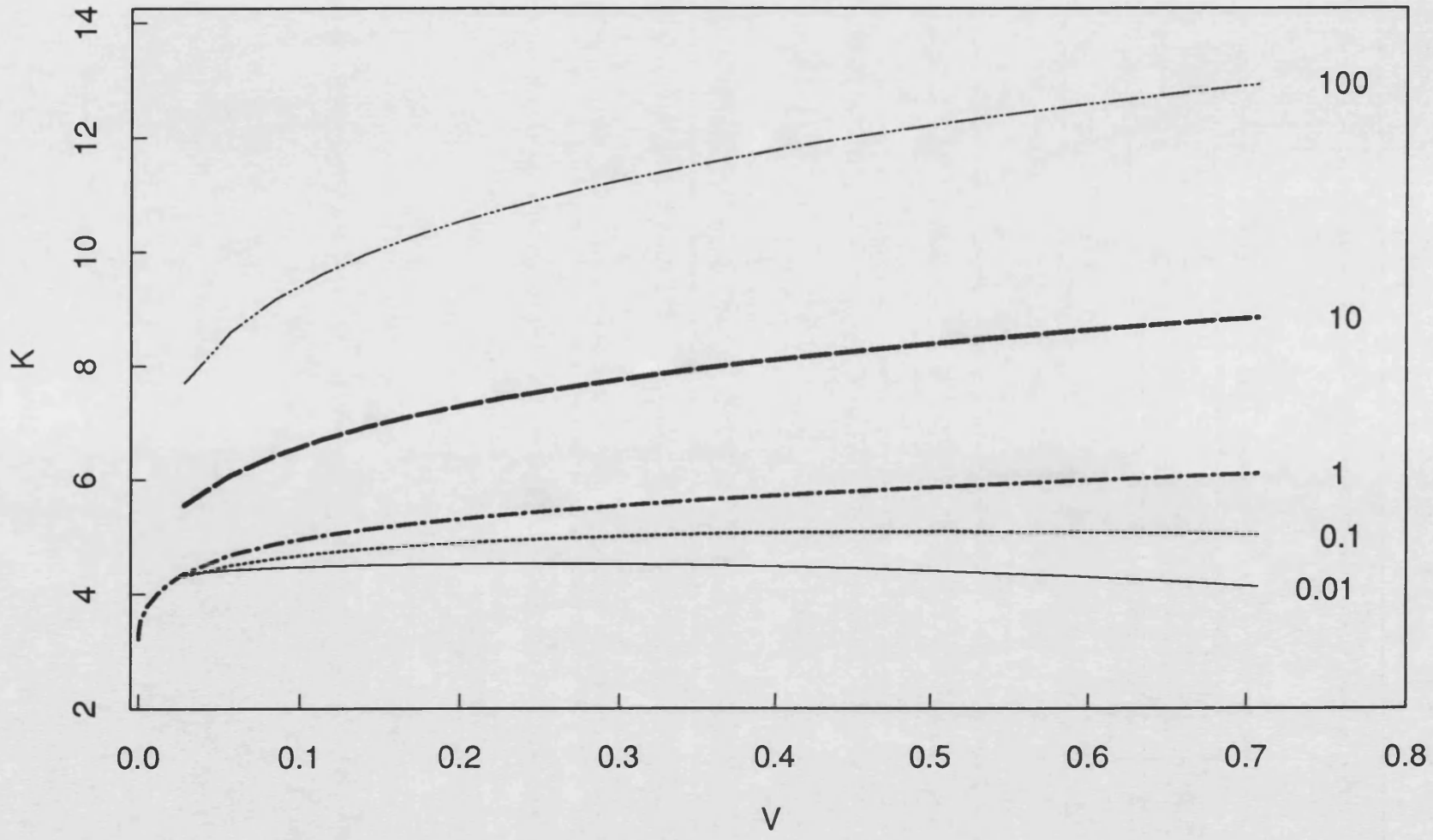

Figure 6.7:
n varies

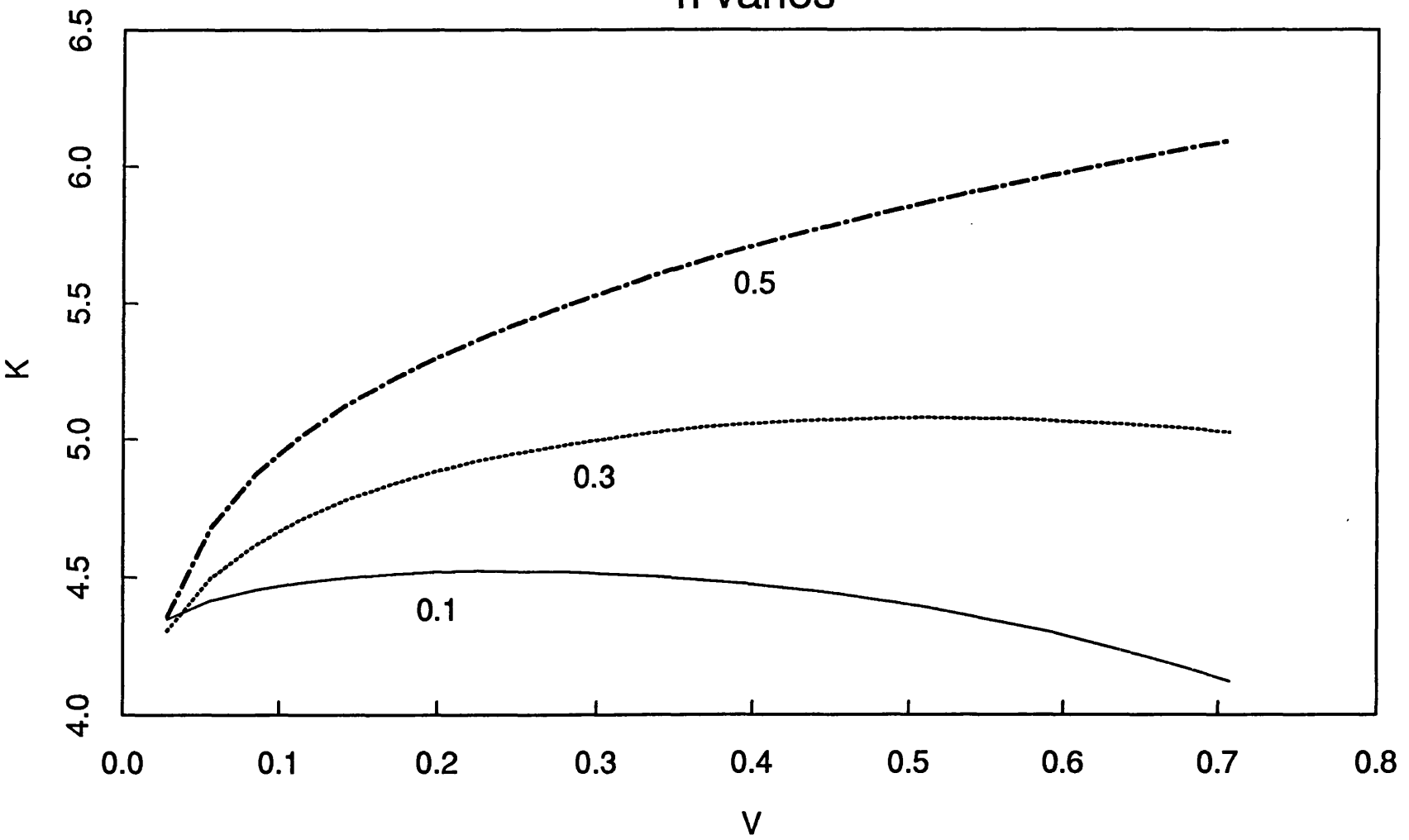

Figure 6.8:
cohesive stresses vary

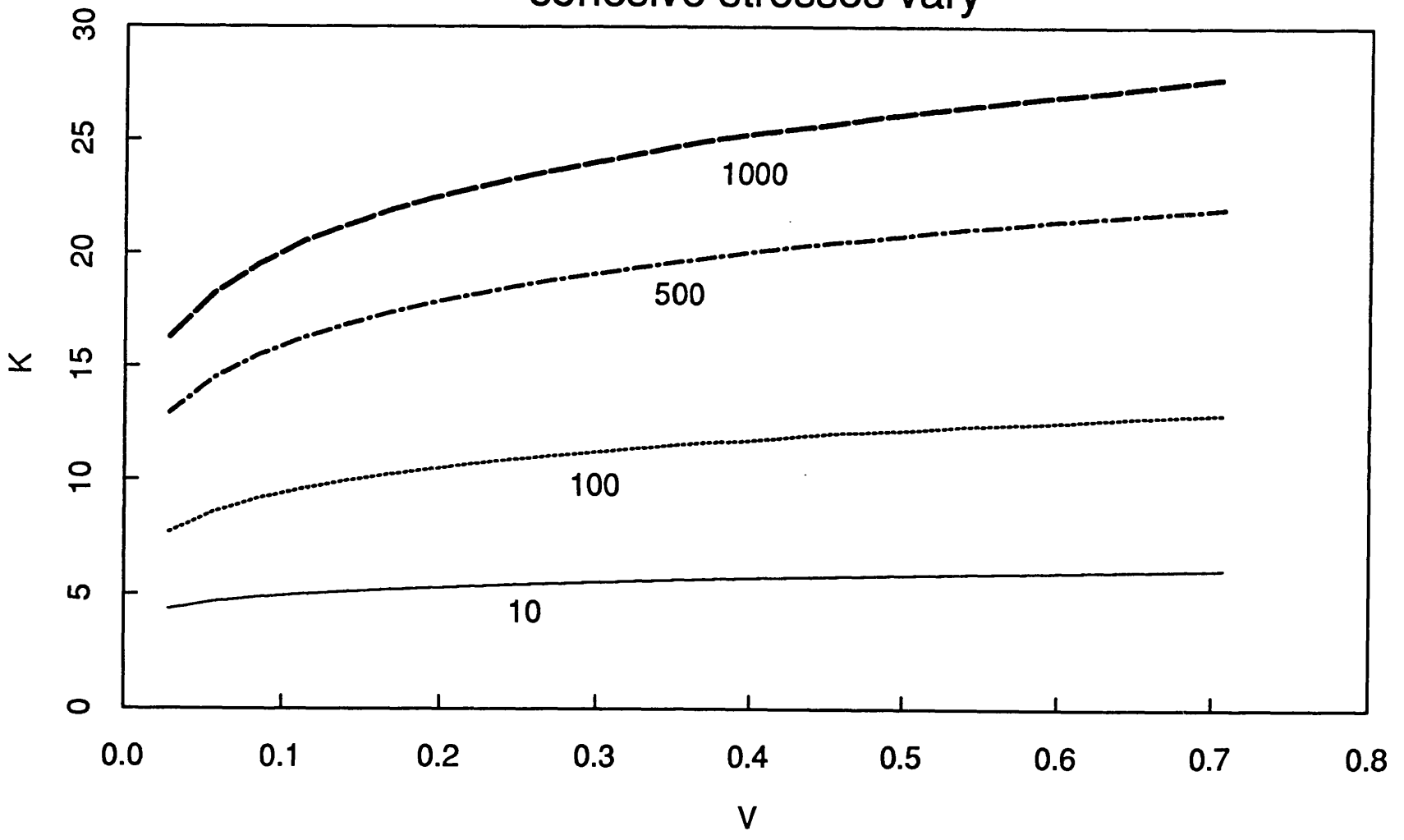

Conclusions and comments on possible future work.

This thesis has addressed a variety of time-dependent fracture problems in linear viscoelastic materials, taking into account the effect of finite, as opposed to infinitesimal, craze zones throughout. These problems naturally fall into two categories depending on whether the inertia term is kept or not, dynamic and quasi-static. The results from investigations in the latter category (chapters 3 and 4) lead to the conclusion that, in the presence of a craze zone, there is a range of loading in which quasi-static crack motion is possible. This is not the case if a sharp crack in a viscoelastic material is considered; also quasi-static crack motion in an elastic material is not possible whether or not a craze zone is present (dynamic terms must be allowed for from the onset of motion). These conclusions seem to be relatively independent of the precise geometry and loading chosen, in view of the rather different models of chapters 3 and 4 yielding similar conclusions.

Steady-state crack propagation with crack face traction loading was investigated in chapter 2 for the Maxwell liquid and in chapter 6 for the standard linear solid. The critical crack opening displacement fracture criterion was used to generate plots of nominal stress intensity factor and work-rate of applied tractions against crack velocity. It can be seen that the curves corresponding to finite craze zones deviate considerably from those approaching the sharp crack limit.

Accelerating crack growth in the subsonic crack velocity range of the standard linear solid is treated in chapter 5 using the method of matched asymptotic expansions. It is believed that the matching could easily be extended to the supersonic regime, and an attempt is made to deal with the inner problem for

this case in section 2 of chapter 5. Unfortunately, the values of K needed for matching are the ones closest to the long-time elastic limit and these prove to be the most troublesome to compute to reasonable accuracy: further work to obtain these particular values would be necessary before matching was attempted. There is, however, no conceptual problem as regards carrying out the matching. The main problem to overcome lies in the breakdown of the subsonic matching just before the transition wave speed.

The analogue of the matched asymptotic expansions inner problem of chapter 5 is treated for the power law material in the final section of chapter 6. Its two parameter relaxation function does not fall into the same class as those of the other materials considered (i.e. the class of linear combinations of step functions and exponentials). Together with the fact that the power law material does not possess a finite short-time modulus, this warrants separate investigation: the K vs V curves generated do not behave in the same way as those for e.g. the standard linear solid. Non-uniqueness of solutions to the fracture criterion equation for certain values of the parameter n is a new feature: for more realistic material models with five or more parameters, the loss of uniqueness will become more likely, and then it will be necessary to decide which of the generated curves is consistent with physical behaviour. An attempt to rationalise the non-uniqueness for these values of n would be worthwhile.

Computations based on the constant COD fracture criterion are inevitably time-consuming as they are displacement-intensive. For realistic loadings and relaxation functions, use of this criterion is undesirable. However, in a sense, it is the most appropriate choice when a craze zone is present.

References

[1] C.Atkinson, A Note on Some Dynamic Crack Problems in Linear Viscoelastity; *Archiwum Mechaniki Stosowanej*, **31** (1979) 829-849.

[2] C.Atkinson and C.J.Coleman, On Some Steady-state Moving Boundary Problems in the Linear Theory of Viscoelasticity; *Journal of the Institute of Mathematics and its Applications*, **20** (1977), 85-106.

[3] C.Atkinson and R.D.List, A Moving Crack Problem in a Viscoelastic Solid; *International Journal of Engineering Science*, **10** (1972), 309-322.

[4] C.Atkinson and C.H.Popelar, Antiplane Dynamic Crack Propagation in a Viscoelastic Strip; *Journal of the Mechanics and Physics of Solids*, **27** (1979), 431-439.

[5] B.A.Bilby, A.H.Cottrell and K.H.Swinden, The Spread of Plastic Yield From a Notch, *Proceedings of the Royal Society (London)*, **A272** (1963) 304-314.

[6] D.R.Bland, *The Theory of Linear Viscoelasticity*, Pergamon Press, Oxford (1960).

[7] R.L.Burden and J.D.Faires, *Numerical Analysis, 3rd edition*, Prindle, Weber and Schmidt, Boston (1981).

[8] R.M.Christensen, *Theory of Viscoelasticity: An Introduction, 2nd edition*, Academic Press, New York (1982).

[9] D.S.Dugdale, Yielding of Steel Sheets Containing Slits; *Journal of the Mechanics and Physics of Solids*, **8** (1960) 100-104.

[10] A.Erdelyi *et al.*, *Tables of Integral Transforms*, Vol. 1, McGraw-Hill, New York (1954).

[11] L.B.Freund, Crack Propagation in an Elastic Solid Subjected to General Loading - I. Constant Rate of Extension; *Journal of the Mechanics and Physics of Solids*, **20** (1972), 129-140.

[12] L.B.Freund, - II. Non-uniform rate of extension; *Journal of the Mechanics and Physics of Solids*, **20** (1972), 141-152.

[13] L.B.Freund, - III. Stress Wave Loading; *Journal of the Mechanics and Physics of Solids*, **21** (1973), 47-61.

[14] L.B.Freund and J.W.Hutchinson, High Strain-rate Crack Growth in Rate-dependent Plastic Solids; *Journal of the Mechanics and Physics of Solids*, **33** (1985), 169-191.

[15] L.B.Freund, J.W.Hutchinson and P.S.Lam, Analysis of High Strain-rate Elastic-Plastic Crack Growth; *Engineering Fracture Mechanics*, **23** (1986), 119-129.

[16] I.M.Gel'fand and G.E.Shilov, *Generalised Functions, Vol.I: Properties and Operations*, Academic Press, New York (1964).

[17] G.A.C.Graham, The Correspondence Principle of Linear Viscoelasticity Theory for Mixed Boundary Value Problems Involving Time-Dependent Boundary Regions; *Quarterly of Applied Mathematics*, **26** (1968) 167-174.

[18] G.A.C.Graham, Two Extending Crack Problems in Linear Viscoelasticity Theory; *Quarterly of Applied Mathematics*, **27** (1969) 497-507.

[19] G.A.C.Graham and G.C.W.Sabin, The Correspondence Principle of Linear Viscoelasticity For Problems that Involve Time-dependent Regions; *International Journal of Engineering Science*, **11** (1973) 123-140.

[20] G.A.C.Graham and G.C.W.Sabin, The Opening and Closing of a Growing

Crack in a Linear Viscoelastic Body That is Subject to Alternating Tensile and Compressive Loads; *International Journal of Fracture*, **14** (1978) 639-649.

[21] G.A.C.Graham and G.C.W.Sabin, Steady State Solutions For a Cracked Standard Linear Viscoelastic Body; *Mechanics Research Communications*, **8** (1981) 361-368.

[22] G.A.C.Graham, Stresses and Displacements in Cracked Linear Viscoelastic Bodies That Are Acted Upon by Alternating Tensile and Compessive Loads, *International Journal of Engineering Science*, **14** (1976) 1135-1142.

[23] J.M.Herrmann and J.R.Walton, On the Energy Release Rate for Dynamic Transient Anti-Plane Shear Crack Propagation in a General Linear Viscoelastic Body; Preprint, Texas A&M University (1988).

[24] W.G.Knauss, On the Steady Propagation of a Crack in a Viscoelastic Sheet: Experiments and Analysis; *Proceedings of the Batelle Colloquium on the Deformation and Fracture of High Polymers*, Kronberg, Germany (1972).

[25] W.G.Knauss, The Mechanics of Polymer Fracture; *Applied Mechanics Reviews*, (1973) 1-17.

[26] W.G.Knauss, Delayed Failure - The Griffith Problem for Linearly Viscoelastic Materials, *International Journal of Fracture*, **6** (1970) 7-20.

[27] W.G.Knauss and H.Dietman, Crack Propagation Under Variable Load Histories in Linearly Viscoelastic Materials, *International Journal of Engineering Science*, **8** (1970) 643-656.

[28] J.F.Knott, *Fundamentals of Fracture Mechanics*, Butterworths, London (1973).

[29] B.V.Kostrov, Unsteady Propagation of Longitudinal Shear Cracks;

J.Appl.Math.Mech. (PMM), **30** (1966) 1241-.

[30] B.V.Kostrov, Crack propagation at variable velocity; *J.Appl.Math.Mech. (PMM)*, **30** (1966) 1042-1049.

[31] B.V.Kostrov and L.V.Nikitin, Some General Problems of Mechanics of Brittle Fracture, *Archiwum Mechaniki Stosowanej*, **22** (1970) 749-776.

[32] M.J.Lighthill, *Introduction to Fourier Analysis and Generalised Functions*, Cambridge University Press (1958).

[33] A.H.Nayfeh, *Perturbation Methods*, Wiley Interscience, New York (1973).

[34] L.V.Nikitin, Application of the Griffith's approach to analysis of rupture in viscoelastic bodies; *International Journal of Fracture*, **24** (1984) 149-157.

[35] W.Mendes, The Numerical Solution of Wiener-Hopf Integral Equations, University of Bath Ph.D. Thesis (1988).

[36] H.K.Mueller and W.G.Knauss, Crack Propagation in a Linearly Viscoelastic Strip; *Journal of Applied Mechanics*, (1971) 483-488.

[37] N.I.Muskhelishvilli, *Singular Integral Equations*, Wolters-Noordhoff, Groningen (1972).

[38] B.Noble, *Methods based on the Wiener-Hopf Technique for the Solution of Partial Differential Equations*, Pergamon, London (1958).

[39] E.Passaglia, Relaxation of Stresses in Crazes at Crack Tips and Rate of Craze Extension; *Polymer*, **23** (1982), 754-760.

[40] C.H.Popelar and C.Atkinson, Dynamic Crack Propagation in a Viscoelastic Strip; *Journal of the Mechanics and Physics of Solids*, **28** (1980), 79-93.

[41] J.R.Rice, *Mathematical Analysis in the Mechanics of Fracture*, Fracture, Vol.II, Academic Press, New York (1968).

[42] R.A.Schapery, A Theory of Crack Initiation and Growth in Viscoelastic Media, I.Theoretical Development; *International Journal of Fracture*, **11** (1975) 141-158.

[43] R.A.Schapery, A Theory Of Crack Initiation and Growth in Viscoelastic Media, II.Approximate Methods of Analysis; *International Journal of Fracture*, **11** (1975) 369-388.

[44] R.A.Schapery, A Theory Of Crack Initiation and Growth in Viscoelastic Media, III.Analysis of Continuous Growth, *International Journal of Fracture*, **11** (1975) 549-562.

[45] R.A.Schapery, A Method For Predicting Crack Growth in Nonhomogenous Viscoelastic Media; *International Journal of Fracture*, **14** (1978) 293-309.

[46] R.A.Schapery, Correspondence Principles and a Generalised J-integral For Large Deformation and Fracture Analysis of Viscoelastic Media; *International Journal of Fracture*, **25** (1984) 195-223.

[47] G.Strang, *Introduction to Applied Mathematics*, Wellesley-Cambridge Press (1986).

[48] M.Van Dyke, *Perturbation Methods in Fluid Mechanics*, Academic Press, New York & London (1964).

[49] J.R.Walton, On the Steady-State Propagation of an Antiplane Shear Crack in an Infinite General Linearly Viscoelastic Body; *Quarterly of Applied Mathematics*, **40** (1982), 37-52.

[50] J.R.Walton, The Dynamic Steady-State Propagation of an Antiplane Shear Crack in a General Linearly Viscoelastic Layer; *Journal of Applied Mechanics*, **52** (1985), 853-856.

[51] J.R.Walton, The Dynamic Energy Release Rate for a Steadily Propagating Anti-plane Shear Crack in a Linearly Viscoelastic Body; *Journal of Applied Mechanics*, **54** (1987), 635-641.

[52] J.R.Walton and Y.Weitsman, Deformations and Stress Intensities Due to a Craze in an Extended Elastic Material, *Journal of Applied Mechanics*, **51** (1984) 84-92.

[53] M.L.Williams, Initiation and Growth of Viscoelastic Fracture; (1965), 292-310.

[54] J.R.Willis, A Comparison of the Fracture Criteria of Griffith and Barenblatt; *Journal of the Mechanics and Physics of Solids*, **15** (1967), 151-162.

[55] J.R.Willis, Crack Propagation in Viscoelastic Media; *Journal of the Mechanics and Physics of Solids*, **15** (1967), 229-240.

[56] J.R.Willis, Equations of Motion for Propagating Cracks; *Mechanics and Physics of Fracture*, The Metals Society (1975) 57-67.

[57] J.R.Willis, *Nonlinear Fracture Mechanics - a Short Review*, United Kingdom Atomic Energy Authority, AERE Harwell, LWRSG(PV)/78/P11 (1978).

[58] J.R.Willis, *Dynamic Fracture - an Outline*, Report to Royal Society Subcommitee on Fracture (1983).

[59] M.P.Wnuk and W.G.Knauss, *International Journal of Solids and Structures*; **6** (1970), 995-1009.

[60] E.H.Yoffé, *Phil. Mag.*; **42** (1951), 739-750.

Published material

The contents of chapter 2, minus most of the analysis, appear in the following research note, which is bound into the back of this thesis:

G.Goleniewski, Dynamic Crack Growth in a Viscoelastic Material, *International Journal of Fracture*, **37** (1988) R39-44.

Appendix 1: Integration techniques used for Chapter 2.

$$\int_{-\infty+i\delta}^{\infty+i\delta} \frac{e^{i\lambda u}d\lambda}{(\lambda+i\frac{b}{a})_+^{1/2}} = 2\sqrt{\frac{\pi}{i}}\frac{e^{\frac{b}{a}u}}{(-u)^{1/2}}H(-u). \qquad \text{(A1.1)}$$

where $\delta\in\mathbf{R}^+$ is infinitesimal.

This integral is evaluated around a keyhole contour (mainly in the lower half plane), consisting of a large semi-circle indented to skirt round the branch cut (which is taken to be $\mathrm{Re}(\lambda)=0$, $-\frac{b}{a}\geq\mathrm{Im}(\lambda)$). As the radius of the semi-circle tends to infinity, the contributions from the arcs disappear, and the integral just above the real line can be expressed in terms of the branch cut integrals using Cauchy's Residue Theorem (there are no poles inside the contour). One of these branch cut integrals turns out to be a copy of the other, and the result follows on making a change of variable and using the fact that

$$\mathrm{erf}(x)\to 1 \text{ as } x\to\infty.$$

$$\int_{-\infty}^{\infty} \frac{e^{ipt}dp}{vp^{1/2}(p+i\frac{b}{a})^{1/2}} = \frac{\frac{vb}{a}e^{\frac{bt}{2a}}}{\sqrt{t^2+v^2}}K_1\left(\frac{b}{2a}\sqrt{t^2+v^2}\right) \qquad \text{(A1.2)}$$

where $v=ya^{1/2}$.

A symmetrising change of variable

$$p=p'-i\frac{b}{a}$$

followed by a rescaling

$$q'=vp'$$

reduces the integral to

$$\frac{e^{\frac{bt}{2a}}}{v}\int_{-\infty}^{\infty} e^{i\frac{t}{v}q'-[q'+\frac{v^2b^2}{4a^2}]^{\frac{1}{2}}}\,dq',$$

which is a known Fourier transform to be found in Erdelyi (1954).

$$w(x,y)\sim\frac{-2k}{\pi^{\frac{1}{2}}}(-x)^{\frac{1}{2}}H(-x)\text{as}|x|\to\infty. \qquad \text{(A1.3)}$$

Providing p is small, the term

$$e^{-ya^{\frac{1}{2}}p^{\frac{1}{2}}(p+i\frac{b}{a})^{\frac{1}{2}}}$$

which appears in the exact formula for $w(-x,y)$ can be approximated to first order by 1. Therefore

$$\hat{w}(p,y)\sim\frac{c_*}{p^{\frac{3}{2}}}\text{ for small } p.$$

Using the relations between the values of a function at 0 (∞) and its transform at ∞ (0) (Lighthill, 1958), this gives (A1.3) as a first approximation.

The more accurate formula (2.3.5) is obtained by replacing the above exponential by

$$e^{-yp^{\frac{1}{2}}(ib)^{\frac{1}{2}}}$$

and evaluating the resulting integral by the method of steepest descent.

Appendix 2: Derivation of static stresses in Mode III.

Consider the antiplane strain static crack problem in a linearly elastic material without the presence of body forces. On the crack faces, σ_{23} is specified to be a given function:

$$\sigma_{23}=g, \quad x<0. \tag{A2.1}$$

Since the equilibrium equation can be written in the form

$$\frac{\partial\sigma_{13}}{\partial x}=-\frac{\partial\sigma_{23}}{\partial y} \tag{A2.2}$$

and

$$\frac{\partial\sigma_{13}}{\partial y}=\frac{\partial\sigma_{23}}{\partial x}=\mu\frac{\partial^2 w}{\partial x\partial y}, \tag{A2.3}$$

i.e. σ_{23}, σ_{13} satisfy the Cauchy-Riemann equations, the function defined by the following equation is analytic:

$$F(z)=\sigma_{23}+i\sigma_{13}. \tag{A2.4}$$

The boundary conditions on the crack faces in terms of F are

$$\left.\begin{matrix}F(x+0i)+\bar{F}(x-0i)\\ F(x-0i)+\bar{F}(x+0i)\end{matrix}\right\}=+2g(x), \quad -\infty<x<x_1, \tag{A2.5}$$

from which it may be deduced that

$$(F-\bar{F})(x+0i)=(F-\bar{F})(x-0i), \tag{A2.6}$$

Therefore $F-\bar{F}$ is an entire function identically equal to zero.

Hence

$$F(x+0i)+F(x-0i)=+2g(x). \tag{A2.7}$$

If a function G is now defined by

$$G(z)=(z-x_1(t))^{1/2}F(z), \tag{A2.8}$$

equation (A2.7) becomes

$$G(x+0i)-G(x-0i)=+2ig(x)(x_1(t)-x)^{1/2}, \tag{A2.9}$$

which, on use of the Plemelj formulae (Muskhelishvilli, 1953), yields

$$G(z)=\frac{1}{\pi}\int_{-\infty}^{x_1}\frac{(x_1-x)^{1/2}g(x)dx}{x-z}. \qquad \text{(A2.10)}$$

Equations (A2.4,9,10) taken together give the final result for static stresses:

$$\sigma_{23}+i\sigma_{13}=\frac{1}{\pi\sqrt{(z-x_1(t))}}\int_{-\infty}^{x_1}\frac{(x_1-x)^{1/2}g(x)dx}{x-z}. \qquad \text{(A2.11)}$$

Appendix 3: Kostrov's solution for an accelerating crack in an elastic medium.

Kostrov (1966) solved the problem of a finite accelerating crack propagating under mode III conditions in an elastic medium, described by equations (5.1.7,8a,8b) for the special case $x_1(t)=-\infty$. What follows is essentially a summary of his method, except that here we keep c, the shear wave speed, and μ, the shear modulus, general. In keeping with the original paper, we shall use τ to signify σ_{23}.

The displacement at a point on the crack line is given by the formula

$$w(x_0,0,t_0)=\frac{1}{2\pi}\iint_S \frac{\tau(x,t)\,dx\,dt}{\sqrt{(t_0-t)^2-((x_0-x)/c)^2}} \qquad \text{(A3.1)}$$

where S is the triangular region defined by

$$(t_0-t)^2-((x_0-x)/c)^2\geq 0,\quad 0\leq t\leq t_0. \qquad \text{(A3.2)}$$

The crack path $x=x_2(t)$ splits the triangle S into two regions: S_1, where τ is known and S_2, where it is not. We are aiming to find a formula for τ ahead of the crack: to this end, rewrite equation (A3.1) for $x>x_2(t)$ in the form

$$\iint_{S_2} \frac{\tau(x,t)\,dx\,dt}{\sqrt{(t_0-t)^2-((x_0-x)/c)^2}}=\iint_{S_1} \frac{p(x,t)\,dx\,dt}{\sqrt{(t_0-t)^2-((x_0-x)/c)^2}}. \qquad \text{(A3.3)}$$

If we introduce characteristic co-ordinates by the equations

$$\xi=\frac{(ct-x)}{\sqrt{2}}, \qquad \text{(A3.4a)}$$

$$\eta=\frac{(x+ct)}{\sqrt{2}}, \qquad \text{(A3.4b)}$$

the equation becomes

$$\int_{-\frac{x_2(0)}{\sqrt{2}}}^{\xi_0} \frac{d\xi}{\sqrt{\xi_0-\xi}} \int_{\eta_2(\xi)}^{\eta_0} \frac{\tau_1(\xi,\eta)\,d\eta}{\sqrt{\eta_0-\eta}} \qquad \text{(A3.5)}$$

$$=\int_{-\frac{x_2(0)}{\sqrt{2}}}^{\xi_0} \frac{d\xi}{\sqrt{\xi_0-\xi}} \int_{-\xi}^{\eta_2(\xi)} \frac{p_1(\xi,\eta)\,d\eta}{\sqrt{\eta_0-\eta}},$$

where (x_0,t_0) becomes (ξ_0,η_0) in the new co-ordinate system. This reduces to the Abel equation

$$\int_{\eta_2(\xi)}^{\eta_0} \frac{\tau_1(\xi,\eta)d\eta}{\sqrt{\eta_0-\eta}} = \int_{-\xi}^{\eta_2(\xi)} \frac{p_1(\xi,\eta)d\eta}{\sqrt{\eta_0-\eta}}. \qquad \text{(A3.6)}$$

This has solution

$$\eta_1(\xi_0,\eta_0)=\frac{1}{\pi\sqrt{\eta_0-\eta_2(\xi_0)}}\int_{-\xi}^{\eta_2(\xi)} \frac{p_1(\xi_0,\eta)\sqrt{\eta_2(\xi_0)-\eta}\,d\eta}{\sqrt{\eta_0-\eta}}, \quad \eta_0>\eta_2(\xi_0). \qquad \text{(A3.7)}$$

In the original co-ordinates, this can be expressed as

$$\tau(x_0,t_0)=\frac{1}{\pi\sqrt{x_0-x_2(t_2)}}\int_{x_0-ct_0}^{x_2(t_2)} \frac{p(\frac{ct_0-x_0+x}{c})\sqrt{x_2(t_2)-x}\,dx}{x_0-x}, \quad x_0>x_2(t_0), \qquad \text{(A3.8)}$$

where t_2 is the solution of

$$ct_0-x_0=ct_2-x_2(t_2).$$

A parallel analysis gives a similar result for the stress at the left edge of the crack, were it to be finite - this is not required for the semi-infinite crack problem posed in Chapter 5.

Appendix 4: Correspondence between the two different notations used in this thesis for the constitutive equation of the standard linear solid.

The constitutive relation in Willis's 1967b paper can be rewritten as

$$\sigma_{ij}=\frac{2\mu}{1+f}\{e_{ij}(t)+f\frac{d}{dt}((\exp(-\frac{1+f}{\tau}t)H(t))*e_{ij}(t))\}. \qquad \text{(A4.1)}$$

where

$$f*g=\int_{-\infty}^{\infty}f(t-u)g(u)du. \qquad \text{(A4.2)}$$

With this convention, μ is the short time modulus.

Using the same definition for the convolution of two functions, the relation in Chapter 5 is

$$\sigma_{ij}=2\mu\{e_{ij}+\alpha\frac{d}{dt}((\exp(-\frac{t}{\varepsilon\tau})H(t))*e_{ij}(t))\}. \qquad \text{(A4.3)}$$

Now μ is the long-time modulus.

Henceforth we shall denote μ, τ in equation (A4.3) by μ_*, τ_* respectively. This facilitates comparison between the two conventions. The two sets of constants are related by the trio of equations

$$\alpha=f, \qquad \text{(A4.4a)}$$

$$\mu_*=\frac{\mu}{1+f}, \qquad \text{(A4.4b)}$$

$$\varepsilon\tau_*=\frac{\tau}{1+f}. \qquad \text{(A4.4c)}$$

International Journal of Fracture 37: R39–R44 (1988)

DYNAMIC CRACK GROWTH IN A VISCOELASTIC MATERIAL

G. Goleniewski
School of Mathematical Sciences, University of Bath,
Claverton Down, Bath, BA2 7AY, U.K.

Freund and Hutchinson [1] investigated high strain-rate crack growth in an elastic-plastic material. Their model consisted of three zones of material, each corresponding to a strain-rate range. The two highest ranges of strain-rate values described the material behaviour in the plastic zone. A critical near-tip energy release rate was used as a fracture criterion. A similar model is investigated here. The material description chosen is that of a Maxwell liquid, this resulting from taking the dominant term of the constitutive equation from [1] in the region of the plastic zone nearest the crack tip (i.e., the region corresponding to the highest strain-rate range of the three). In contrast with [1], here we shall take the same rate-dependent constitutive equation in all of the material as opposed to only in the zone within which strain-rates are high. This reduces the problem to a linear one which can be solved explicitly. Apart from the wish to facilitate comparison with [1], the choice of the material model is governed in part by the need to minimise the scale of the computations. Reference [2] contains numerical work based on the approximate analysis of [1], using as an example the growth of a macroscopic cleavage crack in mild steel - from this work the authors deduce that the approximations appear acceptably accurate except in a higher temperature range.

A new feature of the present analysis is the consideration of the effects of a finite cohesive zone, in which a constant cohesive stress σ_0 acts, whose extent may be comparable with the length scale of the applied loads. A critical crack opening displacement fracture criterion is used. When σ_0 is sufficiently large, this is demonstrated to reduce to the energy release rate criterion, while finite σ_0 provides a rudimentary model of a craze zone such as exists adjacent to a crack tip in a viscoelastic polymer. The solution to be presented thus serves the dual purpose of providing an explicit realisation of the near-tip situation discussed in [1], and of assessing the influence of a craze zone during dynamic fracture of a polymer.

Willis [3] used the Wiener-Hopf technique to solve for stress and displacement fields for steady-state motion in antiplane strain. Atkinson and Popelar [4] dealt with a similar problem in a viscoelastic strip, giving numerical results for stress intensity factor as a function of crack speed. The Wiener-Hopf equation is numerically factored. Popelar and Atkinson [5] dealt with the corresponding mode I problem. Having reformulated the Wiener-Hopf problem as a Riemann-Hilbert problem, and considering a general visco - elastic material, Walton [6] obtained expressions for stress fields in the plane of the crack as well as the stress intensity factor. His work includes an infinitesimal cohesive zone. The same methodology is used to solve the corresponding problem for a layer of general viscoelastic material [7] and to derive an expression for an energy release rate [8].

Steady state motion with uniform velocity V is studied, the crack faces being loaded with stresses travelling in tandem. Only antiplane strain (mode III) is considered, and body forces are ignored. The Wiener-Hopf technique is used to solve for stress and displacement in the manner of Willis [3] which dealt with a parallel calculation for the standard linear solid. The loading

is then specialised to a step function to enable a simpler formula (in terms of single integrals) for the displacement to be obtained. Plots of the work performed by the loading forces per unit of crack extension (which is analogous to G as used in [1], vs V, crack velocity, are drawn showing a similar U-shape to the G/G^{c}_{tip} vs V curves in [1]. The behaviour at V=0 is consistent with the relation $K^2=2\mu G$, since $\mu\to 0$ as $t\to\infty$ and K, the stress intensity factor, is finite.

The constitutive equations for the Maxwell liquid (in shear) are

$$\mu\frac{\partial \dot{w}}{\partial x_i} = \dot{\sigma}_{i3} + \frac{\sigma i3}{t_*} \ , \ i=1,2 \tag{1}$$

where $w=w(x_1,x_2,t)=u_3$ is the 3-component of displacement, σ_{i3}, i=1,2 are the two non-zero components of the stress tensor, μ is a shear modulus and t_* is the relaxation time.

Using the techniques of Willis [3] gives the following formulae for stress and displacement:

$$\sigma_{23}(x,0)=\frac{\exp(-\frac{b}{a}x)}{\pi x^{\frac{1}{2}}}\int_{-\infty}^{0}\frac{\exp(\frac{b}{a}u)f(u)(-u)^{\frac{1}{2}}du}{u-x} \ , \ x>0 \tag{2}$$

$$\frac{d}{ds}w(-s,0)=\frac{-1}{\pi\mu a^{\frac{1}{2}}}\left(\frac{1}{Vt_*}+\frac{d}{ds}\right)\int_{\infty}^{0} f(u)du \int_{u}^{\xi}\frac{\exp(\frac{b}{a}u')du'}{(-u')^{\frac{1}{2}}(s+u-u')^{\frac{1}{2}}} \ , \ s>0 \tag{3}$$

where $\xi=\min\{(s+u),0\}$, V is the uniform crack velocity, and

$$\frac{b}{a}=\frac{1}{ct_*}\Phi\left(\frac{V}{c}\right) \tag{4a}$$

where

$$\Phi(\alpha)=\frac{\alpha}{1-\alpha^2} \tag{4b}$$

and

$$c=\sqrt{\mu}/\rho \tag{4c}$$

(ρ denotes density).

The step function

$$f(x) = \begin{cases} -\sigma_0, & -d<x<0 \\ F, & -(d+L)<x<-d \\ 0, & x<-(d+L) \end{cases} \tag{5}$$

provides for both a shearing stress along a length L of the crack from the crack tip x=-d and a cohesive stress $-\sigma_0$ from the crack tip to the end of the cohesive zone at x=0. A relation between F and σ_0 is established by specifying that the stress intensity factor for the crack tip at x=0 identically vanish:

$$\int_{-\infty}^{0} \frac{\exp(\frac{b}{a}u)f(u)du}{(-u)^{\frac{1}{2}}} = 0 \tag{6}$$

This gives

$$\frac{F}{\sigma_0} = \frac{\operatorname{erf}\sqrt{\frac{b}{a}d}}{\operatorname{erf}\sqrt{\frac{b}{a}(d+L)} - \operatorname{erf}\sqrt{\frac{b}{a}d}} \tag{7}$$

Evaluating (3) in integrated form for the step function given by (5) leads to to

$$w(-s,0) = \frac{\sigma_0}{\pi\mu a^{\frac{1}{2}}}\{A_1(s)+B_1(s)\} \tag{8}$$

where

$$A_1(s) = -2\exp(-\frac{b}{a}d)H(s,d,1)[1+\frac{F}{\sigma_0}(d)]+2\exp[-\frac{b}{a}(d+L)]H(s,d+L,1)\frac{F}{\sigma_0}(d) \tag{9}$$

$$B_1(s) = \frac{1}{Vt_*}\int_0^s A_1(s')ds'$$

$$= \frac{1}{Vt_*}\{-\frac{4}{3}\exp(-\frac{b}{a}d)H(s,d,3)[1+\frac{F}{\sigma_0}(d)]+\frac{4}{3}\exp[-\frac{b}{a}(d+L)]H(s,d+L,3)\frac{F}{\sigma_0}(d)\} \tag{10}$$

and $H(s,x,\alpha)$ is defined as

$$\int_0^{\min\{x,s\}} \exp(\frac{b}{a}\nu)\frac{(s-\nu)^{\frac{\alpha}{2}}}{(x-\nu)^{\frac{1}{2}}}d\nu. \tag{11}$$

Formula (8) was checked by taking elastic ($t_* \to \infty$) and static ($\rho \to 0$) limits and these were in agreement with known results.

Using the fracture criterion COD=δ (δ constant), the equation $w(-d,0)=\delta/2$ was solved numerically (using bisection) for each V, yielding a value of d. The corresponding values of K=K(d,V), nominal stress intensity factor, are plotted in Fig. 1 for various σ_0,δ pairs such that $\sigma_0\delta=2\gamma$, where γ is the surface energy per unit width ($\sigma_0\delta$ represents the energy dissipated in the cohesive zone per unit of crack extension). K is defined by $K=2\sqrt{\frac{2}{\pi}}F\sqrt{L}$. This is done for the values $\alpha=0.125$ and $\mu=1$, where α is a dimensionless parameter defined by $\alpha=\frac{ct_*}{L}$. All the curves tend to the origin, except in the Griffith limit itself. The monotone increasing nature of the K vs V graphs implies that crack motion is stable at all speeds $V\in(0,c)$ for the particular value of α chosen. Increasing α makes the material more elastic, and a decreasing section appears in each of the

K vs V curves in an ever larger interval strictly contained in (0,c).

The total work done by the applied loading, per unit of crack extension, $2F[w(-(d+L))-w(-d)]$ is plotted against V in Fig. 2, again for various σ_0,δ such that $\sigma_0\delta=2\gamma$ and $\alpha=0.125,\mu=1$. This total work per unit of extension corresponds to the total rate of energy absorption, both by viscoelastic dissipation in the bulk of the material and by absorption of energy in the craze zone, and is analogous to the overall energy release rate in the sense used by Freund and Hutchinson [1]. This latter quantity, $\sigma_0\delta=2\gamma$, is also plotted in Fig. 2, and is seen to represent only a small fraction of the total energy absorbed. Stored energy does not enter into the energy balance as it is constant, this being a steady state problem. Walton [8] defined the energy release rate G as the work done by cohesive forces: thus in Walton's terminology, $G=\sigma_0\delta$ for the present model.

As σ_0 increases, the curves converge to what we choose to call the Griffith limit, in which the cohesive zone shrinks to a point but nevertheless a finite amount of energy, 2γ per unit of crack extension is absorbed there. This can be viewed either as plastic dissipation or, alternatively, the cohesive stress σ_0 can be regarded as resisting the breaking of bonds and hence giving rise to a specific surface energy γ. The curves demonstrate that a finite yielding zone (with σ_0 small) induces more dissipation throughout the material than does the Griffith limit, except for small V. As σ_0 increases, the domain of the stable branch of the curves ($V>V_{min}$, the velocity where the minimum is attained) is reduced. However, Fig. 1 suggested that crack motion is stable for all velocities (with small α) with the dead loading that we have been using. A precise stability comparison with [1] is made difficult by the differences in loading, and the nonlinearity which is present in that model.

Walton [8] also includes a finite cohesive zone, but considers exponential forms for both the applied loading and the cohesive stresses. Unlike the current model, the zones of application for the two types of loading are not disjoint, and the assumption is made that $\varepsilon=a_f/a_e<<1$ where a_f,a_e are length scales associated with the cohesive stresses and applied loads, respectively. An expression is derived for the energy release rate, and this is mainly studied as a function of crack speed for the cases of a standard linear solid and power law material, when $\varepsilon<<1$. The analogous parameter in the present work would be $\varepsilon=d/L$. The present work is less general than that of Walton [8] in that it concentrates on a Maxwell liquid but the case of finite σ_0 and δ (and hence d) is considered so that deviations from the limit $\varepsilon<<1$ are shown explicitly.

Acknowledgement: This work was carried out during the tenure of a SERC Research Studentship. The author would like to thank Professor J.R. Willis for many helpful discussions and Professor J.R. Walton for several enlightening comments on an earlier draft.

REFERENCES

[1] L.B. Freund and J.W. Hutchinson, *Journal of the Mechanics and Physics of Solids* 33 (1985) 169-191.

[2] L.B. Freund, J.W. Hutchinson and P.S. Lam, *Engineering Fracture Mechanics* 23 (1986) 119-129.

[3] J.R. Willis, *Journal of the Mechanics and Physics of Solids* 15 (1967) 229-240.

[4] C. Atkinson and C.H. Popelar, *Journal of the Mechanics and Physics of*

Solids 27 (1979) 431-439.

[5] C.H. Popelar and C. Atkinson, *Journal of the Mechanics and Physics of Solids* 28 (1980) 79-93.

[6] J.R. Walton, *Quarterly of Applied Mathematics* 40 (1982) 37-52.

[7] J.R. Walton, *Journal of Applied Mechanics* 52 (1985) 853-856.

[8] J.R. Walton, *Journal of Applied Mechanics* 54 (1987) 635-641.

[9] A. Erdelyi et al., *Tables of Integral Transforms*, Vol. 1, McGraw-Hill, New York (1954).

[10] B. Noble, *Methods Based on the Wiener-Hopf Technique for the Solution of Partial Differential Equations*, Pergamon, London (1958).

10 February 1988

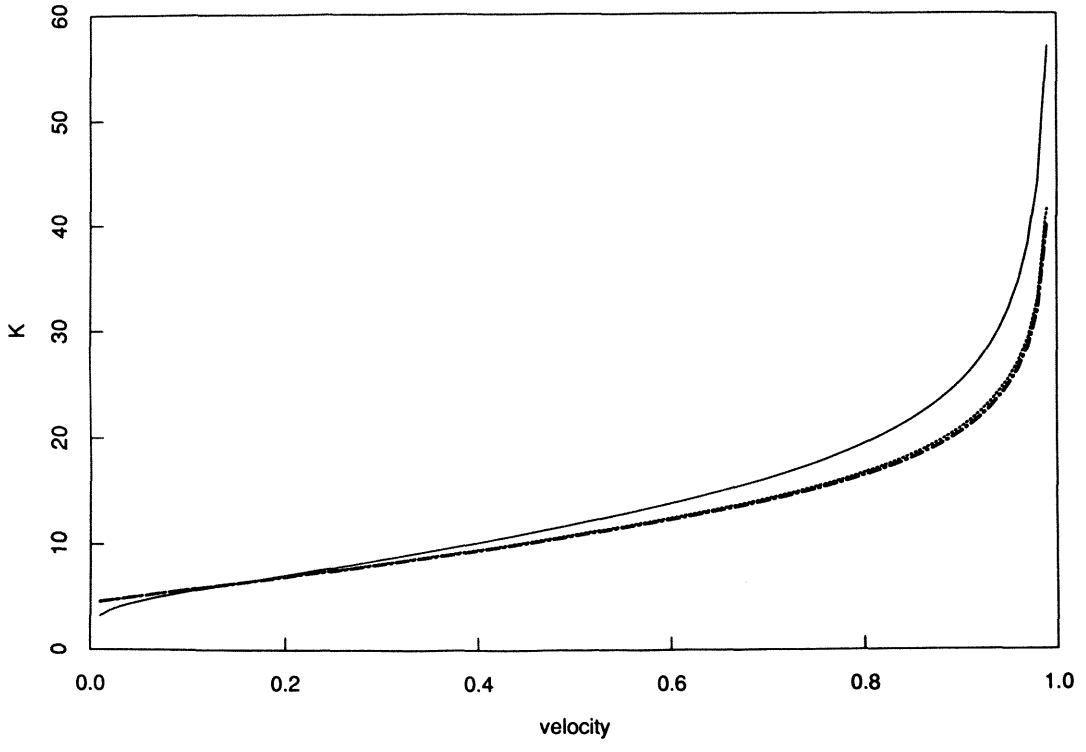

Figure 1. K, nominal stress intensity factor, vs velocity: σ_0, δ varied subject to $\sigma_0\delta=10$.
———— $\sigma_0=10, \delta=1$
..... $\sigma_0=100, \delta=0.1$
-•-•-•-•-•- $\sigma_0=1000, \delta=0.01$

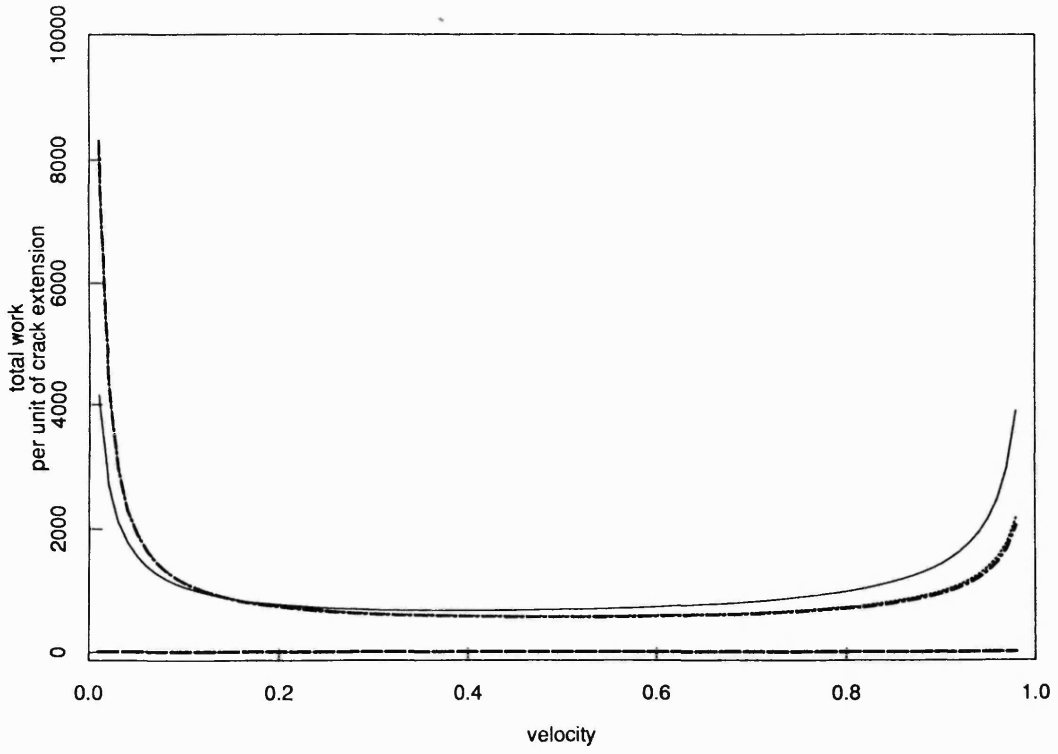

Figure 2. Total work per unit of crack extension vs velocity: σ_0, δ varied subject to $\sigma_0\delta=10$.

———————— $\sigma_0=10, \delta=1$

. . . . . $\sigma_0=100, \delta=0.1$

- - - - - - $\sigma_0=1000, \delta=0.01$

---------- $\sigma_0\delta=10$